IS OUR BREATHING OPTIMAL?

Syed Muhammad Faheem Zaidi

School of Natural and Computational Sciences

Massey University

This dissertation is submitted for the degree of

Doctor of Philosophy

December 2019

I would like to dedicate this thesis to my loving parents.

Acknowledgements

It has been an exceptional journey. One that I had never dreamed of. All have been done because of the blessing of Almighty, Allah for giving me determination and strength to complete my doctoral thesis.

I would like to thank my main supervisor, Alona Ben-Tal, whose advice, appreciation and valuable feedback have given me inspiration throughout my Ph.D. journey. She allowed me to work together with her. I would not have achieved this without her support. I would also like to extend my gratitude to my co-supervisor Mick Roberts, for his valuable inputs, feedbacks and thought-provoking discussions on my research.

I would like to thank people who have contributed their knowledge during my post-graduate study at Massey University: Shaun Cooper, Winston Sweatman, Robert McKibbin, Carlo Laing and GraemeWake. I am also thankful to Freda, Annette and Linh for their administrative support and assistance, and Anil and Zhou for their timely IT support.

I convey my sincere thanks to my family, especially my parents for always believing in me and their support in my decision. Without whom I could not have made it here. Thank you, Azeem and Sabika for supporting me and for being the best sibling anyone could ask for. Special thanks to my beloved wife, Nabila for her patience, understanding and support throughout my studies. And of course Zahra, my daughter for her hugs and love.

Special thanks to Khalid Siddiqui, Mariam Sultana, Husna, Kazim and Rais H. Zaidi (my late uncle) whose sincerity and encouragement I will never forget.

Finally, yet importantly, I am also grateful to Massey University, New Zealand, for awarding me a doctoral scholarship for my Ph.D. studies.

Abstract

One of the open questions in relation to the control of amplitude and frequency of breathing is why a particular pattern of breathing is observed. This thesis explores the hypothesis that the particular combination of breathing frequency and amplitude realised, is optimal with respect to some objective function. Several objective functions have been suggested in the literature, such as the rate of work during inhalation, the average force exerted by the respiratory muscles, and the weighted sum of volumetric acceleration and work during inhalation; all of these objective functions were studied using $1D$ models and all provided physiologically acceptable minima under normal conditions. The thesis investigates optimal solutions of mathematical models that range from $2D$ to 6D and reflect more accurately the coupling between lung mechanics and gas exchange. It shows how published $6D$ and $5D$ models can be reduced to new $3D$ and $2D$ models. At its simplest, the $2D$ model consists of two piecewise linear differential equations. The use of higher dimension models require a new definition of the optimization problem as minimizing a given objective function subject to several constraints, such as satisfying the differential equations and maintaining one of the variables at a given average value. The optimal problem can be solved analytically in the case of the simplest $2D$ model, using concepts from optimal control theory. The analytical solution is used to verify a numerical algorithm that is then used to solve the more complex models. Solutions of the optimization problem for the different objective functions, previously suggested in the literature have been calculated. In all the optimal solutions found in this thesis, the duration of inhalation is equal to the duration of exhalation. However, under normal conditions, the time duration of inhalation is expected to be shorter than that of exhalation. This might be resolved by imposing additional constraints or by proposing a different hypothesis to explain why a particular pattern of breathing is observed.

Table of contents

List of Figures

Nomenclature

Variables and parameters used in this thesis

Symbol	Meaning	Unit
t	Time (Independent variable)	s
P_L	Pleural pressure	$mmHg$
P_A	Alveolar pressure	$mmHg$
V_A	Alveolar volume	l
f_o	Alveolar concentration of O_2	
f_c	Alveolar concentration of CO_2	
p_o	Partial pressure of O_2 in the blood	$mmHg$
p_c	Partial pressure of CO_2 in the blood	$mmHg$
p_{ao}	Partial pressure of O_2 in alveoli	$mmHg$
p_{ac}	Partial pressure of CO_2 in alveoli	$mmHg$
z	Concentration of HCO_3	
q	Airflow though airways	ls^{-1}
$\bar{p_o}$	Average partial pressure of O_2 in the blood	$mmHg$
$\bar{p_c}$	Average partial pressure of CO_2 in the blood	$mmHg$
$R(t)$	Ramp signal	
x_m	Muscle displacement	m
F	Driving force ($2D$ Model)	$l\ s^{-1}$
Y_c	Linear transformation of f_c ($2D$ Model)	s^{-1}
Y_o	Linear transformation of f_o ($2D$ Model)	s^{-1}

Table 1: Variables used in the various models.

Symbol	Meaning		Value
k_1	Recoil rate constant of muscles		$2\ s^{-1}$
k_2	Conversion constant		$1\ m\ s^{-1}$
k_p	Conversion constant		$2.5\ mmHg\ m^{-1}$
P_m	Mouth pressure		$760\ mmHg$
p_w	Vapor pressure of water at 37^oC		$47\ mmHg$
P_{L0}	Constant related to pleural pressure		$5.5\ mmHg$
E	Lung's elasticity	(Normal)	$2.5\ mmHg\ l^{-1}$
		(Diseased)	$1.4\ mmHg\ l^{-1}$ *
R	Resistance to flow	(Normal)	$1.0\ mmHg\ s\ l^{-1}$
		(Diseased)	$2.6\ mmHg\ s\ l^{-1}$ *
f_{om}	Concentration of O_2 in the mouth		0.21
f_{cm}	Concentration of CO_2 in the mouth		0
V_T	Tidal volume		$0.4\ l$
V_D	Dead space volume		$0.15\ l$
V_c	Capillaries volume		$0.07\ l$
T	Respiratory period		$5\ s$
T_L	Heart beat period		$60/72\ s$
ω	Respiratory angular frequency		$2\pi/4\ rad\ s^{-1}$
D_o	Diffusion capacity of O_2	(Normal)	$3.5\times10^{-4}\ l\ s^{-1}\ mmHg^{-1}$
		(Diseased)	$0.875\times10^{-4}\ l\ s^{-1}\ mmHg^{-1}$ *
D_c	Diffusion capacity of CO_2	(Normal)	$7.08\times10^{-3}\ l\ s^{-1}\ mmHg^{-1}$
		(Diseased)	$1.77\times10^{-3}\ l\ s^{-1}\ mmHg^{-1}$ *
C_u	unit conversion factor		$25.426\ l\ mol^{-1}$
σ	Solubility of O_2 in plasma		$1.4\times10^{-6}\ mol\ l^{-1}\ mmHg^{-1}$
σ_c	Solubility of CO_2 in plasma		$3.3\times10^{-5}\ mol\ l^{-1}\ mmHg^{-1}$
T_h	Concentration of hemoglobin		$2\times10^{-3}\ mol\ l^{-1}$
h	Concentration of H^+		$10^{-7.4}\ mol\ l^{-1}$
r_2	Dehydration reaction rate		$0.12\ s^{-1}$
l_2	Hydration reaction rate		$164\times10^3\ l\ s^{-1}\ mol^{-1}$
δ	Acceleration rate		$10^{1.9}$
K_T	Equilibrium constant in the hemoglobin saturation function		$10^4\ l\ mol^{-1}$
K_R	"		$3.6\times10^6\ l\ mol^{-1}$
L	"		1.712
α	Parameter of the $2D$ model		$2.5\ s^{-1}$ *
β	"		$2.295\ s^{-1}$ *
γ	"		$-0.058\ mmHg\ l^{-1}\ s^{-1}$ *

Table 2: Parameters used in the various models. All the values are taken from [7] except values with * which have been estimated in this thesis.

Chapter 1

Introduction

Respiration in mammals is a continuous process, which starts from the moment of birth until the end of life. The primary function of the respiratory system is to bring air from the atmosphere into a close contact with blood in the lungs, where gas exchange takes place. Blood circulation around the body delivers oxygen (O_2) from the lungs to the tissues and carbon dioxide (CO_2) from the tissues to the lungs to meet metabolic demands [35]. The breathing control system is set up to maintain partial pressures of CO_2 and O_2 within a physiological range. Variations in blood CO_2 and O_2 levels trigger a change in the rate and amplitude of breathing; in turn, breathing affects the amount of CO_2 and O_2 in the blood.

The ventilatory response to lack of O_2 or excess of CO_2 can vary significantly between individuals. In some cases, the response consists mainly of an increase in breathing amplitude, in others it consists mainly of an increase in breathing frequency and in some cases, an increase in both amplitude and frequency is observed. Furthermore, physiological levels of O_2 and CO_2 in the blood can be achieved with multiple combinations of breathing frequency and tidal volume (volume of air inhaled in one breath). But why a specific combination of amplitude and frequency is observed remains a mystery.

The aim of this thesis is to check the hypothesis that the particular combination of breathing frequency and amplitude realized, is optimal with respect to some objective function. Several objective functions are explored using a range of mathematical models. In this Chapter, we review the relevant physiology of the control system. We then discuss the optimization of the respiratory system

and models that incorporate both mechanical and chemical components. At the end we discuss the theory of optimal control and its application to the respiratory system.

1.1 The Respiratory Control System and its Modelling

The respiratory control system consists of receptors, controller and affectors that work collectively to ensure that physiological levels of O_2 and CO_2 are maintained in the blood. There are two types of sensors that provide feedback to the respiratory control system, chemical and mechanical, known as chemoreceptors and mechanoreceptors respectively [10], [16]. These inputs play the most important role in adjusting the respiration in terms of tidal volume and the duration of inhalation and exhalation.

There are two types of chemoreceptors: the peripheral chemoreceptors and central chemoreceptors. The peripheral chemoreceptors are located in the aortic and carotid bodies [41], [52], [59]. They sense and react to variations in blood partial pressure of O_2 as well as CO_2; a decrease in the blood partial pressure of oxygen stimulates the carotid sinus nerve which leads to a change in ventilation and brings the oxygen level back to normal [3], [72]. The central chemoreceptors are located in the brainstem and are sensitive to changes in the level of partial pressure of CO_2 and pH in their close environment [21], [26], [33]. The central chemoreceptors are the main respiratory receptors in the breath-by-breath control of ventilation under normal conditions [75]. However, in extreme conditions, O_2 (through the peripheral chemoreceptors) also affects the breath-by-breath control of respiration.

Alongside these chemoreceptors, the mechanoreceptors are responsible for non-chemical respiratory regulation. These receptors are located in the bronchi's wall[1] of the lungs [20]. The response of these sensors is higher with a decrease in lung compliance (measure of the lung's ability to expand and stretch) [76]. During inflation, these sensors become active and send signals to the brainstem via the vagus nerve [22]. There are pure deflation activated receptors, which only respond to deflation of the lungs and are mainly observed in small mammals like mice, cat and rabbit [1], [45], [54].

[1] Bronchi are the tubes through which the air travels to and from the lungs.

The respiratory controllers are located jointly in the region of the medulla oblongata and pons in the brainstem [10], [16], [19], [48], [55]. Studies suggest that the respiratory neurons have a dense population in three centers: (1) the dorsal respiratory group (DRG) which is located in a dorsal portion of the medulla, (2) the ventral respiratory group (VRG) located in ventrolateral portion of the medulla , and (3) the pontine respiratory region (PRG) located in pons [10], [30]. All together, the DRG, VRC and PRG create the central pattern generator (CPG) of respiration [44], [68]. They receive signals from respiratory related mechanoreceptors and chemoreceptors, adjust the breathing pattern and send signals to the motor nerves to generate movement of the respiratory muscles [18], [71].

Mathematical modelling of the respiratory system started after World War II, during which many fields of science and technology have emerged. One of them was control theory which later was used to study the quantitative nature of ventilation control. Gray [27] introduced the first model in which the controller as well as the controlled system were considered as black boxes and the system was restricted to a static view (steady state). This formed a simple relationship between lung ventilation and partial pressures of O_2 and CO_2 in the arteries.

The first dynamical control model of the respiratory system was proposed by Grodin et al. [29], where the arterial CO_2 was considered as a respiratory regulator and a variation in it affected the minute ventilation. In 1967, Grodin et al. [28] upgraded their previous model by introducing several sources of delay along with cerebral blood flow and cerebrospinal fluid (CSF) compartment that exhibited the effects of pH on ventilation. This upgraded model was tested for a few different scenarios such as the increased inspired fraction of CO_2, exercise test and holding the breath. Mixed results were achieved in general, but the result of the exercise test did not match the experimental observations. Saunders et al. [67] modified the model of [28] by incorporating cyclic ventilation, variable lung volume, dead space volume, a blood shunt and a different equation of the controller along with the elimination of CSF compartment. In 1999, Cabera et al. [12] presented a model with four compartments including an alveolar compartment and different tissue compartments such as skeletal muscle (muscles in the lower extremities), splanchnic (e.g. liver, stomach and intestines) and other tissues (which include the heart,

brain, and the rest of the tissues). The model used the same ventilation controller equations as those developed by [28] and [67]. Farhi and Rahn [23] proposed a model of CO_2 storage, in which the total CO_2 of the body was stored in four compartments and connected through the circulation of blood. This model expressed more accurately the impact of variation in ventilation on the stored CO_2 at steady state. However, during the initial few minutes of either hyperventilation or apnea (pauses in breathing), the rate of change of CO_2 was higher than those predicted by other studies [14], [25]. A model with a nonlinear controller was used to study the stability properties of the respiratory control system [40]. The model included two compartments: lumped body tissues and lungs, which were connected by the blood circulation. In 1991, this model was upgraded to stimulate breathing during sleep [39]. The Grodin model was still used recently [58].

While the Grodin model evolved, other envelopments were taking place. The publication of the Hodgkin Huxley model in 1952 [36] revolutionized the field of physiology by introducing electro-physiology and modelling at the neural level. More details about the respiratory neural network were discovered and models of the respiratory central pattern generator (CPG) were developed. Of note is the discovery of the Pre-Bötzinger Complex [70]- a population of excitatory neurons that are essential for breathing. Models of the neural circuitry range from 3 equations [11] to hundreds of equations [64], [65]. See [2], [24], [60] and [61] for a review of the different models developed at the neural level. There were a few attempts to couple the models at the neural level with models of the lungs [7], [8], [49]. However, none of these models can control both frequency and amplitude of breathing in response to inputs from all the chemoreceptors and mechanoreceptors. For example, in [8], amplitude is controlled in response to changes in O_2 and CO_2 but there is no control of frequency. While in [7] there is control of amplitude and frequency but only in response to changes in CO_2. One of the difficulties in coupling mechanical models of the lungs to models of the neural circuitry is our lack of understanding of why a particular combination of breathing frequency and amplitude is selected by the neural system.

This thesis is motivated by the need to understand how the respiratory CPG regulates the breathing amplitude and frequency . Early and recent models that treated the respiratory CPG as a black box provided some useful insights about the res-

piratory system but did not distinguish between the frequency and amplitude of breathing; instead they considered minute ventilation as a control variable. This prevents the use of studies at the neural level which found that there is separate control of amplitude and frequency of breathing. Observations of the breathing response to changes in O_2 and CO_2 concentrations led physiologists to look out for criteria by which the body sets a particular breathing frequency and amplitude. We discuss these studies in the next section.

1.2 Optimization of the Respiratory System

Rohrer [62] was one of the first to indicate that the frequency of breathing may be selected by minimizing the mechanical respiratory work rate with the assumptions of passive expiration, equal durations of inspiration and expiration and constant flow rate during inhalation. He used a simple lung model in which the relationship between the respiratory pressure and volume is given by:

$$P_{rs} = E_{rs}\, V + R_{rs}\, \dot{V} \tag{1.1}$$

where, P_{rs} represents the respiratory pressure required for breathing. V represents the lung's volume. E_{rs} and R_{rs} represent the respiratory elastance and resistance to airflow respectively. Rohrer developed the following formula for the work rate (energy consumption per unit time) of the respiratory muscles during inhalation:

$$WR_{Rohrer} = \left(\frac{E_{rs}}{2f} + 2R_{rs}\right)\left(\dot{V}_A + f V_D\right)^2 \tag{1.2}$$

where $\dot{V}_A$, V_D and f are the alveolar minute ventilation (the amount of air involved in gas exchange per minute), dead space volume and respiratory frequency respectively. The values obtained by minimizing Eq. (1.2) were similar to human resting breathing frequency. Otis. et al. [53] added non-linear resistance into the model in Eq. (1.1) and represented it as:

$$P_{rs} = E_{rs}\, V + R_{rs}\, \dot{V} + Q_{rs}\, \dot{V}^2 \tag{1.3}$$

where Q_{rs} represents the respiratory resistance due to turbulence. By considering a sinusoidal airflow pattern, this gave the following mathematical expression for

the work rate during inhalation for a given constant alveolar ventilation [53]:

$$WR_{Otis} = \left(\frac{E_{rs}}{2f} + \frac{\pi^2}{4}R_{rs}\right)\left(\dot{V}_A + fV_D\right)^2 + \frac{2\pi^2}{3}Q_{rs}\left(\dot{V}_A + fV_D\right)^3 \tag{1.4}$$

The optimal breathing frequency that minimizes Eq. (1.4) was again consistent with observations. The work rate criterion was confirmed by observations during light exercise [46], however, Mead [47] found that the work rate criterion did not explain the variations in breathing frequency during light to severe exercise. So, he came up with a new criterion − that the optimal frequency is close to that which minimizes the average force developed by the respiratory muscles. By considering a sinusoidal airflow and the resistance due to turbulence, he found the following formula for the optimal frequency :

$$f_{Mead} = \left(\frac{\dot{V}_A}{V_D}\right)^{1/3}\left(\frac{E_{rs}}{2\pi R_{rs}}\right)^{2/3} \tag{1.5}$$

The optimal frequency from the above expression is slightly higher than that which optimizes Eq. (1.4). Mead found that the frequency from Eq. (1.5) is close to human breathing frequency at all levels of exercise. This gave a better prediction for breathing frequency than work rate mainly during exercise.

It was also suggested that neither the pressure integral nor the mechanical work are individually minimized over an inspiration. This means that the optimization criterion may involve the weighted sum of energy expenditure and work [4]. It was believed that the quick variations in the rate of airflow might have certain harmful effects. The weighted criterion sum was introduced as [31]:

$$J(\dot{V}_A) = \int_0^{T_i}\left[\ddot{V}_A^2 + \theta_1 P_{rs}\dot{V}_A\right]dt + \int_{T_i}^{T}\left[\ddot{V}_A^2 + \theta_2 P_{rs}^2\right]dt \tag{1.6}$$

where θ_1 and θ_2 represent the weights; T and T_i are the durations of inhalation and whole breath respectively. In Eq. (1.6), the criterion for inspiration consists of the weighted sum of the square of the alveolar acceleration and the mechanical work produced by the respiratory muscles during inhalation while during expiration, the term of mechanical work was substituted by the integral square of the driving pressure. The cost function of inspiration was modified further by adding a term that was responsible for the efficiency loss of gas exchange with muscular load [32].

It was suggested that an optimum controller might balance the energetic needs with metabolic needs of the body [57].

In all of these studies, a simple lung model was used (see Eq. (1.1)) where the function of gas exchange was not involved directly (instead, effective minute ventilation was used). In our study, we consider more detailed lung models, which can calculate how a variation in breathing frequency leads to a change in alveolar gas concentrations. The use of more detailed lung models requires a new definition of the optimization problem which we introduce in Chapter 3. We then solve the newly defined optimization problem directly (i.e. for a given driving function) similar to what has been done before. In Chapter 4 and 5, we search for an optimal "driving function", i.e. we do not assume a particular shape of this function. This signifies another difference between our work and previous studies and also requires the development of new methodologies for solving the optimization problem. In the following sections we describe the lung models we use that have already been published in the literature. We then review the literature for solving an optimal driving function.

1.3 A 6D Lung Model

In our study, we consider a flexible lung model with gas exchange and gas transport developed by Ben-Tal [5]. It includes both mechanical (pressure, volume and airflow) and chemical (level of carbon dioxide and oxygen) components of the respiratory system. In the flexible model, the airways are represented by a single pipe with resistance R. The alveolar region is considered as a container with a moving plate as shown in Fig. 1.1 (a). Gas exchange and gas transport are modelled by a 'conveyor' model, shown in Fig. 1.1 (b), in which the transit time of blood in the lungs (where gas exchange takes place) is the same as the interval between two consecutive heart beats. The system of differential equations for the 6D lung

model is [5]:

$$\frac{dP_A}{dt} = \frac{E}{R}(P_m - P_A) + \frac{dP_L}{dt} \tag{1.7}$$

$$\frac{df_c}{dt} = \frac{1}{V_A}\left[D_c\left(p_c - p_{ac}\right) + \left(f_{ci} - f_c\right)q_i - f_c\left(D_o\left(p_o - p_{ao}\right) + D_c\left(p_c - p_{ac}\right)\right)\right] \tag{1.8}$$

$$\frac{df_o}{dt} = \frac{1}{V_A}\left[D_o\left(p_o - p_{ao}\right) + \left(f_{oi} - f_o\right)q_i - f_o\left(D_o\left(p_o - p_{ao}\right) + D_c\left(p_c - p_{ac}\right)\right)\right] \tag{1.9}$$

$$\frac{dp_c}{dt} = \frac{D_c}{C_u\sigma_c V_c}(p_{ac} - p_c) + \frac{\delta l_2}{\sigma_c}hz + \delta r_2 p_c \tag{1.10}$$

$$\frac{dp_o}{dt} = \frac{D_o}{C_u\sigma V_c}\left(1 + \frac{4T_h}{\sigma}\frac{dS(p_o)}{dp_o}\right)^{-1}(p_{ao} - p_o) \tag{1.11}$$

$$\frac{dz}{dt} = \delta r_2\sigma_c p_c - \delta l_2 hz \tag{1.12}$$

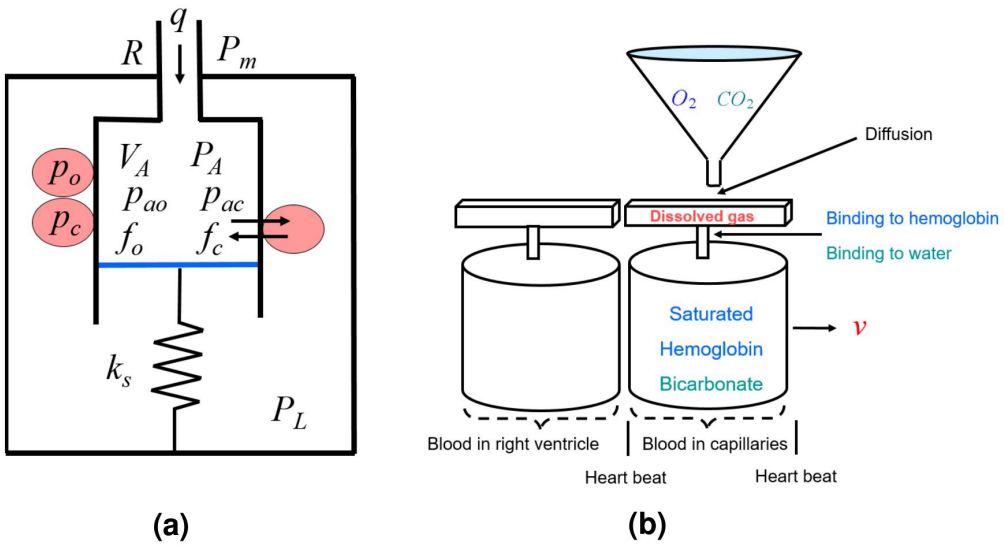

Fig. 1.1: Schematic description of the 6D model. (a) The lung is assumed to be a single container with a moving plate. (b) Blood transport is modelled as a conveyor model. R−overall resistance to airflow; k_s−spring constant (lung elastance, E, is equivalent to k_s/s^2, where s is the area of moving plate), q−airflow. P_A−pressure in the lung, P_m−pressure at the mouth. f_o and f_c are the concentrations of O_2 and CO_2 in the alveoli. p_{ao} and p_{ac} are the partial pressures of O_2 and CO_2 in the alveoli. p_o and p_c are the partial pressures of O_2 and CO_2 in the blood [5].

Where, P_A is the pressure in the alveoli; f_c and f_o are the concentrations of carbon dioxide and oxygen respectively in the alveoli; p_c and p_o represent the blood partial pressures of carbon dioxide and oxygen respectively; z is the blood concentration

of bicarbonate, P_L and P_m are the pleural and mouth pressures respectively (the mouth pressure is assumed to be constant in this study); V_A is the lung's volume. The airflow, q is assumed to be proportional to the pressure difference between the mouth and the alveolar region; p_{ac} and p_{ao} are the alveolar partial pressures of carbon dioxide and oxygen respectively- they are calculated as $p_{ac} = f_c(P_A - p_w)$ and $p_{ao} = f_o(P_A - p_w)$ where p_w is the vapor pressure of water at $37°C$. D_c and D_o are the diffusion capacities of carbon dioxide and oxygen respectively; q_i is the inspired airflow; f_{ci} and f_{oi} are the inspired concentrations of oxygen and carbon dioxide respectively; V_c is the capillary volume; σ and σ_c are the solubility of oxygen and carbon dioxide in plasma respectively; T_h is the concentration of hemoglobin; l_2 is the hydration reaction rate; δ is the acceleration rate; r_2 is the dehydration reaction rate; h is the concentration of hydrogen ions and $S(p_o)$ is the saturation function of hemoglobin. The volume of the lungs V_A is:

$$V_A = \frac{1}{E}(P_A - P_L) \tag{1.13}$$

The airflow, q is:

$$q = \frac{1}{R}(P_m - P_A) \tag{1.14}$$

The inspired concentration of oxygen is:

$$f_{oi} = \begin{cases} f_o & V_T < V_D \\ \frac{1}{V_T}\left(f_o V_D + f_{om}(V_T - V_D)\right) & V_T \geq V_D \end{cases} \tag{1.15}$$

where V_T , V_D and f_{om} are the tidal volume, dead space and the concentration of oxygen in the mouth. By replacing f_{oi} , f_o and f_{om} in Eq. (1.15) by f_{ci}, f_c and f_{cm} respectively we get the inspired alveolar concentrations of carbon dioxide..

The saturation function of hemoglobin is [5], [50]:

$$S\left(p_o\right) = \frac{LK_T\sigma p_o\left(1 + K_T\sigma p_o\right)^3 + K_R\sigma p_o\left(1 + K_R\sigma p_o\right)^3}{\left(1 + K_T\sigma p_o\right)^4 + \left(1 + K_R\sigma p_o\right)^4} \tag{1.16}$$

where L, K_T and K_R are parameters.

The model assumes that after every heartbeat, a new bolus of blood enters the lungs. Therefore, we re-initialize p_o, p_c and z after every heart period, T_L. We

also store the values of p_o and p_c just before the re-initialization as p_{oe} and p_{ce}, where, p_{oe} and p_{ce} represent the partial pressure of O_2 and CO_2 in the arterial blood, which is supplied to the body.

1.4 A $5D$ Lung Model

The $6D$ lung model introduced in the previous section was later reduced by Ben-Tal et al. [6]. This was done by averaging the partial pressure of O_2 (p_o) and CO_2 (p_c) over one heart period. In the $6D$ model, we have to reinitialize the values of p_o and p_c after every heartbeat which makes them discontinuous. The $5D$ model does not require a re-initialization of the blood partial pressures, therefore it is easier to find the optimal breathing pattern by using this model. This model is continuous and smooth during inhalation and exhalation but not necessarily in the transition from inhalation to exhalation.

Let T_L be the transition time of the blood in the lungs, which is also assumed to be the duration between two consecutive heartbeats. The average p_o and p_c during this transition time is represented by $\bar{p}_o = \frac{1}{T_L}\int_0^{T_L} p_o\,dt$ and $\bar{p}_c = \frac{1}{T_L}\int_0^{T_L} p_c\,dt$.

By rearranging Eq. (1.11) and using $\frac{dS}{dp_o}\frac{dp_o}{dt} = \frac{dS}{dt}$, we get:

$$\frac{dp_o}{dt} = \frac{D_o}{C_u \sigma V_c}(p_{ao} - p_o) - \frac{4T_h}{\sigma}\frac{dS(p_o)}{dt} \tag{1.17}$$

By using Eq. (1.10) and (1.12), we have:

$$\frac{dp_c}{dt} = \frac{D_c}{C_u \sigma_c V_c}(p_{ac} - p_c) - \frac{1}{\sigma_c}\frac{dz}{dt} \tag{1.18}$$

Now we integrate both sides of Eq. (1.17) and (1.18) from 0 to T_L and by assuming that the partial pressures of O_2 and CO_2 in the lungs do not change much during this short transition time, the following system of differential equations is obtained

[6]:

$$\frac{d\bar{p}_c}{dt} = \frac{D_c}{C_u \sigma_c V_c}(p_{ac} - \bar{p}_c) + \frac{r_2}{l_2 h T_L}\left[p_{c0} - \bar{p}_c\right] \tag{1.19}$$

$$\frac{d\bar{p}_o}{dt} = \frac{D_o}{C_u \sigma V_c}(p_{ao} - \bar{p}_o) + \frac{4T_h}{\sigma T_L}\left[S(p_{o0}) - S(\bar{p}_o)\right] \tag{1.20}$$

where, p_{c0} and p_{o0} represent the level of partial pressures of CO_2 and O_2 in the blood when it enters the lungs for gas exchnage. The alveolar concentrations of $O_2\left(f_o\right)$ and $CO_2\ \left(f_c\right)$ do not change much during the transition time. Therefore, the differential equations for P_A, f_c and f_o in this model are the same as for the $6D$ model. However, the variables p_c and p_o are replaced by $\bar{p}_c$ and $\bar{p}_o$ respectively in Eq. (1.8) and (1.9) and represented as:

$$\frac{df_c}{dt} = \frac{1}{V_A}\left[D_c\left(\bar{p}_c - p_{ac}\right) + \left(f_{ci} - f_c\right)q_i - f_c\left(D_o\left(\bar{p}_o - p_{ao}\right) + D_c\left(\bar{p}_c - p_{ac}\right)\right)\right] \tag{1.21}$$

$$\frac{df_o}{dt} = \frac{1}{V_A}\left[D_o\left(\bar{p}_o - p_{ao}\right) + \left(f_{oi} - f_o\right)q_i - f_o\left(D_o\left(\bar{p}_o - p_{ao}\right) + D_c\left(\bar{p}_c - p_{ac}\right)\right)\right] \tag{1.22}$$

The differential equations for the $5D$ model, consists of Eq. (1.7) and (1.19) - (1.22). The expression representing the volume of the lungs, airflow and inspired concentration of O_2 and CO_2 are the same as in the $6D$ model (see Eq. (1.13), (1.14) and (1.15)).

1.5 Optimal Control Theory

Optimal control theory of ordinary differential equations was first introduced by Lev Semonovich Pontryagin and his students [56] and is now well known. It is fundamentally an expansion of the classical variation technique of Lagrange, Euler and Hamilton [15]. This method is used to find an optimal controller of a dynamical system in the presence of constraints.
Consider the minimization of

$$W = \int_{t_0}^{t_f} J(t, \mathbf{x}, u)\, dt \tag{1.23}$$

subject to the differential equation:

$$\dot{\mathbf{x}}(t) = \mathbf{g}(t, \mathbf{x}, u) \tag{1.24}$$

with boundary conditions:

$$\mathbf{x}(t_0) = \mathbf{x_0}, \qquad \mathbf{x}\left(t_f\right) = \mathbf{x_f}$$

where $\mathbf{x}$ and u are the state and control variables respectively. Let H be the Hamiltonian of the problem which is:

$$H = J(t, \mathbf{x}, u) + \boldsymbol{\lambda}^{\top}(t)\, \mathbf{g}(t, \mathbf{x}, u) \tag{1.25}$$

where $\boldsymbol{\lambda}(t)$ is an unknown adjoint vector function, also known as Lagrange multiplier. By substituting Eq. (1.25) into Eq. (1.23) we get:

$$W = \int_{t_0}^{t_f} \left(H - \boldsymbol{\lambda}^{\top}(t)\, \dot{\mathbf{x}}(t)\right) d\, t \tag{1.26}$$

If t_0 and t_f are fixed and the system of differential equations is continuous, the optimization problem can be transformed into a boundary value problem of an augmented set of differential equations [56], [43]. The augmented set of differential equations is:

$$\dot{\lambda_i}(t) = -\frac{\partial H}{\partial x_i} \tag{1.27}$$

where, λ_i is the Lagrange multiplier asociated with state variable x_i.

The optimization problem can also be solved when the terminal time is free [42], [73] and the state variables are fixed and/or free at the initial and terminal times ($\mathbf{x_0}$ and/or $\mathbf{x_f}$ are fixed and/or free) [42], [73] . The constrains can also be augmented by adding an algebraic constraint (i.e. the control and state variables satisfy an algebraic relationship) [9], [42] and an interior point constraint (a state variable has a particular value at some point of time between the initial and terminal times) [9], [34], [74], [17]. The optimization problem can also be solved if the system of differential equations is piecewise continuous with fixed and free time durations [37].

The idea of optimal control theory was used to study the breathing pattern. By

considering a simple lung model (Eq. (1.1)) and minimizing the work of breathing, the airflow pattern during inhalation was found to be constant [77]. Similarly, another study [63] showed that when the work rate was taken as a cost function, the optimal flow was a constant. The same study also investigated minimizing the average force and found that there was no optimal solution for a constant resistance. However, the optimal air flow had a triangular shape (i.e. it increased linearly with time during inspiration) for a dynamic resistance when Q_{rs} was included (see Eq. 1.3) [63]. When the work was optimized and the resistance to flow was taken as nonlinear (Eq. 1.3), an optimal ratio between the inhalation and exhalation durations satisfied the following cubic equation [38]:

$$\left(\frac{T_I}{T_E}\right)^3 - \frac{R_I}{R_E + \left(\frac{2Q_E V_T}{T_E}\right)}\left(\frac{T_I}{T_E}\right) - \frac{Q_I}{Q_E + \left(\frac{R_E T_E}{2V_T}\right)} = 0 \tag{1.28}$$

Here, subscripts I and E represent the parameters and variables during inhalation and exhalation respectively. T is the time duration, R and Q represent the resistance to airflow and resistance to turbulent flow respectively, and V_T is the tidal volume. By ignoring the resistance to turbulent flow ($Q_I = Q_E = 0$) and assuming that the resistance to airflow is the same during inhalation and exhalation ($R_I = R_E > 0$), then the solution of Eq. (1.28) shows that the durations of inhalation and exhalation are the same.

All the studies described in this section, where the optimal breathing pattern (optimal shape of driving force) was found, have used a $1D$ linear model for the lungs in which gas exchange was not taken into account directly. In most of the studies, the duration of inhalation and exhalation was considered as a fixed constant value. Compared with more general optimal problems that have been solved in the past, our problem has some additional difficulties. Our system of differential equations is piecewise and the transition between phases is defined by the rate of change of one of the state variables. Additionally, one of the parameters in the model (the tidal volume) as well as the time durations are part of the optimization problem. We therefore had to develop some new methodologies for solving the optimization problem which we describe in Chapter 4.

1.6 Conclusions

Physiological levels of oxygen and carbon dioxide in the blood are tightly regulated. This is mainly done by varying the frequency and amplitude of breathing. Early models of respiratory control treated the system as a black box model, where minute ventilation (the amount of inhaled air per minute) was taken as the controlled variable. This did not provide a distinction between frequency and amplitude of breathing because the same minute ventilation can be achieved by various combinations of frequency and amplitude. Studies of breathing control at the neural circuitry level found that there are distinct mechanisms for controlling the amplitude and frequency of breathing. However, why a specific combination of breathing frequency and amplitude is observed, remains a mystery. This thesis explores the hypothesis that the observed combination of breathing frequency and amplitude is optimal with respect to some objective function. Different objective functions were studied previously such as the work rate and the average force developed by the respiratory muscles during inhalation; all used $1D$ models. In this thesis, we consider higher dimension models that reflect more accurately the coupling between lung mechanics and gas exchange. We reviewed two previously published models, which we will use in this thesis, labelled as the $6D$ model (see Section 1.3) and the $5D$ model (see Section 1.4). We present in Chapter 2 other models we will use in this thesis that have not yet been published. These are simplifications of the $5D$ model and a slight modification of the $6D$ model. The use of more detailed lung models requires a new definition of the optimization problem, which we present in Chapter 3. We also show in Chapter 3 solutions of the optimization problem when the driving force is a given function. Following previous studies (see Section 1.2), we solve the problem for a sinusoidal driving force. We go further by comparing solutions for other driving functions. The optimization problem is more difficult when the driving force is not given. In Section 4.1, we reviewed methods for solving similar optimization problems using ideas from optimal control theory. Our problem has additional difficulties as the system of differential equations contains piecewise nonlinear equations with a few of the parameters (tidal volume, and the durations of inhalation and exhalation) that are unknown. This requires the development of new methodologies for solving the optimization problem, which we present in Chapter 4. We also show in Chapter 4 an analytical solution of the optimization problem for a 2D piecewise linear

model and a numerical algorithm we developed and used to solve the optimization problem when the objective function is the work of breathing. The methodology developed in Chapter 4 is used in Chapter 5 to solve the optimization problem for other objective functions.

Chapter 2

Lung Models

The respiratory system is a highly complex control system and it is very difficult to define or explain its behavior without the aid of some form of a mathematical model. In this thesis, we use several models that represent the respiratory system at various degrees of complexity. Some of these models have been published before and have already been described in detail (see Sections 1.3 and 1.4). In this chapter, we discuss additional modifications of the $6D$ model. First we show how we couple the $6D$ model to a neural signal. We then discuss a reduction of the $5D$ model to $3D$ and $2D$ models. A summary of all the models we use in this thesis is given in Fig. 2.3.

2.1 Coupling a Neural Signal with the $6D$ Model

To represent the pleural pressure more accurately, we couple the the $6D$ model (see Section 1.3) with a representation of a neural signal. Fig. 2.1 shows a schematic description of the coupled model. In this model the brainstem transmits an electric signal to generate contraction of the respiratory muscles. We assume that at the muscle level, the force generator is in the waveform shown in Fig. 2.1 and depicted by $R_p(t)$ (this mimics a "ramp signal"). The ramp signal enables us to generate a more realistic pleural pressure with inspiration time different from expiration time.

The movement of the muscles x_m is modelled by [7]:

$$\frac{dx_m}{dt} = -k_1 x_m + k_2 R_p(t) \tag{2.1}$$

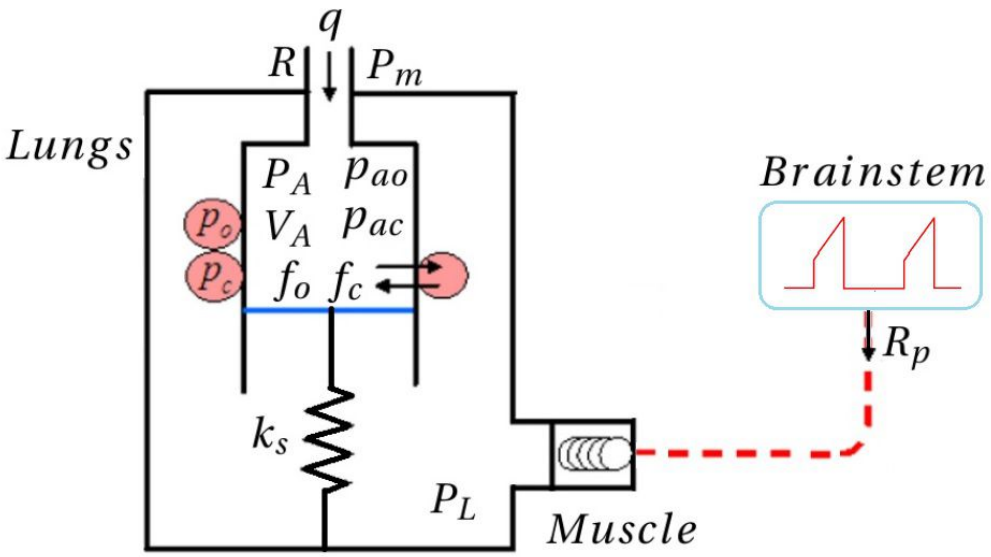

Fig. 2.1: Coupling a neural signal with the 6D model. R_p is a representation of ramp signal from the brainstem. All other symbols have been described in Fig. 1.1.

and the pleural pressure, P_L is taken as [7]:

$$P_L = P_m - P_{L0} - k_p x_m \tag{2.2}$$

where P_m and P_{L0} represent the pressure at the mouth and the pressure difference that normally exists between the pleural cavity and the atmospheric pressure respectively. k_1 represents the recoil rate constant of muscles whereas k_2 and k_p are conversion constants. The other equations of the 6D model are unchanged and are given in Section 1.3 (see Eq. 1.7 to 1.12).

Under normal conditions, the brainstem sends a signal to the breathing muscle during inhalation only. We assume that the ramp signal starts with amplitude k_n and increases linearly as shown in Fig. 2.2. The parameter k_n is also a control parameter that changes the amplitude of the pleural pressure [7]. We also assume that the rate of increase of the ramp signal during inhalation, α, is constant and is independent of other parameters.

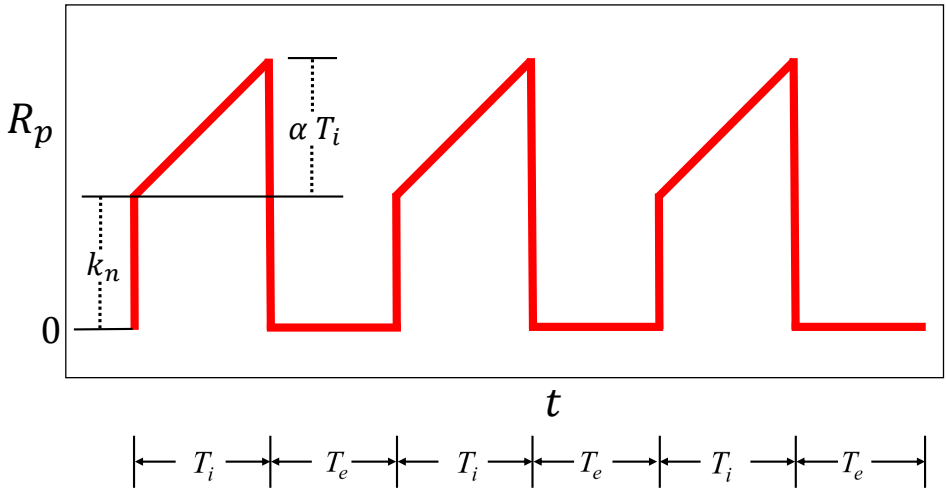

Fig. 2.2: The ramp signal, R_p. T_i and T_e are the durations of inhalation and exhalation respectively

The ramp signal $R_p(t)$ is:

$$R_p = \begin{cases} k_n + \alpha t & 0 \le t \le T_i \\ 0 & T_i < t \le T \end{cases} \tag{2.3}$$

By solving Eq. (2.1), the muscle movement becomes:

$$x_m = \begin{cases} (x_{m0} - A)\, e^{-k_1 t} + A + B t & 0 \le t \le T_i \\ \left((x_{m0} - A)\, e^{-k_1 T_i} + A + B T_i\right) e^{-k_1 (t - T_i)} & T_i < t \le T \end{cases} \tag{2.4}$$

where, $x_{m0} = \frac{\left(-A e^{-k_1 T_i} + A + B T_i\right) e^{-k_1 (T - T_i)}}{1 - e^{-k_1 T_i}}$, $B = \frac{k_2 \alpha}{k_1}$ and $A = \frac{k_2 k_n - B}{k_1}$. T and T_i represent the breathing period and the duration of inhalation respectively. The plueral pressure can then be written as:

$$P_L = P_m - P_{L0} - k_p \begin{cases} (x_{m0} - A)\, e^{-k_1 t} + A + B t & 0 \le t \le T_i \\ \left((x_{m0} - A)\, e^{-k_1 T_i} + A + B T_i\right) e^{-k_1 (t - T_i)} & T_i < t \le T \end{cases} \tag{2.5}$$

2.2 Reduction of the $5D$ Model

The aim of model reduction is to replace a high dimensional model with a simpler model that contains the essence of the original behavior under study. Therefore by solving a simpler model one can still observe the behavior of the original model. In this section, we discuss the reduction of the $5D$ model to $3D$ and $2D$ models.

2.2.1 $3D$ Models

By using Eq. (1.13) and Eq. (1.7), we get:

$$\frac{dV_A}{dt} = -\frac{E}{R}V_A + \frac{1}{R}\Big(P_m - P_L\Big) \tag{2.6}$$

Following [6], Assume that the rate of change of the alveolar volume represents the airflow $\left(q = \dot{V}_A\right)$ and the respiratory exchange ratio is one, that is $D_o\left(p_o - p_{ao}\right) = -D_c\left(p_c - p_{ac}\right)$. This assumption decouples the components of CO_2 and O_2 in the model, therefore, Eq. (1.21) and (1.22) become

$$\frac{df_c}{dt} = \frac{1}{V_A}\left[D_c\left(\bar{p_c} - p_{ac}\right) + \left(\frac{V_T - V_D}{V_T}\right)\left(f_{cm} - f_c\right)\dot{V}_{Ai}\right] \tag{2.7}$$

and

$$\frac{df_o}{dt} = \frac{1}{V_A}\left[D_o\left(\bar{p_o} - p_{ao}\right) + \left(\frac{V_T - V_D}{V_T}\right)\left(f_{om} - f_o\right)\dot{V}_{Ai}\right] \tag{2.8}$$

where, $\dot{V}_{Ai} = \begin{cases} \dot{V}_A(t) & ; \quad \dot{V}_A(t) > 0 \\ 0 & ; \quad \dot{V}_A(t) \leq 0 \end{cases}$

As we have $p_{ac} = f_c(P_A - p_w) = f_c(EV_A + P_L - p_w)$, $p_{ao} = f_o(EV_A + P_L - p_w)$ and $f_{cm} = 0$, we get:

$$\frac{df_c}{dt} = -D_c f_c\left[E + \frac{(P_L - p_w)}{V_A}\right] + D_c\frac{\bar{p_c}}{V_A} - \frac{f_c}{V_A}\left(\frac{V_T - V_D}{V_T}\right)\dot{V}_{Ai} \tag{2.9}$$

and

$$\frac{df_o}{dt} = -D_o f_o\left[E + \frac{(P_L - p_w)}{V_A}\right] + D_o\frac{\bar{p_o}}{V_A} + \frac{\left(f_{om} - f_o\right)}{V_A}\left(\frac{V_T - V_D}{V_T}\right)\dot{V}_{Ai} \tag{2.10}$$

Eq. (2.6), (2.9) and (1.19) represent the 3D model that explains the variation in the level of CO_2 in the lungs and blood during gas exchange, whereas Eq. (2.6), (2.10) and (1.20) represent the 3D O_2 model. These models are similar to a model described in [6]. The difference is that here we assume that the airflow is equal to the rate of change of the alveolar volume ($q = \dot{V}_A$). Another difference is that Eq. (2.6) describes the rate of change of the alveolar volume rather than the rate of change of the alveolar pressure as is done in [6].

2.2.2 2D Models

Let us assume that the blood flow in the lungs is so fast that there are no changes in the level of partial pressures of CO_2 and O_2 in the blood during gas exchange. This assumption further reduces the dimension of the models. Let $\bar{\bar{p}}_c$ and $\bar{\bar{p}}_o$ represent the constant value of the partial pressure of CO_2 and O_2 respectively. This gives:

$$\frac{df_c}{dt} = -D_c f_c \left[E + \frac{(P_L - p_w)}{V_A} \right] + D_c \frac{\bar{\bar{p}}_c}{V_A} - \frac{f_c}{V_A} \left(\frac{V_T - V_D}{V_T} \right) \dot{V}_{Ai} \tag{2.11}$$

and

$$\frac{df_o}{dt} = -D_o f_o \left[E + \frac{(P_L - p_w)}{V_A} \right] + D_o \frac{\bar{\bar{p}}_o}{V_A} + \frac{\left(f_{om} - f_o\right)}{V_A} \left(\frac{V_T - V_D}{V_T} \right) \dot{V}_{Ai} \tag{2.12}$$

where, $\dot{V}_{Ai} = \begin{cases} \dot{V}_A(t) & ; \quad \dot{V}_A(t) > 0 \\ 0 & ; \quad \dot{V}_A(t) \leq 0 \end{cases}$

Eq. (2.6) and (2.11) form the 2D non-linear model , which represents the variation in the level of CO_2 in the lungs during gas exchange. Similarly, Eq. (2.6) and (2.12) represent the variation in the level of O_2.

We now assume that the oscillations in $\frac{(P_L - p_w)}{V_A}$, $\frac{\bar{p}_c}{V_A}$, $\frac{f_c}{V_A}$, $\frac{\bar{p}_o}{V_A}$ and $\frac{(f_{om} - f_o)}{V_A}$ are relatively small compared to their average values. By taking these ratios as constant we eliminate the non-linearity from the 2D models. Let $\frac{(P_L - p_w)}{V_A} = K_1$, $\frac{\bar{p}_c}{V_A} = K_2$, $-\frac{f_c}{V_A} = K_3$, $\frac{\bar{p}_o}{V_A} = K_4$ and $\frac{(f_{om} - f_o)}{V_A} = K_5$, we get:

$$\frac{df_c}{dt} = -D_c f_c (E + K_1) + D_c K_2 + K_3 \left(\frac{V_T - V_D}{V_T} \right) \dot{V}_{Ai} \tag{2.13}$$

and

$$\frac{df_o}{dt} = -D_o f_o (E + K_1) + D_o K_4 + K_5 \left(\frac{V_T - V_D}{V_T} \right) \dot{V}_{Ai} \tag{2.14}$$

Eq. (2.6) and (2.13) (or (2.14)) represent the $2D$ linear model of gas exchange for CO_2 (or O_2) in the lungs (here we assume that V_T is constant). By using the transformations $Y_c = D_c f_c (E + K_1) - D_c K_2$ and $Y_o = D_o f_o (E + K_1) - D_o K_4$, we can rewrite the $2D$ linear model in the form:

$$\frac{dY_c}{dt} = -D_c (E + K_1) Y_c + D_c (E + K_1) K_3 \left(\frac{V_T - V_d}{V_T} \right) \dot{V}_{Ai} \tag{2.15}$$

and

$$\frac{dY_o}{dt} = -D_o (E + K_1) Y_o + D_o (E + K_1) K_5 \left(\frac{V_T - V_d}{V_T} \right) \dot{V}_{Ai} \tag{2.16}$$

Now let $F = \dfrac{P_m - P_L}{R}$, $\alpha = \dfrac{E}{R}$, $\beta = D_c (E + K_1)$ and $\gamma = D_c (E + K_1) K_3$, therefore we have:

$$\dot{V}_A (t) = -\alpha V_A (t) + F (t) \tag{2.17}$$

$$\dot{Y}_c (t) = -\beta Y_c (t) + \begin{cases} \gamma \left(\frac{V_T - V_D}{V_T} \right) \dot{V}_A (t) & ; \quad \dot{V}_A (t) > 0 \\ 0 & ; \quad \dot{V}_A (t) \leq 0 \end{cases} \tag{2.18}$$

If we assume that T is the period of $F(t)$, that is $F(t + T) = F(t)$ for all T and $T_i \in (0, T)$ such that V_A is strictly increasing in the interval $(0, T_i)$ and strictly decreasing in the interval (T_i, T) then equation (2.18) can be expressed as:

$$\dot{Y}_c (t) = -\beta Y_c (t) + \begin{cases} \gamma \left(\frac{V_T - V_D}{V_T} \right) \dot{V}_A (t) & ; \quad 0 < t \leq T_i \\ 0 & ; \quad T_i < t \leq T \end{cases} \tag{2.19}$$

and we add two more boundary values for $V_A(t)$: $V_A(T_i) = V_T + B$ and $V_A(T) = B$, where B represents the volume at the end of expiration. When we substitute actual values, we get α and $\beta > 0$ and $\gamma < 0$.

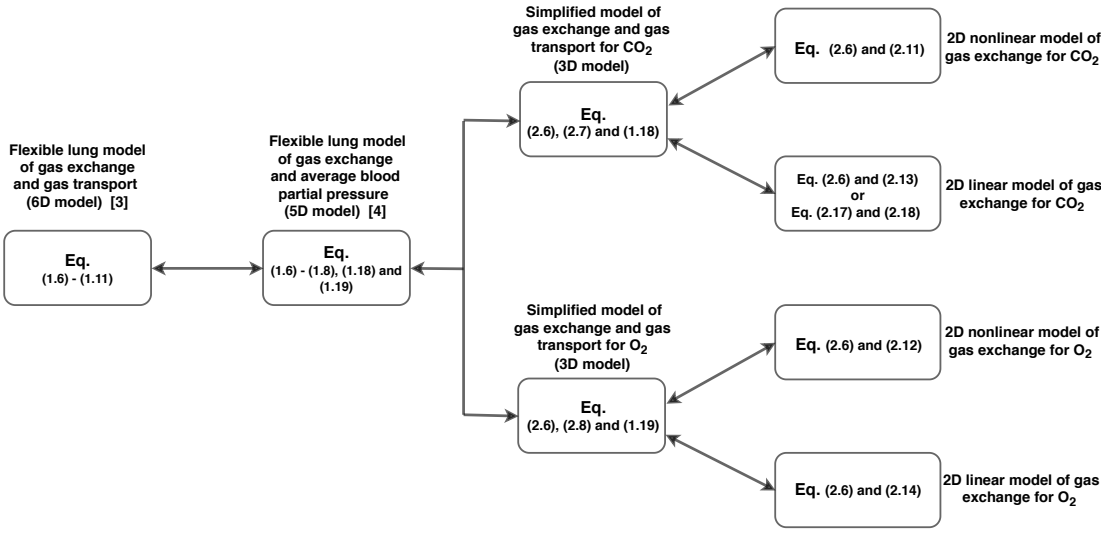

Fig. 2.3: A summary of the models used in this thesis.

2.3 Checking the Assumptions We Made

In sectiom 2.3, we have reduced the $5D$ model to the $3D$ and $2D$ models by using some assumptions. In this section, we discuss the effect of those assumptions on the variables. For this, we consider the pleural pressure as a sinusoidal [5]:

$$P_L = P_m - R\omega\frac{V_T}{2}\sin(\omega t) - E\left(B - \frac{V_T}{2}\right)\cos(\omega t) \tag{2.20}$$

Now we solve the $5D$ model by using the sinusoidal pleural pressure defined above. We computed $\frac{P_L - p_w}{V_A}$, $\frac{f_{om} - f_o}{V_A}$, $\frac{\bar{p}_o}{V_A}$, $\frac{f_c}{V_A}$ and $\frac{\bar{p}_c}{V_A}$. Fig. 2.4 shows the variation in these ratios over time for the $5D$ model, we have observed that the variations in these ratios are within 5% of their average values.

For the $2D$ model, we consider these ratios as constants and take their average values. Fig. 2.5 shows a comparison of the $5D$ and the $2D$ models. It shows that the average values of f_c for the $5D$ and $2D$ models are close to each other for the same tidal volume (V_T) and breathing frequency (f).

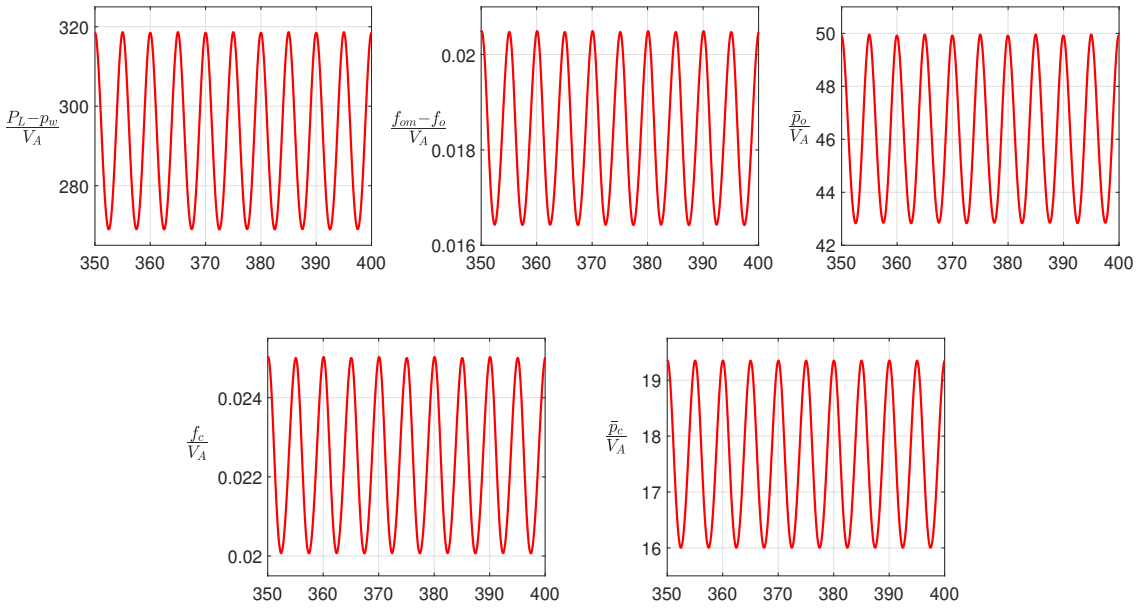

Fig. 2.4: Variations in ratios over time for the $5D$ model using a sinusoidal P_L, when $V_T = 0.4\ l$ and $f = \frac{12}{60}\ s^{-1}$.

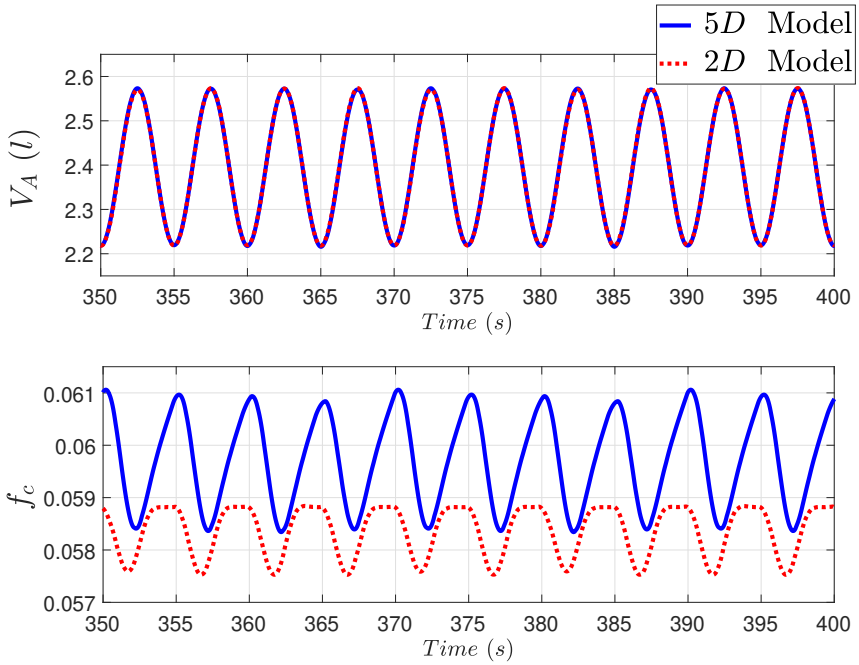

Fig. 2.5: Comparison of the solution of V_A and f_c for the $5D$ and $2D$ models for a sinusoidal P_L, when $V_T = 0.4\ l$ and $f = \frac{12}{60}\ s^{-1}$.

Chapter 3

Optimization Problem

Breathing frequency and amplitude are regulated so that gases levels in arterial blood are maintained at physiological levels. It is therefore natural to raise the question under what criteria the system selects a particular combination. In this chapter, we explore the hypothesis that the selected combination of frequency and amplitude of breathing is an optimal solution. First, we define the optimization problem in general and when the shape of the driving force for breathing is given. We then solve the optimization problem with the predefined driving force for the $6D$ and $2D$ models.

3.1 General Formulation of the Optimization Problem

The aim of this study is to find the optimal combination of breathing frequency (f) and amplitude (V_T) that minimizes some cost function (CF), with certain constraints.

$$\min_{f,V_T} \; CF \tag{3.1}$$

subject to:

(i) The model equations are satisfied.

(ii) The system is at steady state. For our purpose this means periodic with period T.

(iii) The average value of one or two variables at steady state are constants.

In the $2D$ linear model, constraint (iii) refers to the average value of Y_c (or Y_o) over one period, which is maintained at a constant given value, Y_{av},

$$Y_{av} = \frac{1}{T}\int_0^T Y_c(t)\, dt \tag{3.2}$$

The variable Y_c provides a measure of CO_2 concentration in the lungs (recall that $Y_c = D_c(E+K_3)f_c - D_cK_1$, where, f_c is the concentration of CO_2 in the lungs). Similarly, Y_o provides a measure of O_2 concentration in the lungs. In the $6D$ model, constraint (iii) refers to the average values of partial pressures of O_2 and CO_2 in arterial blood which are maintained constant at steady state. This reflects the observation that the breathing pattern tightly regulates the blood levels of O_2 and and in particular the levels of CO_2.

Solving the optimization problem using the $6D$ model is too difficult, so we address it instead in two steps. First, we compute the combinations of frequency and amplitude of breathing that maintain specific level of gases in the blood. Then, we substitute the calculated values into the given cost function and find its minimum.

Step 1: We compute the combinations of breathing frequency and amplitude that minimize a new cost function: $\chi_1\left[\frac{S(\bar{p}_{oe})-S(p_o^\star)}{S(\bar{p}_o^\star))}\right]^2+\chi_2\left[\frac{p_{ce}-p_c^\star)}{p_c^\star)}\right]^2$, where $\bar{p}_{oe}\left(\frac{1}{t}\int_0^t p_{oe}d\tau\right)$ and $\bar{p}_{ce}\left(\frac{1}{t}\int_0^t p_{ce}d\tau\right)$ are the averages of p_{oe} and p_{ce} respectively over a long time, $p_o^\star$ and $p_c^\star$ represent the fixed level of partial pressure of oxygen and carbon dioxide respectively which we try to maintain and $S(\bar{p}_{oe})$ represents the saturation function of hemoglobin at $\bar{p}_{oe}$. It is observed that the ventilation of breathing is more sensitive towards p_{ce} than to p_{oe}, that is why we have used the saturation function of hemoglobin in our cost function instead of partial pressure of oxygen directly. The constants χ_1 and χ_2 represent the weights for maintaining the level of O_2 and CO_2 in the arterial blood. In order to maintain the specific level of p_{oe} only, we need to substitute $\chi_1 = 1$, $\chi_2 = 0$, and $\chi_1 = 0$, $\chi_2 = 1$ for maintaining the level of p_{ce} only.

We minimize this new cost function subject to the following constraints:

(a) The system of differential equations (1.7 – 1.12) is satisfied.

(b) The system is at steady state with period T.

(c) p_{oe} and p_{ce} have constant average values at steady state, $\bar{p}_{oe} = \frac{1}{T}\int_0^T p_{oe}dt$ and $\bar{p}_{ce} = \frac{1}{T}\int_0^T p_{ce}dt$.

Step 2: We solve Expression (3.1) using the specific combinations of frequency and amplitude we found in Step 1 and compute the optimal combination among them that minimizes the mechanical cost of breathing. So,

$$\min_{f,V_T} \; CF \tag{3.3}$$

Subject to the combinations of breathing frequency and amplitude from **Step 1**.

Our study is in two parts. In this chapter, we solve the optimization problem as defined in expression 3.1 directly by providing the shape of the driving force ($P_L(t)$ for the 6D model and $F(t)$ for the 2D model) following Steps 1 and 2. In Chapter 4, we find the optimal trajectory of the driving force by using ideas from optimal control theory.

3.2 Direct Calculation Using the 6D Model

In this section we consider two different representations of the pleural pressure: a sinusoidal function and a function that mimics the result of neural excitation.

3.2.1 Sinusoidal Pleural Pressure

The breathing of mammals is periodic in nature, hence, we consider the pleural pressure as a sinusoidal function:

$$P_L = P_m - P_{L0} - \frac{A}{2}\left[1 - \cos(\omega t + \phi)\right] \tag{3.4}$$

where P_m is the mouth pressure, P_{L0} is the pressure difference that generally exists between the mouth and the pleural cavity, A is the amplitude of the pleural pressure and ϕ is a phase shift. After substituting P_L into Eq. (1.7) and solving the differential equation at steady state, we get:

$$P_A(t) = P_m + \frac{AR\omega}{2(E^2 + R^2\omega^2)}\left[R\omega\cos(\omega t + \phi) - E\sin(\omega t + \phi)\right] \tag{3.5}$$

From Eq. (1.13), the alveolar volume V_A is:

$$V_A(t) = \frac{A+2P_0}{2E} - \frac{A}{2(E^2+R^2\omega^2)}\left[E\cos(\omega t+\phi) - R\omega\sin(\omega t+\phi)\right] \tag{3.6}$$

Now, we can find a phase shift ϕ such that inhalation starts at $t=0$ regardless of other parameters. By using $\frac{dV_A}{dt}\Big|_{t=0} = 0$ and $\frac{d^2V_A}{dt^2}\Big|_{t=0} > 0$, we get $\phi = \tan^{-1}\left(\frac{R\omega}{E}\right)$. Inhalation takes place from $t=0$ to $t=\frac{\pi}{\omega}$, therefore, the tidal volume can be calculated as:

$$V_T = V_A\left(\frac{\pi}{\omega}\right) - V_A(0) = \frac{A}{\sqrt{E^2+R^2\omega^2}} \tag{3.7}$$

this implies,

$$A = V_T\sqrt{E^2+R^2\omega^2} \tag{3.8}$$

As $\omega = 2\pi f$, the pleural pressure in terms of f and V_T can be written as:

$$P_L(t) = P_m - P_0 - \frac{1}{2}V_T\sqrt{E^2+4\pi^2f^2R^2}\left[1-\cos(2\pi f t+\phi)\right] \tag{3.9}$$

and

$$\phi = \tan^{-1}\left(\frac{2\pi fR}{E}\right) \tag{3.10}$$

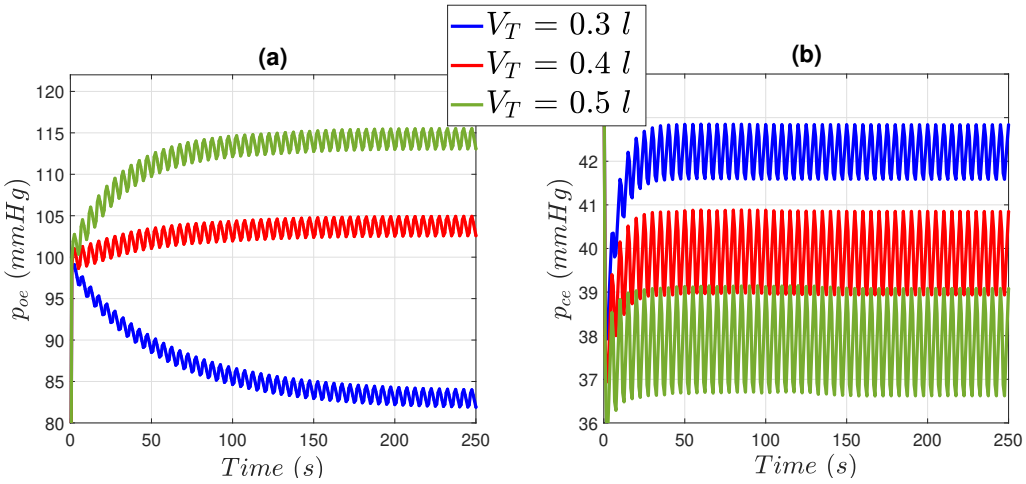

Fig. 3.1: Numerical simulation of the $6D$ model showing that breathing at the same frequency with different amplitudes leads to different blood partial pressures. (a) Arterial partial pressure of oxygen at the end of each heartbeat. (b) Arterial partial pressure of carbon dioxide at the end of each heartbeat. In both figures, $\left(f = \frac{12}{60}s^{-1},\ T_L = \frac{60}{72}s\right)$. See Table 2, for all other values of parameters.

We solved the 6D model with the pleural pressure given in Eq. (3.9) using the built-in MatLab function $ode15s$. At the end of every heart period we stored the values of p_o and p_c as p_{oe} and p_{ce} respectively, and reinitialized p_o, p_c and z. These stored values represent the level of p_o and p_c in arterial blood. Fig. 3.1 shows how the levels of partial pressure of O_2 and CO_2 in arterial blood vary due to changes in the tidal volume with fixed breathing frequency and heart beat. Now, we find the combinations of breathing amplitude and frequency that maintain given levels of p_{oe} and p_{ce}.

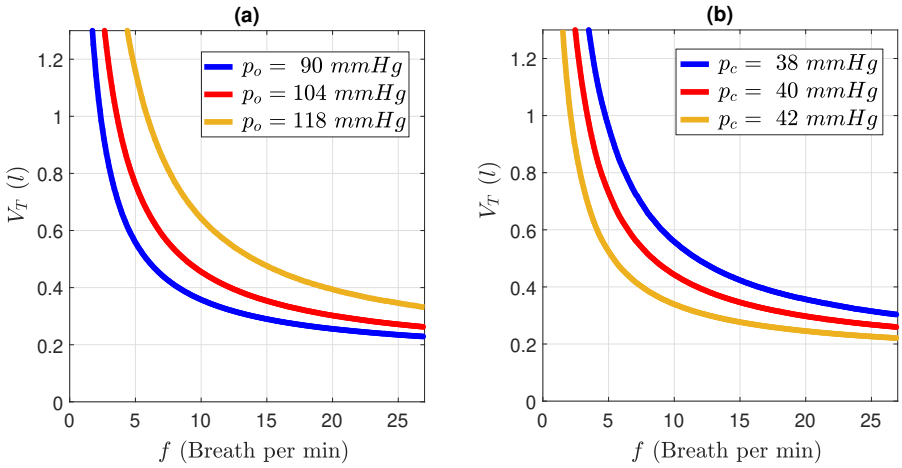

Fig. 3.2: The combinations of frequency and tidal volume that maintain the specific level of (a) arterial O_2 only, (b) arterial CO_2 only.

Fig. 3.2 shows the numerical relationship between the tidal volume and the breathing frequency that maintains the specific level of partial pressure of O_2 or CO_2 in arterial blood under normal conditions. It shows that in order to maintain the specific level of gases in the blood, if the breathing rate increases the amount of inhaled air during each breath (tidal volume) has to reduce as expected. Under normal conditions, the partial pressures of O_2 and CO_2 in the blood arteries are about 104 $mmHg$ and 40 $mmHg$ respectively. In other words, we minimize

$$\left[\left(\frac{S(\bar{p_{oe}}) - S(104)}{S(104)}\right)^2 + \left(\frac{\bar{p_{ce}} - 40}{40}\right)^2\right] \tag{3.11}$$

As the model is nonlinear, this optimization was done using the iterative numerical algorithm that is the Nelder-Mead simplex method and the Gauss-Newton method

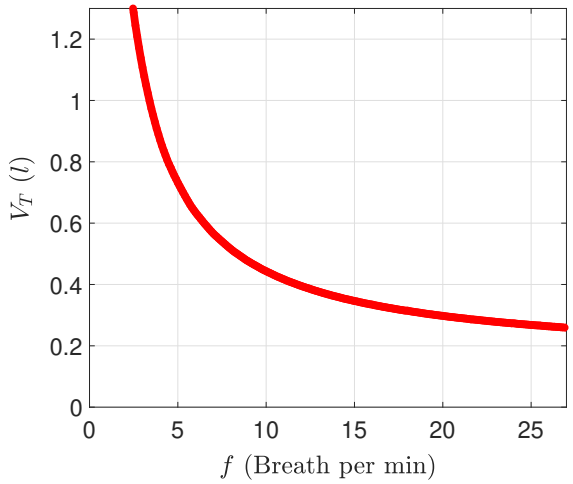

Fig. 3.3: Combinations of frequency and tidal volume that minimize 3.11.

to evaluate the optimal value of tidal volume against the given frequency of breathing. For this, the MatLab built-in tool called fminsearch which is an application of the Nelder-Mead simplex method was used to estimate the tidal volume. Fig. 3.3 shows the numerical relationship between the breathing amplitude and frequency that maintains arterial partial pressures of O_2 and CO_2 at 104 $mmHg$ and 40 $mmHg$ receptively by minimizing Eq. (3.11). Next, Eq. (3.3) gives the optimal combination of tidal volume and breathing frequency among these, by minimizing the mechanical cost CF. We tested different mechanical cost functions under normal conditions as well as on disease-affected lungs to find which of them could represent physiological observations better.

Work Rate of Breathing

The work rate of breathing is one of the costs functions previously suggested in the literature (see Section 1.2). The differential expression for work is:

$$dW = \Delta P_{rs} \cdot dV_A \tag{3.12}$$

where, $P_{rs} = P_m - P_L$ is the respiratory pressure required for breathing and $\Delta P_{rs} = P_{rs}(t) - P_{rs}(0)$ represents the change in the respiratory pressure from the end of

expiration. The work done by the respiratory muscles during inhalation is:

$$W_I = \int_0^{\frac{\pi}{\omega}} \Delta P_{rs} \cdot \frac{dV_A}{dt}\, dt \tag{3.13}$$

By substituting (3.6), (3.8) and (3.9) into Eq. (3.13) and calculating the integral, we get:

$$W_I = \frac{V_T^2}{8}\left(4\cos\phi\left(E\cos\phi + R\omega\sin\phi\right) + \pi R\omega\right) \tag{3.14}$$

Using $\tan\phi = \frac{R\omega}{E}$ (see Eq. (3.10)), we get:

$$\sin\phi = \frac{R\omega}{\sqrt{E^2 + R^2\omega^2}} \tag{3.15}$$

$$\cos\phi = \frac{E}{\sqrt{E^2 + R^2\omega^2}} \tag{3.16}$$

Let $\omega = 2\pi f$ and substituting Eq. (3.15) and (3.16) into Eq. (3.14), we get:

$$W_I = \frac{1}{2}EV_T^2 + \frac{1}{4}\pi^2 f R V_T^2 \tag{3.17}$$

Here, the first term in the above expression represents elastic work which shows the work done by the diaphragm and the intercostal muscles and the second term represents the work done against the resistance of airflow. The work rate (power, WR_I) is the work per breath times the frequency of breathing.

$$WR_I = f \cdot W_I = \frac{1}{2}EfV_T{}^2 + \frac{1}{4}\pi^2 R f^2 V_T{}^2 \tag{3.18}$$

The work rate during inhalation can be computed numerically by substituting the function shown in Fig. 3.3 into Eq. (3.18). Fig. 3.4 shows the relationship between WR_I and the breathing frequency while maintaining the specific levels of gases in the arterial blood. It shows that under normal conditions, the optimal frequency is about 11.2 breaths per min and the corresponding tidal volume is 0.408 liters (see Fig. 3.3), these values are within the observed physiological range for normal conditions at rest.

We tested this mechanical cost function on disease-affected lungs, in which the

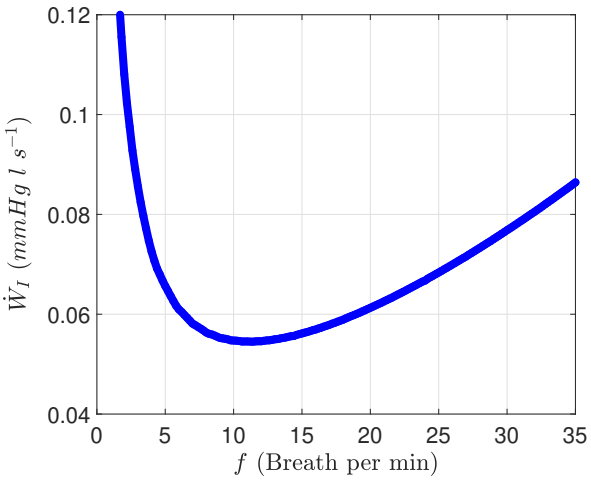

Fig. 3.4: Work rate (WR_I) as a function of breathing frequency for normal conditions. Calculations are done using the $6D$ model for a sinusoidal pleural pressure. See Table 2, for all values of the parameters.

patient loses the elasticity of the lungs and has difficulty to breathe due to high resistance to airflow in and out of the lungs. The diffusion capacities of O_2 and CO_2 reduce due to a decrease in the surface area between the alveoli and the blood capillaries. This mimics a mild chronic obstructive pulmonary disease ($COPD$) condition.

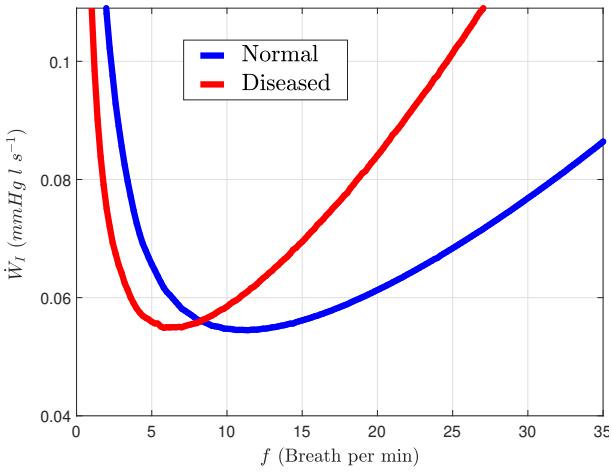

Fig. 3.5: Comparison of work rate (WR_I) as a function of breathing frequency for normal and diseased conditions. Calculations are done using the $6D$ model for a sinusoidal pleural pressure. See Table 2, for all values of the parameters.

It is observed that a patient with affected lungs breathe with a higher rate compared to normal [51]. However, Fig. 3.5 shows that the optimal frequency for

disease-affected lungs is lower than for the normal condition. Hence, this shows a movement of the optimal frequency in the wrong direction.

Total Work of Breathing

The total work of breathing is the sum of the work done by the respiratory muscles during inhalation and exhalation. If we assume that the same amount of work against the resistance to air flow must be overcome during expiration as during inspiration, and that the elastic energy stored during inspiration is available to aid expiration, then the inspiration work can be calculated by Eq. (3.17) and the expiatory work by:

$$W_E = -\frac{1}{2}E{V_T}^2 + \frac{1}{4}\pi^2 R f {V_T}^2 \tag{3.19}$$

The first term in the above expression represents the release of energy which was stored due to the elasticity of the lungs. The total work of respiration becomes

$$Total\ Work = \frac{1}{2}\pi^2 R f {V_T}^2 \tag{3.20}$$

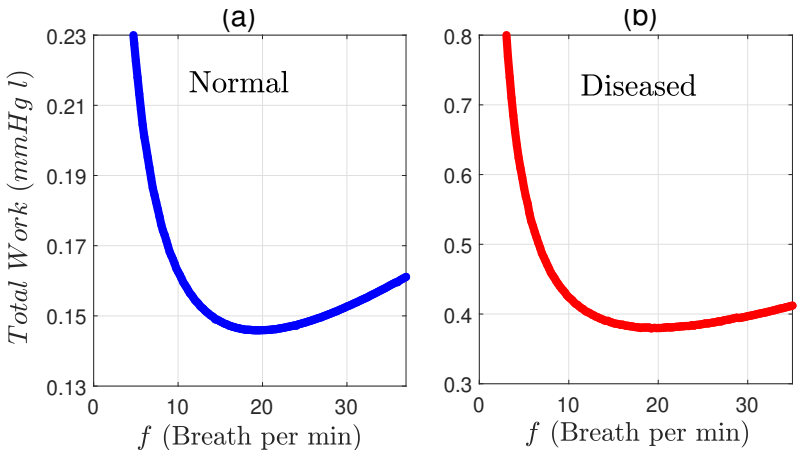

Fig. 3.6: Total work as a function of breathing frequency for (a) normal and (b) diseased conditions. Calculations are done using the 6D model with a sinusoidal pleural pressure. See Table 2, for all values of the parameters.

Fig 3.6 shows the total work as a function of breathing frequency. Panel (a) shows the total work under normal conditions and Panel (b) shows the total work in diseased lungs. The optimal frequency in Fig. 3.6 (b) is about the same as the

optimal value under normal conditions at rest. Hence, minimizing the WOB gives a movement of the optimal frequency in the right direction. This cost function might be worth considering with a different pleural pressure.

Weighted sum of the average square of volume acceleration and work

There is an hypothesis that the efficiency of muscle contraction is expected to reduce with high accelerations as it does with high shortening velocities [13], although there is no experimental evidence. The two-level hierarchical model [31] used the following performance functional to be minimized during inspiration:

$$J_I = \int_0^{\pi/\omega} \left[\ddot{V}_A^2 + \zeta_1 \Delta P_{rs} \dot{V}_A\right] dt \tag{3.21}$$

This criterion may be interpreted as a weighted sum of the average square of volume acceleration and the mechanical work performed by the respiratory muscles during inhalation. The coefficient ζ_1 is the weighting parameter and we used the value calculated by [31] (ζ_1=2.5 $l\ s^{-3}\ mmHg^{-1}$). By substituting for ΔP_{rs} and V_A, we get:

$$J_I = \pi^4 f^3 V_T^2 + \frac{1}{2}\zeta_1 E {V_T}^2 + \frac{1}{4}\pi^2 \zeta_1 f R {V_T}^2 \tag{3.22}$$

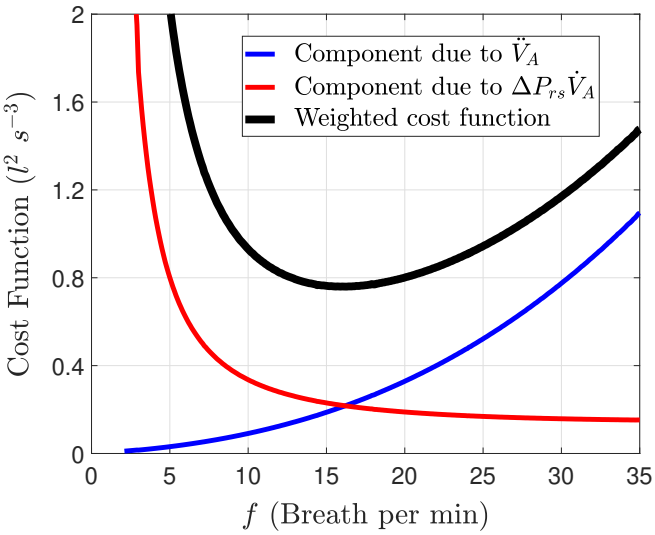

Fig. 3.7: Weighted cost function and its components as a function of breathing frequency under normal conditions. Calculations are done using the 6D model with a sinusoidal pleural pressure. See Table 2, for all values of the parameters.

In Fig. 3.7, the blue and red lines represent the partition of the cost function due to square volumetric acceleration and mechanical work respectively, and black represents the total cost function. It also shows that at a low breathing rate, the cost function is affected mostly by work done by the respiratory muscles because the lung is almost maximally inflated due to high tidal volume. However, with the higher breathing frequency and lower tidal volume, most of the cost function is due to volumetric acceleration, whereas the work done is reduced due to the small tidal volume. The weighted cost function of breathing has its lowest value within the physiological range for normal conditions at rest. However, when we test this weighted cost function on disease effected lungs, the optimal frequency is slightly lower than the one under normal conditions which shows a movement of the optimal breathing frequency in the wrong direction as shown in Fig 3.8.

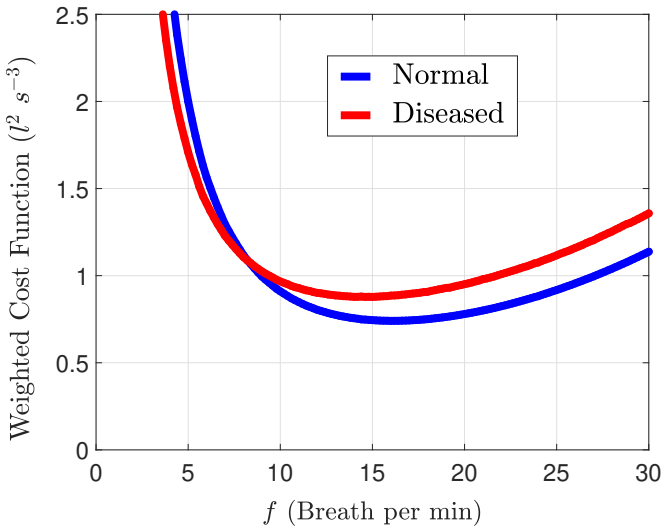

Fig. 3.8: Comparison of the weighted cost function (Eq. (3.22)) as a function of breathing frequency under normal and diseased conditions. Calculations are done using the 6D model with a sinusoidal pleural pressure. See Table 2, for all values of the parameters.

3.2.2 Exponential Pleural Pressure

In the previous section we took the pleural pressure as sinusoidal with equal inspiration and expiration durations. In mammals, under normal conditions, the durations of inhalation and exhalation are not the same and expiration is passive.

Therefore, the sinusoidal function does not represent the breathing pattern accurately. To address this we used an exponential pleural pressure calculated by coupling a representation of a neural signal to the lungs (see Section 2.1) which allows for variations in the durations of inspiration and exhalation.

We consider P_L as defined in Eq. (2.5). We fix the duration of inspiration to 1.7, and let the variation in the breathing period be entirely due to the change in the duration of exhalation[1]. First, we solve Eq. (1.7) and (1.13) and find the tidal volume at steady state for a particular breathing frequency and k_n. Then we solve the full system of differential equations (Eq. 1.7 - 1.12) by using the combination of breathing frequency and k_n and their corresponding tidal volume found in the first step.

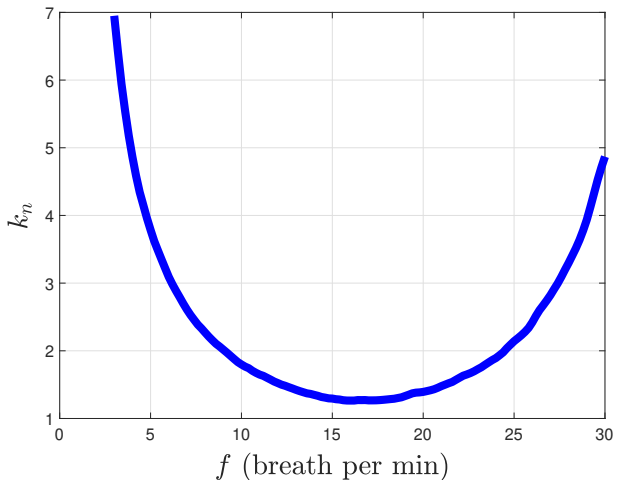

Fig. 3.9: Combinations of k_n and breathing frequency (f) that minimize Eq. (3.11). Calculations are done using the $6D$ model with the exponential pleural pressure (see Eq. (2.5)) for normal conditions. See Table 2, for all values of the parameters.

For a particular breathing frequency, the variation in k_n leads to different arterial partial pressures of oxygen and carbon dioxide. If the arterial partial pressure of O_2 and CO_2 are maintained at 104 mmHg and 40 mmHg respectively (see Eq. (3.11)), we can calculate the breathing frequency as a function of k_n (Fig. 3.9) and the tidal volume as a function of breathing frequency (Fig. 3.10).

We then find the optimal combination of breathing frequency and tidal volume among all the potential combinations shown in Fig. (3.10) for the cost functions

[1] If T_i is not fixed and instead the ratio between T_i and T_e is fixed, there is no minimum.

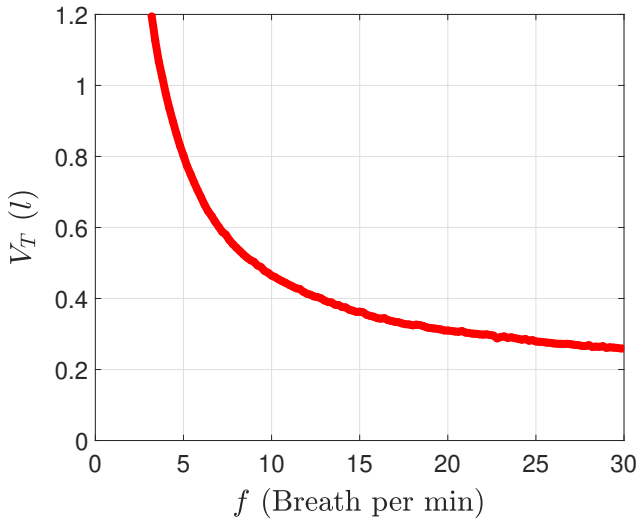

Fig. 3.10: Combinations of V_T and f that minimize Eq. (3.11). Calculations are done using the 6D model with the exponential pleural pressure (see Eq. (2.5)) for normal conditions. See Table 2, for all values of the parameters.

discussed in Section 3.2.1. Unlike the case of a sinusoidal pleural pressure, for the exponential pleural pressure, there is no explicit analytical expression for those cost functions. So, we solved numerically the complete system of differential equations (Eq. 1.7 - 1.12) and computed $\dot{V}_A$ at steady state. This enabled us to find the volumetric acceleration by numerical differentiation. We then computed the different cost functions by numerical integration; for this we used MatLab built-in function $trapz$.

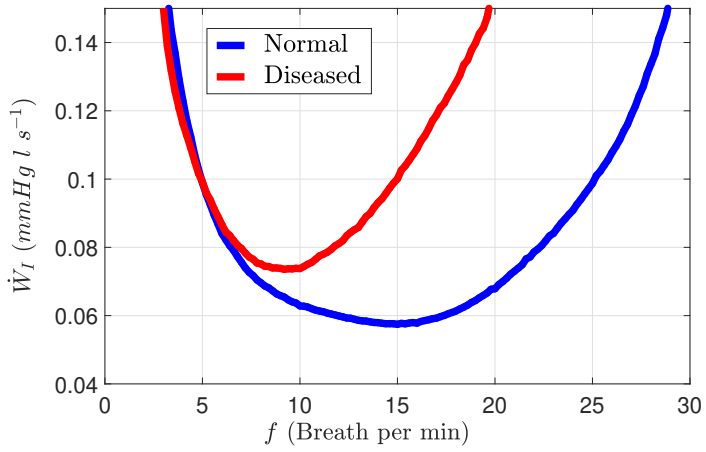

Fig. 3.11: Comparison of $\dot{W}_I$ as a function of breathing frequency under normal and diseased conditions. Calculations are done using the 6D model with an exponential pleural pressure. See Table 2, for all values of the parameters.

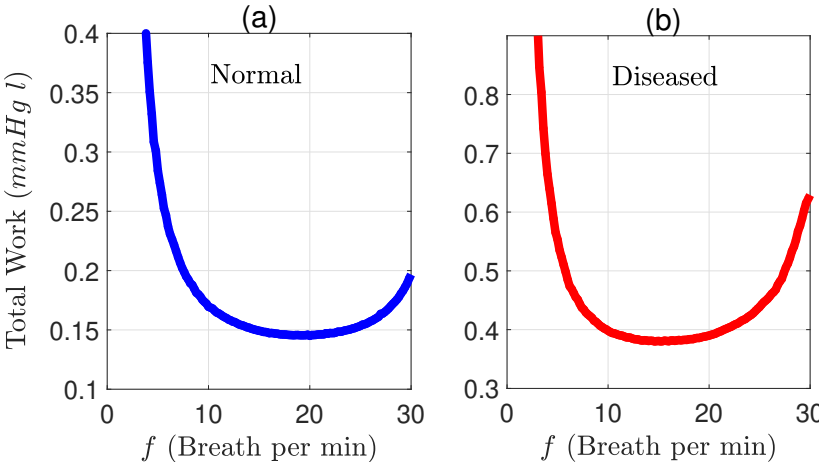

Fig. 3.12: Total work as a function of breathing frequency for (a) normal and (b) diseased conditions. Calculations are done using the $6D$ model with an exponential pleural pressure. See Table 2, for all values of the parameters.

Fig. 3.11, 3.12, and 3.13 show the work rate during inhalation, the total work and weighted cost function respectively, all as functions of the breathing frequency. They show that the optimal breathing frequencies associated with work rate and the weighted cost function are within the physiological range (12-18 breaths per minute) while the optimal frequency associated with the total work is slightly higher under normal conditions. However, the optimal breathing frequencies associated with these cost functions are lower than expected for diseased lungs.

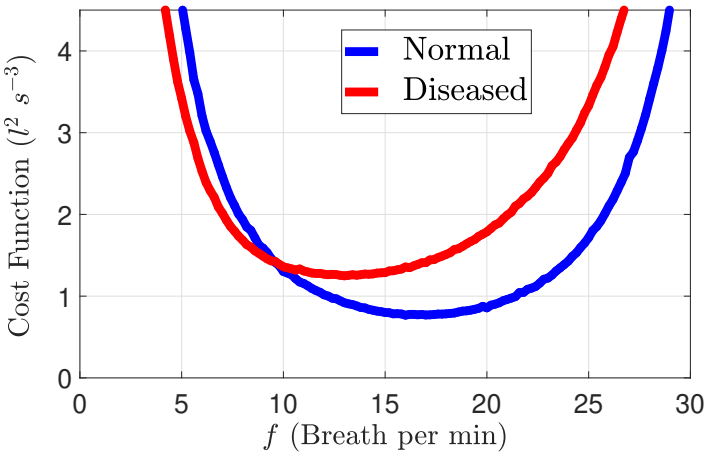

Fig. 3.13: Comparison of the weighted cost function as a function of breathing frequency under normal and diseased conditions. Calculations are done using the $6D$ model with an exponential pleural pressure. See Table 2, for all values of the parameters.

3.3 Calculation Using the $2D$ Model

In this section, we consider $F(t)$ as a predefined function. We solve the $2D$ linear model analytically, and also find the optimal V_T and T that minimizes the given cost function, while maintaining a constant average value of Y_c. As we have $Y_c = D_c f_c (E + K_1) - D_c K_2$, where D_c, E, K_1 and K_2 are constants (see Section 2.2.2),maintaining a constant average value of Y_c is equivalent to maintaining a constant average value of concentration of CO_2 in the lungs, f_c.

3.3.1 A Sinusoidal $F(t)$

Let

$$F(t) = \frac{V_T}{2}(\omega \sin \omega t - \alpha \cos \omega t) + \frac{\alpha V_T}{2} + \alpha B \tag{3.23}$$

where, B represents the volume of the lungs at its minimum under the action of $F(t)$. From equation (2.17), the alveolar volume is:

$$V_A(t) = B + \frac{V_T}{2}\left(1 - \cos \omega t\right) \tag{3.24}$$

It is clear from equation (3.24) that $V_A(t)$ is an increasing function in the interval $t \in \left(0, \frac{\pi}{\omega}\right)$ and a deceasing function in the interval $t \in \left(\frac{\pi}{\omega}, \frac{2\pi}{\omega}\right)$ with a period $T = \frac{2\pi}{\omega}$. By solving equation (2.19) we get an expression of Y_c:

$$Y_c(t) = \begin{cases} C_1\, e^{-\beta t} + \frac{\gamma(V_T - V_D)\omega}{2(\beta^2+\omega^2)}\left[\beta \sin \omega t - \omega \cos \omega t\right] & ; \quad 0 < t \leq \frac{\pi}{\omega} \\ C_2\, e^{-\beta t} & ; \quad \frac{\pi}{\omega} < t \leq \frac{2\pi}{\omega} \end{cases} \tag{3.25}$$

where, C_1 and C_2 are constants. By imposing the conditions of continuity at $t = \frac{\pi}{\omega}$ and periodicity of Y_c, $Y_c(0) = Y_c\left(\frac{2\pi}{\omega}\right)$, we get C_1 and C_2 as:

$$C_1 = \frac{\gamma(V_T - V_D)\omega^2 e^{\frac{\pi\beta}{\omega}}}{2\left(\omega^2 + \beta^2\right)\left(e^{\frac{\pi\beta}{\omega}} - 1\right)} \qquad and \qquad C_2 = \frac{\gamma(V_T - V_D)\omega^2 e^{\frac{2\pi\beta}{\omega}}}{2\left(\omega^2 + \beta^2\right)\left(e^{\frac{\pi\beta}{\omega}} - 1\right)}.$$

Let Y_{av} be the average value of Y_c that we have to maintain during each period at steady state.

$$Y_{av} = \frac{\omega}{2\pi}\int_0^{\frac{2\pi}{\omega}} Y_c(t)\, dt \tag{3.26}$$

By substituting (3.25) into (3.26), the period T can be expressed as:

$$T = \frac{\gamma(V_T - V_D)}{\beta\, Y_{av}} \tag{3.27}$$

This gives a linear relationship between T and V_T (with $V_T > V_D$) that maintains the specified average value Y_{av}. This relationship shows that the alveolar minute ventilation $\left(\frac{V_T - V_D}{T}\right)$ is constant, which is one of the assumptions used by Otis et al. [53]. Fig. 3.14 shows the solution for the alveolar volume V_A and variable Y_c for two different combinations of V_T and T that satisfy Eq. (3.27).

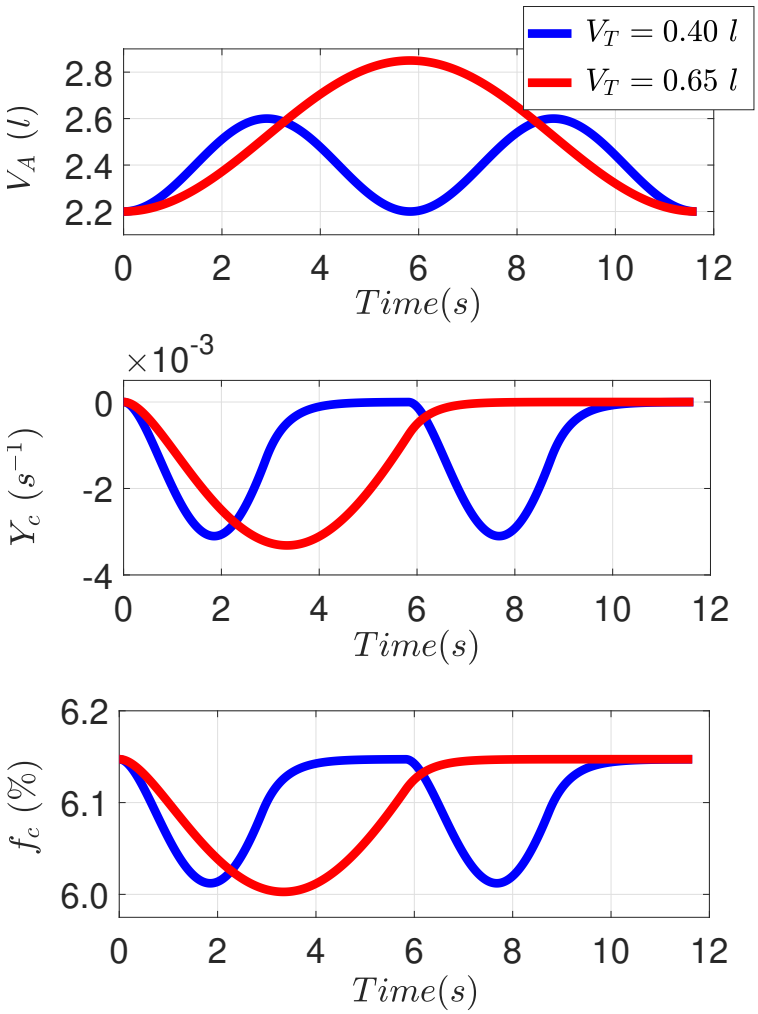

Fig. 3.14: Solutions of $V_A(t)$, $Y_c(t)$ and $f_c(t)$ for two different values of V_T. Both solutions maintain a specific value of $Y_{av} = -0.0013$, which is equivalent to $f_c = 6.1\%$. Calculations are done using the $2D$ model with a sinusoidal $F(t)$. See Table 2, for all values of the parameters.

The total work for the given sinusoidal function is:

$$W = R\int_0^{\frac{2\pi}{\omega}} F\dot{V}_A dt = \frac{1}{4}R\pi\omega {V_T}^2 = \frac{\pi^2 R {V_T}^2}{2T} \tag{3.28}$$

Among all combinations of T and V_T that satisfy Eq. (3.27), we need to find the combination that minimizes the cost function (3.28). By substituting (3.27) into (3.28), the cost function can be represented in terms of V_T only.

$$W = \frac{\pi^2 \beta\ R\ Y_{av} {V_T}^2}{2\gamma(V_T - V_D)} \tag{3.29}$$

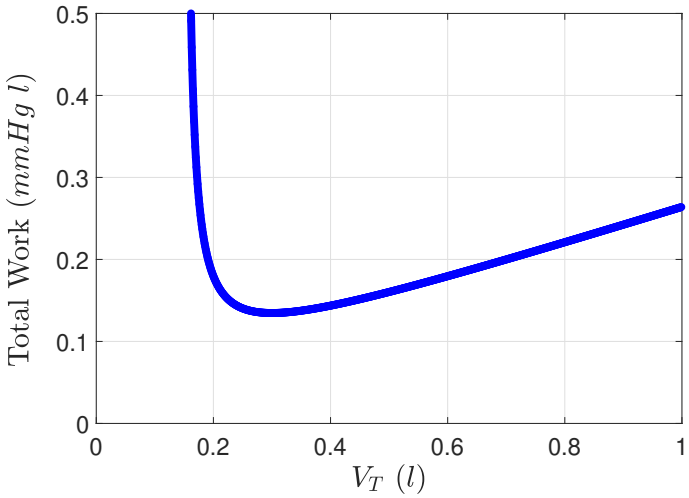

Fig. 3.15: Total work (W) as a function of V_T for the 2D model (see Eq. (3.29)). See Table 2, for all values of the parameters.

For the optimal V_T, we set $\frac{\partial W}{\partial V_T}$=0 which implies that the optimal V_T is:

$$V_T^* = 2V_D \tag{3.30}$$

and the corresponding optimal period T is:

$$T^* = \frac{\gamma V_D}{\beta Y_{av}} \tag{3.31}$$

As can be seen, the optimal amplitude, only depends on the dead space, V_D, while the optimal period, T^*, depends on the dead space (V_D), the average value of Y_c

and the constant $\frac{\gamma}{\beta}$. Fig. 3.16 shows a comparison of the total work done during each breath as a function of the tidal volume for the $6D$ model and the $2D$ linear model. The concentration of CO_2, f_c , was maintained at 6.1% and the driving forces for both models are sinusoidal functions (see Eq. 3.4 and 3.23). As can be seen both models have a minimum at $V_T = 0.3\ l$ which is $V_T = 2V_D$.

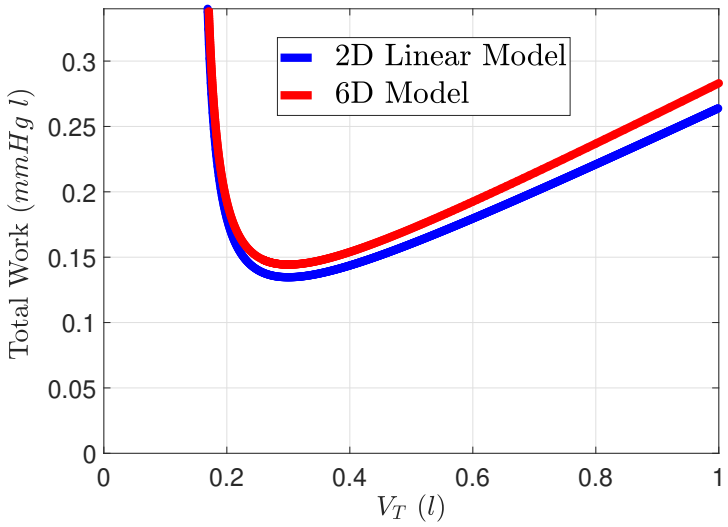

Fig. 3.16: Comparison of total work as a function of V_T for the $6D$ model and $2D$ linear model. For both models, the driving forces are sinusoidal and the average values of CO_2 concentrations are maintained at 6.1%. See Table 2, for all values of the parameters

3.3.2 A Linear $F(t)$

In the previous section, we considered $F(t)$ as a sinusoidal function, in which the duration of inhalation is half of the breathing period. In this section, we consider $F(t)$ as a simple linear function in which both the breathing period and the duration of inhalation are free. The motivation for choosing this function will become clear in Section 4.2. Let

$$F(t) = \begin{cases} \alpha B + \frac{V_T}{T_i}(1+\alpha t) & ; \quad 0 < t \leq T_i \\ \alpha B + \frac{V_T}{T_i - T}(1+\alpha t - \alpha T) & ; \quad T_i < t \leq T \end{cases} \tag{3.32}$$

Substituting Eq. (3.32) into equation (2.17) and solving for the alveolar volume we get:

$$V_A(t) = \begin{cases} B + \frac{V_T}{T_i} t & ; \quad 0 < t \leq T_i \\ B + \frac{V_T}{T - T_i} (T - t) & ; \quad T_i < t \leq T \end{cases} \tag{3.33}$$

The function $V_A(t)$ is increasing in the interval $0 < t \leq T_i$ and decreasing in the interval $T_i < t \leq T$. From equation (2.19) we get:

$$Y_c(t) = \begin{cases} C_3\ e^{-\beta t} + \frac{\gamma(V_T - D)}{\beta T_i} & ; \quad 0 < t \leq T_i \\ C_4\ e^{-\beta t} & ; \quad T_i < t \leq T \end{cases} \tag{3.34}$$

where, C_3 and C_4 are constants. By imposing the conditions of continuity at $t = T_i$ and periodicity of Y, $Y(0) = Y(T)$, we get C_3 and C_4 as:

$$C_3 = \frac{\gamma(V_T - V_D)\left(e^{\beta T} - e^{\beta T_i}\right)}{\beta T_i \left(1 - e^{\beta T}\right)} \qquad and \qquad C_4 = \frac{\gamma(V_T - V_D) e^{\beta T} \left(1 - e^{\beta T_i}\right)}{\beta T_i \left(1 - e^{\beta T}\right)}$$

As Y_{av} is the average value of $Y_c(t)$ that we maintain during each period at steady state:

$$Y_{av} = \frac{1}{T} \int_0^T Y_c(t)\ dt \tag{3.35}$$

By substituting Eq. (3.34) into Eq. (3.35) and solving for the period T we get:

$$T = \frac{\gamma(V_T - V_D)}{\beta\ Y_{av}} \tag{3.36}$$

The relationship between T and V_T in this case is the same as we got when $F(t)$ was sinusoidal (see Eq. (3.27)).

The total work is:

$$W = R \int_0^T F \dot{V}_A dt = \frac{R T {V_T}^2}{T T_i - T_i^2} \tag{3.37}$$

By substituting T from Eq. (3.36) into Eq. (3.37), we get:

$$W = \frac{\gamma R {V_T}^2 (V_T - D)}{T_i(\gamma(V_T - V_D) - \beta T_i Y_{av})} \tag{3.38}$$

By differentiating W with respect to V_T and T_i separately and equating the derivatives to zero we get the optimal amplitude $V_T^* = 2V_D$ and the duration of inhalation $T_i^* = \frac{\gamma V_D}{2\beta Y_{av}}$. Substituting V_T^* into Eq. (3.36) gives the optimal duration $T^* = \frac{\gamma V_D}{\beta Y_{av}}$.

The optimal amplitude V_T^* only depends on the dead space and the optimal duration of inhalation T_i^* is half of the period of breathing, which are the same results as when $F(t)$ was sinusoidal.

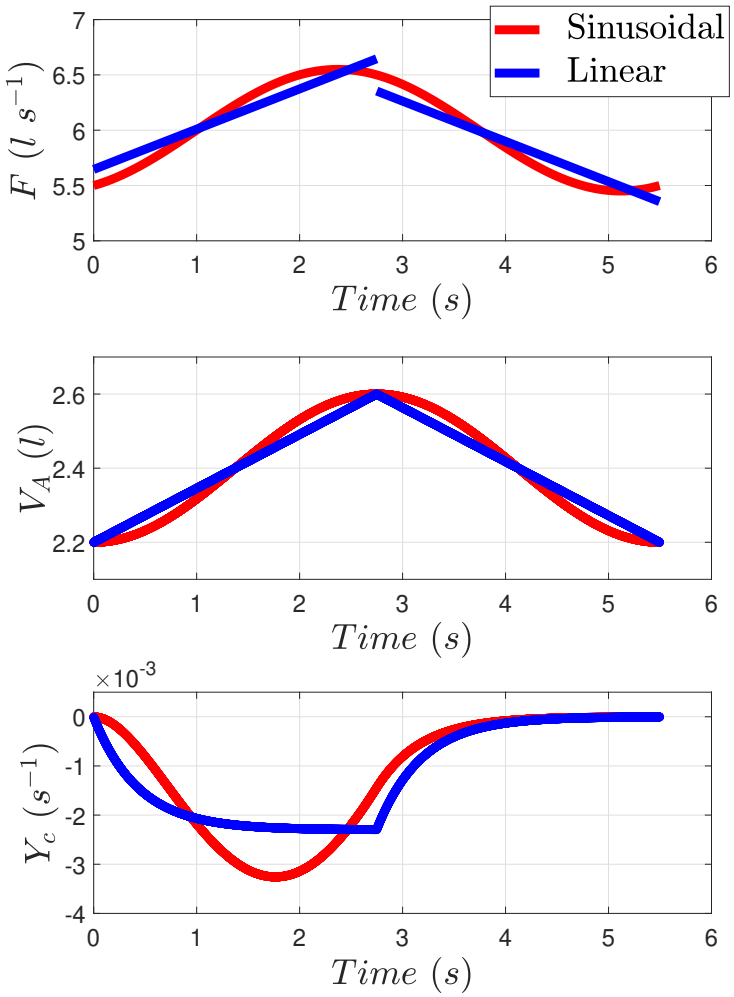

Fig. 3.17: Trajectories of $F(t)$ and solutions of $V_A(t)$ and $Y_c(t)$ when $F(t)$ is sinusoidal and linear. Both solutions maintain a specific value of $Y_{av} = -0.0013$, which is equivalent to $f_c = 6.1\%$. Calculations are done using the $2D$ model. See Table 2, for all values of the parameters.

The solutions obtained when $F(t)$ was linear and sinusoidal, are shown in Fig. 3.17 and the associated cost functions are plotted in Fig. 3.18. Notably, the phase difference between $F(t)$ and $V_A(t)$ that is seen in the sinusoidal case does not exist in the linear case. However, the linear function is discontinuous at $t = 0$, $t = T_i$ and $t = T$. Fig. 3.18 also shows that for every V_T, the linear function gives a lower total

work per breath than the sinusoidal function.

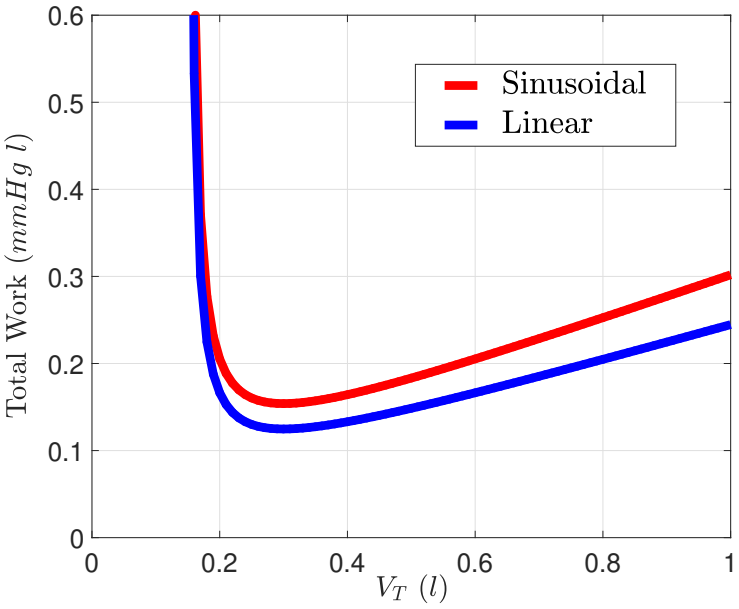

Fig. 3.18: Comparison of the total work as a function of V_T when $F(t)$ is sinusoidal and linear. Both solutions maintain a specific value of $Y_{av} = -0.0013$, which is equivalent to $f_c = 6.1\%$. Calculations are done using the 2D model. See Table 2, for all values of the parameters.

3.4 Effect of Breathing Pattern on Gas Exchange for the 2D Model

Eq. (3.27) and (3.36) show that the relationship between the tidal volume and the breathing period is the same for two different breathing patterns for our 2D linear model. In this section, we consider the alveolar volume (V_A) as a general Fourier series and aim to find the relationship between T and V_T that maintains a specific average value of Y_c, y_{av}, while satisfying the continuity and steady state conditions for V_A and Y_c.

Let us consider $V_A(t)$ as a Fourier series:

$$V_A(t) = a_0 + \sum_{n=1}^{\infty} [a_n \cos(n\omega t) + b_n \sin(n\omega t)] \tag{3.39}$$

Here we assume that the Fourier series converges and can be differentiated term by term; note that this will be the case for a wide range of functions.

By substituting Eq. (3.39) into (2.19), and solving the differential equation for Y_c, we get:

$$Y_c(t) = \begin{cases} C_1 e^{-\beta t} + \frac{\gamma(V_T - V_D)}{V_T} \sum_{n=1}^{\infty} \frac{n\omega}{\beta^2 + n^2\omega^2} \Big[\big(n\omega a_n + \beta b_n\big)\cos(n\omega t) \\ \qquad + \big(n\omega b_n - \beta a_n\big)\sin(n\omega t) \Big] & 0 \le t \le T_i \\ C_2 e^{-\beta t} & T_i < t \le T \end{cases} \tag{3.40}$$

where C_1 and C_2 are constants. By imposing the conditions of continuity at $t = T_i$ and periodicity of Y_c, $Y_c(0) = Y_c(T)$, we get C_1 and C_2 as:

$$C_1 = \frac{\gamma(V_T - V_D)}{V_T\left(1 - e^{\beta T}\right)} \sum_{n=1}^{\infty} \frac{n\,\omega}{\beta^2 + n^2\,\omega^2} \Big[\big(a_n\, n\,\omega + b_n\,\beta\big)\Big(e^{\beta T} - e^{\beta T_i}\cos(n\omega T_i)\Big) - \big(b_n\, n\,\omega - a_n\,\beta\big)\, e^{\beta T_i}\sin(n\omega t) \Big] \tag{3.41}$$

and

$$C_2 = \frac{\gamma(V_T - V_D)}{V_T\left(1 - e^{-\beta T}\right)} \sum_{n=1}^{\infty} \frac{n\,\omega}{\beta^2 + n^2\,\omega^2} \Big[\big(a_n\, n\,\omega + b_n\,\beta\big)\Big(e^{\beta T_i}\cos(n\omega T_i) - 1\Big) + \big(b_n\, n\,\omega - a_n\,\beta\big)\, e^{\beta T_i}\sin(n\omega t) \Big] \tag{3.42}$$

Let Y_{av} be the average value of Y_c that is maintained during each period at steady state.

$$y_{av} = -\frac{1}{T}\int_0^T Y_c(t)\, dt \tag{3.43}$$

By substituting $Y_c(t)$ from Eq. (3.40) into Eq. (3.43) and using (3.41) and (3.42), we get:

$$y_{av} = \frac{\gamma(V_T - V_D)}{T\,\beta\,V_T} \sum_{n=1}^{\infty} \Big[a_n\big(\cos(n\omega T_i) - 1\big) + b_n \sin(n\omega T_i) \Big] \tag{3.44}$$

From the condition $V_A(0) = B$ we get:

$$a_0 + \sum_{n=1}^{\infty} a_n = B \tag{3.45}$$

and from the condition $V_A(T_i) = B + V_T$ we get:

$$a_0 + \sum_{n=1}^{\infty} [a_n \cos(n\omega T_i) + b_n \sin(n\omega T_i)] = B + V_T \tag{3.46}$$

Subracting Eq. (3.45) from (3.46) we get:

$$\sum_{n=1}^{\infty} [a_n (\cos(n\omega T_i) - a_n) + b_n \sin(n\omega T_i)] = V_T \tag{3.47}$$

Subtituting Eq. (3.47) into (3.44), and after rearrangement we get:

$$T = \frac{\gamma(V_T - V_D)}{\beta y_{av}} \tag{3.48}$$

This relationship between the tidal volume and the breathing period is linear and independent of any Fourier coefficient. This shows that in the 2D linear model, the average levels of CO_2 in the lungs are only affected by the tidal volume and the period of breathing and are not affected by the shape of the driving force. This result supports the physiological hypothesis that constant effective minute ventilation, $\frac{V_T - V_D}{T}$, could represent constant gas exchange in the lungs [66], [53] and [47].

Chapter 4

Optimal Control Problem

In the previous chapter, we defined and solved the optimization problem when the driving force was a given function, and the optimal values of V_T and T (or alternatively f^{-1}) were unknown. In this chapter we develop the necessary conditions for the solution of the optimal control problem, which enables us to find the optimal driving force with optimal duration of whole breath (T) and inhalation (T_i) for a given V_T.

4.1 Solution of the Optimal Control Problem

Consider a piecewise system of ordinary differential equations

$$\dot{\mathbf{x}}(t) = \begin{cases} \mathbf{g_1}(t, \mathbf{x}, u) & ; \quad t_0 < t \leq T_i \\ \\ \mathbf{g_2}(t, \mathbf{x}, u) & ; \quad T_i < t \leq T \end{cases} \tag{4.1}$$

where, $\mathbf{x}(t)$ and $u(t)$ are the state and control variables respectively, such that $\mathbf{x}(t) \in \mathbb{R}^n$ and $u(t) \in \mathbb{R}$. Let us assume that u is periodic with period T, that is $u(t) = u(t+T)$, and that $\mathbf{x}(t)$ has some specified values at $t = t_0$, T_i and T.

We would like to find $u(t)$ and T_i such that the cost function $W = \int_{t_0}^{T} J(t, \mathbf{x}, u)\, dt$ is minimized subject to the following constraints:

i The differential system (4.1) is satisfied.

ii The system is in steady state. For our purpose this means periodic with period T, that is, $\mathbf{x}(t_0) = \mathbf{x}(t_0 + T)$.

Following ideas from [42], we assume that there exists an optimal solution $u^*(t)$ and T_i^* such that the cost function W is minimized, and that $\mathbf{x}^*(t)$ is the optimal solution of the differential equations associated with $u^*(t)$ and T_i^*. Suppose $h(t)$ is an arbitrary function and ϵ and δ are small scalar parameters. A non-optimal $u(t)$ can then be represented as $u(t,\epsilon) = u^*(t) + \epsilon h(t)$ and the non-optimal value of T_i can be represented as $T_i = T_i^* + \delta$. The corresponding solution of the differential equations (4.1) is $\mathbf{x}(t,\epsilon,\delta)$, and $\epsilon = \delta = 0$ provides the optimal solution $\mathbf{x}(t,0,0) = \mathbf{x}^*(t)$.

This representation of $u(t,\epsilon,\delta)$, $\mathbf{x}(t,\epsilon,\delta)$ and $T_i(\delta)$ leads to W being a function of ϵ and δ. In addition, we add to the integrand the quantity: $\boldsymbol{\lambda}^\top \mathbf{g}(t,\mathbf{x},u) - \boldsymbol{\lambda}^\top \dot{\mathbf{x}} = 0$ where $\boldsymbol{\lambda}(t)$ is an unknown vector function in the interval $[t_0, T]$. The cost function is then:

$$\begin{aligned} W(\epsilon,\delta) = &\int_{t_0}^{T_i} \left[J(t,\mathbf{x}_1,u_1) + \boldsymbol{\lambda}_1^\top(t)\, \mathbf{g}_1(t,\mathbf{x}_1,u_1) - \boldsymbol{\lambda}_1^\top(t)\, \dot{\mathbf{x}}_1 \right] dt \\ &+ \int_{T_i}^{T} \left[J(t,\mathbf{x}_2,u_2) + \boldsymbol{\lambda}_2^\top(t)\, \mathbf{g}_2(t,\mathbf{x}_2,u_2) - \boldsymbol{\lambda}_2^\top(t)\, \dot{\mathbf{x}}_2 \right] dt \end{aligned} \tag{4.2}$$

here, $\mathbf{x}_1$ and u_1 represent the state and control variable in the interval $t_0 \le t \le T_i$ respectively, whereas $\mathbf{x}_2$ and u_2 represent these variables in the interval $T_i < t \le T$. We construct new quantities: $H_1 = J + \boldsymbol{\lambda}_1^\top \mathbf{g}_1$ and $H_2 = J + \boldsymbol{\lambda}_2^\top \mathbf{g}_2$ and get:

$$\begin{aligned} W(\epsilon,\delta) = &\int_{t_0}^{T_i} \left[H_1(t,\mathbf{x}_1,u_1,\boldsymbol{\lambda}_1) - \boldsymbol{\lambda}_1^\top(t)\dot{\mathbf{x}}_1 \right] dt \\ &+ \int_{T_i}^{T} \left[H_2(t,\mathbf{x}_2,u_2,\boldsymbol{\lambda}_2) - \boldsymbol{\lambda}_2^\top(t)\dot{\mathbf{x}}_2 \right] dt \end{aligned} \tag{4.3}$$

As $u = u^*$, $\mathbf{x} = \mathbf{x}^*$ and $T_i = T_i^*$ are optimal at $\epsilon = \delta = 0$, $W(\epsilon,\delta)$ is optimal when the variation in $W(\epsilon,\delta)$ with respect to ϵ and δ is zero at $\epsilon = \delta = 0$. That is:

$$dW(\epsilon,\delta)\Big|_{\epsilon=0,\delta=0} = 0 \tag{4.4}$$

where:

$$dW(\epsilon,\delta) = \frac{\partial W}{\partial \epsilon} d\epsilon + \frac{\partial W}{\partial \delta} d\delta \tag{4.5}$$

Differentiating Eq. (4.3) with respect to ϵ, by using Leibniz' integral rule,[1] we get:

$$\begin{aligned}\frac{\partial W}{\partial \epsilon} = &\int_{t_0}^{T_i} \left[\frac{\partial H_1}{\partial \mathbf{x}_1} \frac{\partial \mathbf{x}_1}{\partial \epsilon} + \frac{\partial H_1}{\partial u_1} \frac{\partial u_1}{\partial \epsilon} - \boldsymbol{\lambda}_1^\top(t) \frac{\partial \dot{\mathbf{x}}_1}{\partial \epsilon} \right] dt \\ &+ \int_{T_i}^{T} \left[\frac{\partial H_2}{\partial \mathbf{x}_2} \frac{\partial \mathbf{x}_2}{\partial \epsilon} + \frac{\partial H_2}{\partial u_2} \frac{\partial u_2}{\partial \epsilon} - \boldsymbol{\lambda}_2^\top(t) \frac{\partial \dot{\mathbf{x}}_2}{\partial \epsilon} \right] dt \end{aligned} \tag{4.6}$$

Using integration by parts we have:

$$\begin{aligned}\frac{\partial W}{\partial \epsilon} = &- \boldsymbol{\lambda}_1^\top(T_i) \left.\frac{\partial \mathbf{x}_1}{\partial \epsilon}\right|_{t=T_i} + \boldsymbol{\lambda}_1^\top(t_0) \left.\frac{\partial \mathbf{x}_1}{\partial \epsilon}\right|_{t=t_0} - \boldsymbol{\lambda}_2^\top(T) \left.\frac{\partial \mathbf{x}_2}{\partial \epsilon}\right|_{t=T} + \boldsymbol{\lambda}_2^\top(T_i) \left.\frac{\partial \mathbf{x}_2}{\partial \epsilon}\right|_{t=T_i} \\ &+ \int_{t_0}^{T_i} \left[\frac{\partial H_1}{\partial \mathbf{x}_1} \frac{\partial \mathbf{x}_1}{\partial \epsilon} + \frac{\partial H_1}{\partial u_1} \frac{\partial u_1}{\partial \epsilon} + \dot{\boldsymbol{\lambda}}_1^\top(t) \frac{\partial \mathbf{x}_1}{\partial \epsilon} \right] dt \\ &+ \int_{T_i}^{T} \left[\frac{\partial H_2}{\partial \mathbf{x}_2} \frac{\partial \mathbf{x}_2}{\partial \epsilon} + \frac{\partial H_2}{\partial u_2} \frac{\partial u_2}{\partial \epsilon} + \dot{\boldsymbol{\lambda}}_2^\top(t) \frac{\partial \mathbf{x}_2}{\partial \epsilon} \right] dt \end{aligned} \tag{4.7}$$

Now, differentiating eq (4.3) with respect to δ, as $T_i = T_i^* + \delta$, and using Libnitz' rule, we get:

$$\begin{aligned}\frac{\partial W}{\partial \delta} = &H_1(T_i) - \boldsymbol{\lambda}_1^\top(T_i) \dot{\mathbf{x}}_1(T_i) - H_2(T_i) + \boldsymbol{\lambda}_2^\top(T_i) \dot{\mathbf{x}}_2(T_i) \\ &+ \int_{t_0}^{T_i} \left[\frac{\partial H_1}{\partial \mathbf{x}_1} \frac{\partial \mathbf{x}_1}{\partial \delta} + \frac{\partial H_1}{\partial u_1} \frac{\partial u_1}{\partial \delta} - \boldsymbol{\lambda}_1^\top(t) \frac{\partial \dot{\mathbf{x}}_1}{\partial \delta} \right] dt \\ &+ \int_{T_i}^{T} \left[\frac{\partial H_2}{\partial \mathbf{x}_2} \frac{\partial \mathbf{x}_2}{\partial \delta} + \frac{\partial H_2}{\partial u_2} \frac{\partial u_2}{\partial \delta} - \boldsymbol{\lambda}_2^\top(t) \frac{\partial \dot{\mathbf{x}}_2}{\partial \delta} \right] dt \end{aligned} \tag{4.8}$$

Using integration by parts we have:

$$\begin{aligned}\frac{\partial W}{\partial \delta} = &H_1(T_i) - \boldsymbol{\lambda}_1^\top(T_i) \dot{\mathbf{x}}_1(T_i) - H_2(T_i) + \boldsymbol{\lambda}_2^\top(T_i) \dot{\mathbf{x}}_2(T_i) \\ &- \boldsymbol{\lambda}_1^\top(T_i) \left.\frac{\partial \mathbf{x}_1}{\partial \delta}\right|_{t=T_i} + \boldsymbol{\lambda}_1^\top(t_0) \left.\frac{\partial \mathbf{x}_1}{\partial \delta}\right|_{t=t_0} - \boldsymbol{\lambda}_2^\top(T) \left.\frac{\partial \mathbf{x}_2}{\partial \delta}\right|_{t=T} + \boldsymbol{\lambda}_2^\top(T_i) \left.\frac{\partial \mathbf{x}_2}{\partial \delta}\right|_{t=T_i} \\ &+ \int_{t_0}^{T_i} \left[\frac{\partial H_1}{\partial \mathbf{x}_1} \frac{\partial \mathbf{x}_1}{\partial \delta} + \frac{\partial H_1}{\partial u} \frac{\partial u}{\partial \delta} + \dot{\boldsymbol{\lambda}}_1^\top(t) \frac{\partial \mathbf{x}_1}{\partial \delta} \right] dt \\ &+ \int_{T_i}^{T} \left[\frac{\partial H_2}{\partial \mathbf{x}_2} \frac{\partial \mathbf{x}_2}{\partial \delta} + \frac{\partial H_2}{\partial u} \frac{\partial u}{\partial \delta} + \dot{\boldsymbol{\lambda}}_2^\top(t) \frac{\partial \mathbf{x}_2}{\partial \delta} \right] dt \end{aligned} \tag{4.9}$$

[1] Leibniz's rule for differentiation under the integral sign states that:

$$\frac{d}{dx} \int_{u(x)}^{v(x)} f(x,t)\,dt = f(x, v(x)) \frac{dv}{dx} - f(x, u(x)) \frac{du}{dx} + \int_{u(x)}^{v(x)} \frac{\partial f(x,t)}{\partial x}\,dt$$

By using Eq. (4.7) and (4.9), Eq. (4.5) can be written as:

$$\begin{aligned} dW(\epsilon,\delta) = &\left[H_1(T_i) - H_2(T_i)\right] d\delta \\ &- \boldsymbol{\lambda}_1^\top(T_i)\left[d\mathbf{x}_1(T_i) + \dot{\mathbf{x}}_1(T_i)\, d\delta\right] \\ &+ \boldsymbol{\lambda}_2^\top(T_i)\left[d\mathbf{x}_2(T_i) + \dot{\mathbf{x}}_2(T_i)\, d\delta\right] \\ &+ \boldsymbol{\lambda}_1^\top(t_0)\, d\mathbf{x}_1|_{t=t_0} - \boldsymbol{\lambda}_2^\top(T)\, d\mathbf{x}_1|_{t=T} \\ &+ \int_{t_0}^{T_i}\left[\frac{\partial H_1}{\partial \mathbf{x}_1} d\mathbf{x}_1 + \frac{\partial H_1}{\partial u} du + \dot{\boldsymbol{\lambda}}_1^\top(t)\, d\mathbf{x}_1\right] dt \\ &+ \int_{T_i}^{T}\left[\frac{\partial H_2}{\partial \mathbf{x}_2} d\mathbf{x}_2 + \frac{\partial H_2}{\partial u} du + \dot{\boldsymbol{\lambda}}_2^\top(t)\, d\mathbf{x}_2\right] dt \end{aligned} \tag{4.10}$$

From Eq. (4.4), the optimal $dW(\epsilon,\delta)$ is:

$$\begin{aligned} dW(\epsilon,\delta)|_{\epsilon=0,\delta=0} = &\left[H_1\left(T_i^*\right) - H_2\left(T_i^*\right)\right] d\delta \\ &- \boldsymbol{\lambda}_1^\top\left(T_i^*\right)\left[d\mathbf{x}_1\left(T_i^*\right) + \dot{\mathbf{x}}_1\left(T_i^*\right) d\delta\right] \\ &+ \boldsymbol{\lambda}_2^\top\left(T_i^*\right)\left[d\mathbf{x}_2\left(T_i^*\right) + \dot{\mathbf{x}}_2\left(T_i^*\right) d\delta\right] \\ &+ \boldsymbol{\lambda}_1^\top(t_0)\, d\mathbf{x}_1|_{t=t_0} - \boldsymbol{\lambda}_2^\top(T)\, d\mathbf{x}_1|_{t=T} \\ &+ \int_{t_0}^{T_i^*}\left[\frac{\partial H_1}{\partial \mathbf{x}_1} d\mathbf{x}_1 + \frac{\partial H_1}{\partial u} du + \dot{\boldsymbol{\lambda}}_1^\top(t)\, d\mathbf{x}_1\right] dt \\ &+ \int_{T_i^*}^{T}\left[\frac{\partial H_2}{\partial \mathbf{x}_2} d\mathbf{x}_2 + \frac{\partial H_2}{\partial u} du + \dot{\boldsymbol{\lambda}}_2^\top(t)\, d\mathbf{x}_2\right] dt = 0 \end{aligned} \tag{4.11}$$

Borrowing ideas from [43] and [73], we note that the variation in the optimal $\mathbf{x}^*(t)$ at time T_i^* is (see Fig. 4.1):

$$d\mathbf{x}(T_i^*) = \mathbf{x}(T_i^*) - \mathbf{x}^*(T_i^*) = \left.\frac{\partial \mathbf{x}}{\partial \epsilon}\right|_{t=T_i^*} d\epsilon + \left.\frac{\partial \mathbf{x}}{\partial \delta}\right|_{t=T_i^*} d\delta \tag{4.12}$$

and the overall variation from the optimal state at T_i^* is:

$$d\mathbf{x}_{T_i} = \mathbf{x}(T_i^* + \delta) - \mathbf{x}^*(T_i^*) \tag{4.13}$$

To estimate the variation $d\mathbf{x}_{T_i}$ we expand the function $\mathbf{x}(T_i^* + \delta)$ around $\mathbf{x}(T_i^*)$ by using Taylor approximation and obtain:

$$\begin{aligned} d\mathbf{x}_{T_i} &= \mathbf{x}(T_i^*) + \dot{\mathbf{x}}(T_i^*)\delta - \mathbf{x}^*(T_i^*) \\ &= d\mathbf{x}(T_i^*) + \dot{\mathbf{x}}(T_i^*)\,\delta \end{aligned} \tag{4.14}$$

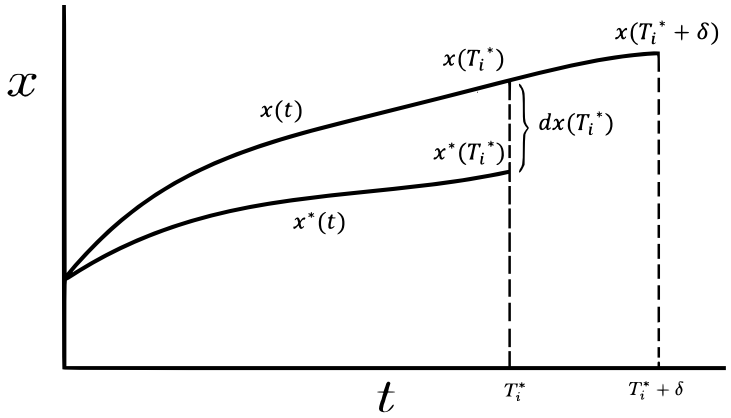

Fig. 4.1: A graph showing the variation of the variable x from the optimum x^* at time T_i^*.

Therefore, Eq. (4.11) can be written as:

$$\begin{aligned} dW(\epsilon,\delta) = &\left[H_1\left(T_i^*\right) - H_2\left(T_i^*\right)\right] d\delta - \boldsymbol{\lambda}_1^\top\left(T_i^*\right) d\mathbf{x}_{1\,T_i} + \boldsymbol{\lambda}_2^\top\left(T_i^*\right) d\mathbf{x}_{2\,T_i} \\ &+ \boldsymbol{\lambda}_1^\top(t_0)\, d\mathbf{x}_1(t_0) - \boldsymbol{\lambda}_2^\top(T)\, d\mathbf{x}_2(T) \\ &+ \int_{t_0}^{T_i^*} \left[\frac{\partial H_1}{\partial \mathbf{x}_1} d\mathbf{x}_1 + \frac{\partial H_1}{\partial u_1} du_1 + \dot{\boldsymbol{\lambda}}_1^\top(t)\, d\mathbf{x}_1\right] dt \\ &+ \int_{T_i^*}^{T} \left[\frac{\partial H_2}{\partial \mathbf{x}_2} d\mathbf{x}_2 + \frac{\partial H_2}{\partial u_2} du_2 + \dot{\boldsymbol{\lambda}}_2^\top(t)\, d\mathbf{x}_2\right] dt \end{aligned} \tag{4.15}$$

For Eq. (4.4) to be satisfied the following conditions are required:

$$(i)\quad \frac{\partial H_1}{\partial u_1} = 0 \qquad (ii)\quad \dot{\boldsymbol{\lambda}}_1^\top = -\frac{\partial H_1}{\partial \mathbf{x}_1}$$

$$(iii)\quad \frac{\partial H_2}{\partial u_2} = 0 \qquad (iv)\quad \dot{\boldsymbol{\lambda}}_2^\top = -\frac{\partial H_2}{\partial \mathbf{x}_2}$$

$$(v)\quad \boldsymbol{\lambda}_1^\top(t_0)\, d\mathbf{x}_1(t_0) - \boldsymbol{\lambda}_2^\top(T)\, d\mathbf{x}_2(T) = 0$$

$$(vi)\quad \boldsymbol{\lambda}_1^\top\left(T_i^*\right) d\mathbf{x}_{1\,T_i} - \lambda_2^\top\left(T_i^*\right) d\mathbf{x}_{2\,T_i} = 0$$

$$(vii) \quad H_1\left(T_i^*\right) - H_2\left(T_i^*\right) = 0$$

Conditions (i) and (iii) are used to find u_1 and u_2 as functions of $\mathbf{x}$ and $\boldsymbol{\lambda}$. Conditions (ii) and (iv) are used to construct additional differential equations for the Lagrange multiplier functions in the interval $0 < t \leq T_i$ and $T_i < t \leq T$ respectively. If the state variable $\mathbf{x}$ is fixed at any boundary point(t_0, T_i and T), then $d\mathbf{x}$ at this point is zero and the associated Lagrange multiplier function at that point is free (unknown). If the state variable is free at any boundary point, then the Lagrange multiplier function at this point needs to be set to zero. However, if the boundary conditions are periodic, that is $d\mathbf{x_1}(t_0) = d\mathbf{x_2}(T)$, condition (v) implies that $\boldsymbol{\lambda}_1(t_0) = \boldsymbol{\lambda}_2(T)$. Similarly, if the state variable is continuous and unknown at $t = T_i$, then we expect that $d\mathbf{x_1}_{T_i} = d\mathbf{x_2}_{T_i}$ and condition (vi) implies that $\boldsymbol{\lambda}_1(T_i^*) = \boldsymbol{\lambda}_2(T_i^*)$.

4.2 Calculating an Optimal Driving Force for the $2D$ Model

In chapter 3 we solved the optimal problem defined in chapter 2 when $F(t)$ was a given function, and the optimal values of V_T and T were unknown. We now use the conditions developed in Section (4.1) to solve the optimization problem when $F(t)$, T_i and T are unknown for a given V_T. We would like to minimize the cost function:

$$W = \int_0^T F(t)\dot{V}_A(t)dt \tag{4.16}$$

which is equivalent to minimizing the total work done by the respiratory muscles during one whole breath (see Eq. (3.28), where R is a constant), subject to the following constraints:

i The differential equations (Eq. 2.17 and 2.19) are satisfied.

ii The system of equations is in periodic steady state with period T, that is $V_A(0) = V_A(T)$ and $Y_c(0) = Y_c(T)$.

iii The initial value and amplitude of $V_A(t)$ are given as B and V_T respectively. That is, $V_A(0) = B$ and $V_A(T_i) = B + V_T$, where T_i is the time to reach a maximum V_A.

iv The average value of Y_c is a given fixed value, $y_{av} = \frac{1}{T}\int_0^T Y_c(t)\,dt$, where y_{av} is a constant.

The constraint (iv) can be replaced by the differential equation

$$\frac{dM}{dt} = Y_c \tag{4.17}$$

with the boundary conditions $M(0) = 0$ and $M(T) = T\ y_{av}$.

Following the general discussion in Section (4.1), let H_1 and H_2 be the Hamiltonians of the problem over the intervals $0 < t \leq T_i$ and $T_i < t \leq T$ respectively such that:

$$H_1 = F_1 \dot{V}_{A1} + \lambda_{11}(t)\dot{V}_{A1} + \lambda_{12}(t)\dot{Y}_{c1} + \lambda_{13}(t)\dot{z}_1 \tag{4.18}$$

$$H_2 = F_2 \dot{V}_{A2} + \lambda_{21}(t)\dot{V}_{A2} + \lambda_{22}(t)\dot{Y}_{c2} + \lambda_{23}(t)\dot{z}_2 \tag{4.19}$$

Here, λ_{ij} are unknown adjoint functions of time (sometimes known as Lagrange multipliers).

For the interval $0 < t \leq T_i$ we can construct three additional differential equations for Lagrange multipliers (see condition (ii) of section 4.1):

$$\dot{\lambda}_{11} = -\frac{\partial H_1}{\partial V_{A1}} = \alpha F_1 + \alpha\lambda_{11} + \hat{\gamma}\lambda_{12} \tag{4.20}$$

$$\dot{\lambda}_{12} = -\frac{\partial H_1}{\partial Y_{c1}} = \beta\lambda_{12} - \lambda_{13} \tag{4.21}$$

$$\dot{\lambda}_{13} = -\frac{\partial H_1}{\partial M_1} = 0 \tag{4.22}$$

where $\hat{\gamma} = \frac{\gamma(V_T - V_D)}{V_T}$. By using the condition $\partial H_1/\partial F_1 = 0$ (see condition (i) of section 4.1), we get:

$$F_1 = \frac{1}{2}\left(\alpha V_{A1} - \lambda_{11} - \hat{\gamma}\lambda_{12}\right) \tag{4.23}$$

Substituting Eq. (4.23) into the differential equations (2.17), (2.19), (4.17) and (4.20)-(4.22) yields the following system of differential equations:

$$\dot{\mathbf{A}}_1 = \begin{bmatrix} -\frac{\alpha}{2} & 0 & 0 & -\frac{1}{2} & -\frac{\hat{\gamma}}{2} & 0 \\ -\frac{\alpha\hat{\gamma}}{2} & -\beta & 0 & -\frac{\hat{\gamma}}{2} & -\frac{\hat{\gamma}^2}{2} & 0 \\ 0 & 1 & 0 & 0 & 0 & 0 \\ \frac{\alpha^2}{2} & 0 & 0 & \frac{\alpha}{2} & \frac{\alpha\hat{\gamma}}{2} & 0 \\ 0 & 0 & 0 & 0 & \beta & -1 \\ 0 & 0 & 0 & 0 & 0 & 0 \end{bmatrix} \mathbf{A}_1 \tag{4.24}$$

where $\mathbf{A_1} = \begin{bmatrix} V_{A1} & Y_{c1} & M_1 & \lambda_{11} & \lambda_{12} & \lambda_{13} \end{bmatrix}^\top$

Similarly, for the interval $T_i < t \leq T$ we can construct three additional differential equations for Lagrange multipliers (see condition (iv) of section 4.1):

$$\dot{\lambda}_{21} = -\frac{\partial H_2}{\partial V_{A2}} = \alpha F_2 + \alpha\lambda_{21} \tag{4.25}$$

$$\dot{\lambda}_{22} = -\frac{\partial H_2}{\partial Y_{c2}} = \beta\lambda_{22} - \lambda_{23} \tag{4.26}$$

$$\dot{\lambda}_{23} = -\frac{\partial H_1}{\partial M_2} = 0 \tag{4.27}$$

By taking the condition $\partial H_2/\partial F_2 = 0$ (see condition (iii) of section 4.1), we get:

$$F_2 = \frac{1}{2}(\alpha V_{A2} - \lambda_{21}) \tag{4.28}$$

Substituting Eq. (4.28) into the differential equations (2.17), (2.19), (4.17) and (4.25)-(4.27) yields the following system of differential equations:

$$\dot{\mathbf{A}}_2 = \begin{bmatrix} -\frac{\alpha}{2} & 0 & 0 & -\frac{1}{2} & 0 & 0 \\ 0 & -\beta & 0 & 0 & 0 & 0 \\ 0 & 1 & 0 & 0 & 0 & 0 \\ \frac{\alpha^2}{2} & 0 & 0 & \frac{\alpha}{2} & 0 & 0 \\ 0 & 0 & 0 & 0 & \beta & -1 \\ 0 & 0 & 0 & 0 & 0 & 0 \end{bmatrix} \mathbf{A}_2 \tag{4.29}$$

where $\mathbf{A}_2 = \begin{bmatrix} V_{A2} & Y_{c2} & M_2 & \lambda_{21} & \lambda_{22} & \lambda_{23} \end{bmatrix}^\top$

By solving the equations (4.24) and (4.29), we obtain:

$$V_{A1} = -C_2\frac{\hat{\gamma}}{\alpha\beta} + C_3\frac{\beta}{\hat{\gamma}} - C_4\frac{2\beta}{\alpha\hat{\gamma}} + C_4\frac{\beta}{\hat{\gamma}}t - C_6\frac{\hat{\gamma}}{2\beta}e^{\beta t} \tag{4.30}$$

$$Y_{c1} = C_4 - C_5\beta e^{-\beta t} - C_6\frac{\hat{\gamma}^2}{4\beta}e^{\beta t} \tag{4.31}$$

$$M_1 = C_1\frac{\hat{\gamma}}{\alpha\beta} + C_3 + C_4 t + C_5 e^{-\beta t} - C_6\frac{\hat{\gamma}^2}{4\beta^2}e^{\beta t} \tag{4.32}$$

$$\lambda_{11} = -C_3\frac{\alpha\beta}{\hat{\gamma}} - C_4\frac{\alpha\beta}{\hat{\gamma}}t + C_6\frac{\alpha\hat{\gamma}}{2\beta}e^{\beta t} \tag{4.33}$$

$$\lambda_{12} = C_2\frac{1}{\beta} + C_6 e^{\beta t} \tag{4.34}$$

$$\lambda_{13} = C_2 \tag{4.35}$$

$$V_{A2} = -\frac{C_8}{\alpha} + \frac{2C_9}{\alpha^2} - \frac{C_9 t}{\alpha} \tag{4.36}$$

$$Y_{c2} = -C_{11}\beta e^{-\beta t} \tag{4.37}$$

$$M_2 = C_{10} + C_{11}e^{-\beta t} \tag{4.38}$$

$$\lambda_{21} = C_8 + C_9 t \tag{4.39}$$

$$\lambda_{22} = \frac{C_7}{\beta} + C_{12}e^{\beta t} \tag{4.40}$$

$$\lambda_{23} = C_7 \tag{4.41}$$

We also have the following 12 boundary conditions (see section 4.1 for more details):

$$\begin{array}{lll} V_{A1}(0) = B, & V_{A1}(T_i) = B + V_T, & V_{A2}(T_i) = B + V_T, \\ V_{A2}(T) = B, & Y_{c1}(0) = Y_{c_2}(T), & Y_{c1}(T_i) = Y_{c_2}(T_i), \\ M_1(0) = 0, & M_1(T_i) = M_2(T_i), & \lambda_{12}(0) = \lambda_{22}(T), \\ \lambda_{12}(T_i) = \lambda_{22}(T_i), & \lambda_{13}(T_i) = \lambda_{23}(T_i), & \lambda_{13}(T) = 0 \end{array} \tag{4.42}$$

Recall that λ_1, λ_2 and λ_3 are the Lagrange multipliers associated with thevariables V_A, Y_c and M respectively. As V_A is fixed at $t = 0$, T_i and T, the Lagrange multiplier λ_1 is free at these boundary points (see conditions (v) and (vi) of section 4.1). The variable Y_c is periodic and free hence λ_2 is also periodic and free (see conditions (v) of section 4.1). Y_c and M are continuous and free at $t = T_i$, therefore λ_2 and λ_3 are also continuous and free at $t = T_i$ (see conditions (vi) of section 4.1). The variable M is fixed at $t = 0$, and free at $t = T$, so λ_3 is free at $t = 0$ and zero at $t = T$.

This allows us to find the coefficients C_1 to C_{12} by using conditions 4.42. We get:

$$\begin{aligned}
C_1 &= -\alpha B + \tfrac{V_T\left(2\beta-(\alpha+2\beta)e^{\beta T}+\alpha e^{\beta T_i}\right)}{\beta T_i\left(e^{\beta T}-1\right)}, & C_2 &= 0,\\
C_3 &= \tfrac{\hat{\gamma}}{\alpha\beta T_i}\left(2V_T+\alpha B T_i\right), & C_4 &= \tfrac{V_T\hat{\gamma}}{\beta T_i},\\
C_5 &= \tfrac{V_T\hat{\gamma}(e^{\beta T}-e^{\beta T_i})}{\beta^2 T_i(e^{\beta T}-1)}, & C_6 &= 0,\\
C_7 &= 0, & C_8 &= -\alpha B - \tfrac{V_T(\alpha T-2)}{T-T_i},\\
C_9 &= \tfrac{\alpha V_T}{T-T_i}, & C_{10} &= \tfrac{V_T\hat{\gamma}}{\beta} + \tfrac{V_T\hat{\gamma}\left(e^{\beta \mathrm{Ti}}-1\right)}{\beta^2 T_i\left(e^{\beta T}-1\right)},\\
C_{11} &= \tfrac{V_T\hat{\gamma}e^{\beta T}\left(1-e^{\beta T_i}\right)}{\beta^2 \mathrm{Ti}\left(e^{\beta T}-1\right)}, & C_{12} &= 0
\end{aligned}$$

Substituting C_1 to C_{12} into Eqs. (4.30) - (4.41), and by using Eqs. (4.23) and (4.28) we then obtain the optimal function $F(t)$ for a given V_T:

$$F(t) = \begin{cases} \alpha B + \frac{V_T}{T_i}(1+\alpha t) & ; \quad 0 < t \le T_i \\ \\ \alpha B + \frac{V_T}{T_i}(\alpha T - \alpha t - 1) & ; \quad T_i < t \le T \end{cases} \tag{4.43}$$

From the conditions $u_2(T) = T\ y_{av}$ and $H_1(T_i) = H_2(T_i)$, the optimal durations T and T_i are found:

$$T = \frac{\gamma\,(V_T - V_D)}{\beta\ y_{av}} \tag{4.44}$$

$$T_i = \frac{\gamma\,(V_T - V_D)}{2\ \beta\ y_{av}} = \frac{T}{2} \tag{4.45}$$

The optimal solution is linear and the optimal period we get by using optimal control theory is the same as that obtained when $F(t)$ was a given function. Likewise, the optimal T_i is half the period, which is the same as was found in Section 3.4.

4.3 Numerical Solution of the Optimal Problem

The algorithm shown in Fig. 4.2, allows us to find the optimal combinations of tidal volume (V_T), breathing period (T) and duration of inhalation (T_i) numerically. First, we provide a range of values for V_T, such that $V_{T\,min} \le V_T \le V_{T\,max}$. For each value of V_T, we initially guess T and T_i and solve the piecewise differential equations (4.24) and (4.29) with boundary conditions (4.42) by using the Matlab built-in function $bvp4c$. We then check the conditions $M_2(T) - T \cdot y_{av} < \epsilon$ and $H_1(T_i) - H_2(T_i) < \epsilon$, where ϵ is the error tolerance ($\epsilon = 10^{-8}$ in all our computations).

If these conditions are not satisfied, we use Newton's method to correct the values of T and T_i.

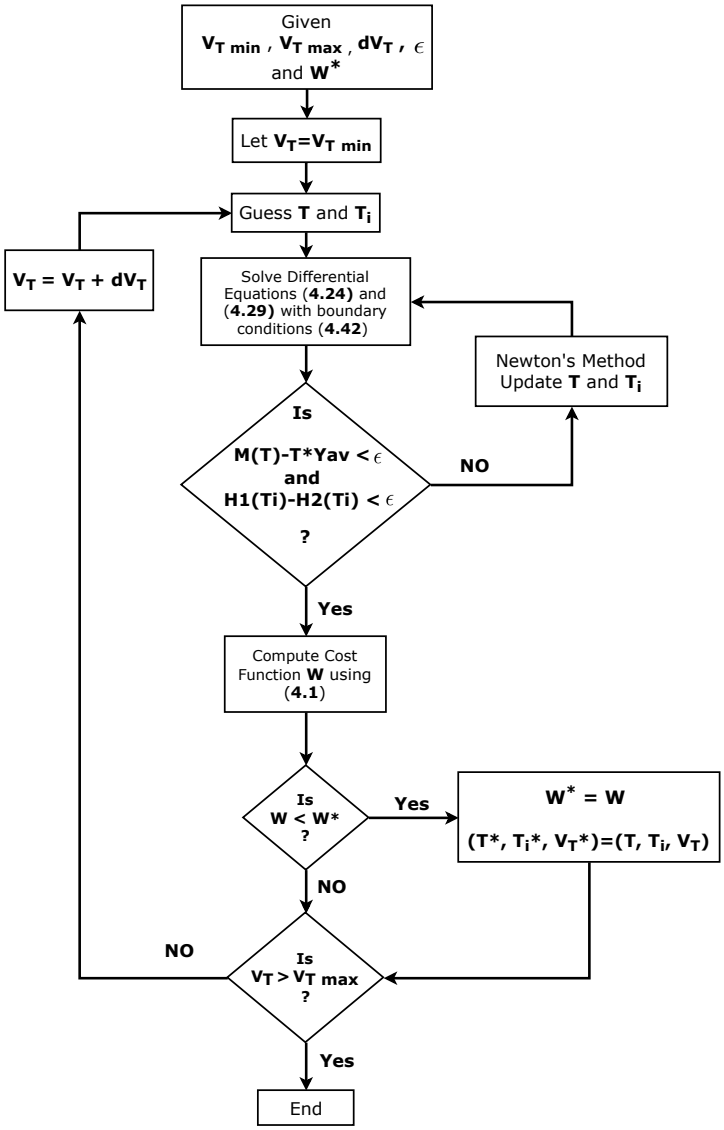

Fig. 4.2: Flowchart of the numerical algorithm.

In order to do this we define the intial guesses as $T^1$and T_i^1 and the subsequent corrcetions as $T^n$and T_i^n, where n represents the n^{th} iteration. We also define $\tau^{\mathbf{n}} = [T^n,\ T_i^n]^\top$ and $\mathbf{e^n} = [e_1^n,\ e_2^n]^\top$, where $e_1^n = M_2(T^n) - T^n \cdot y_{av}$ and $e_2^n = H_1(T_i^n) - H_2(T_i^n)$. We then compute $\mathbf{k^n}$ such that $\mathbf{J^n} \cdot \mathbf{k^n} = \mathbf{e^n}$, where $\mathbf{J^n}$ is the Jacobian matrix computed by numerical differentiation, and update T^n and T_i^n using the equation: $\tau^{\mathbf{n+1}} = \tau^{\mathbf{n}} - \mathbf{k^n}$. The boundary value problem is solved for each iteration n untill e_1^n and e_2^n are less than ϵ.

Finally, W is calculated by numerical integration (we used the trapezoidal rule in all our numerical calculations). Each time W is calculated for a new value of V_T, we compare it with the value of W^* previously calculated (initially we provide a high value of W^*). If it has a lower value, we record it along with the corresponding values of V_T, T and T_i. The values we obtain at the end of this process are the optimal values W^*, V_T^*, T^* and T_i^*. Fig. 4.3 shows a comparison between the optimal numerical solution and the optimal analytical solution. As can be seen, there is a good agreement between these two solutions.

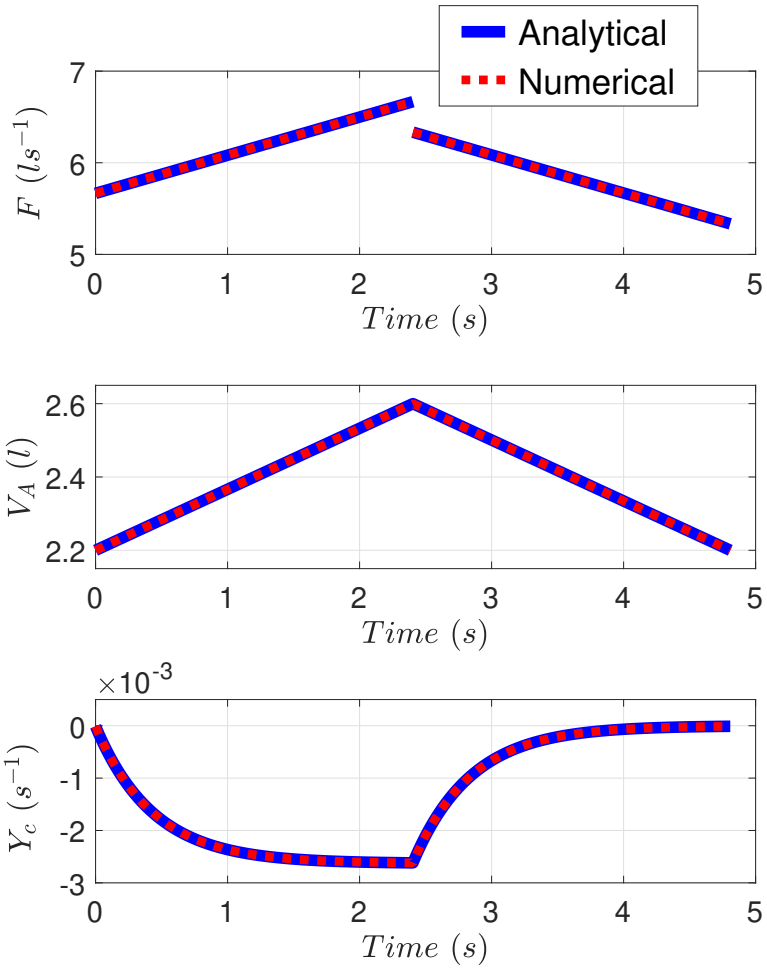

Fig. 4.3: Comparision of the solutions $F(t)$, $V_A(t)$ and $Y_c(t)$ when calculated numerically and analytically for the $2D$ linear model (Eq. (2.17) and (2.19). See Table 2, for all values of the parameters.

As we discussed in Chapter 1, the $5D$ model approximates the $6D$ model. The same combination of breathing frequency and amplitude gives slightly a higher

level of concentration of CO_2 in the lungs for the $5D$ model. To be able to compare the optimal amplitude and frequency of both models, we chose to maintain the concentration of CO_2 in the lungs at about 6.1% in the $5D$ model. If the same amplitude and frequency we used in the $5D$ model with a sinusoidal pleural pressure were used in the $6D$ model with a sinusoidal pleural pressure, the lung concentration of CO_2 would be 5.2%.

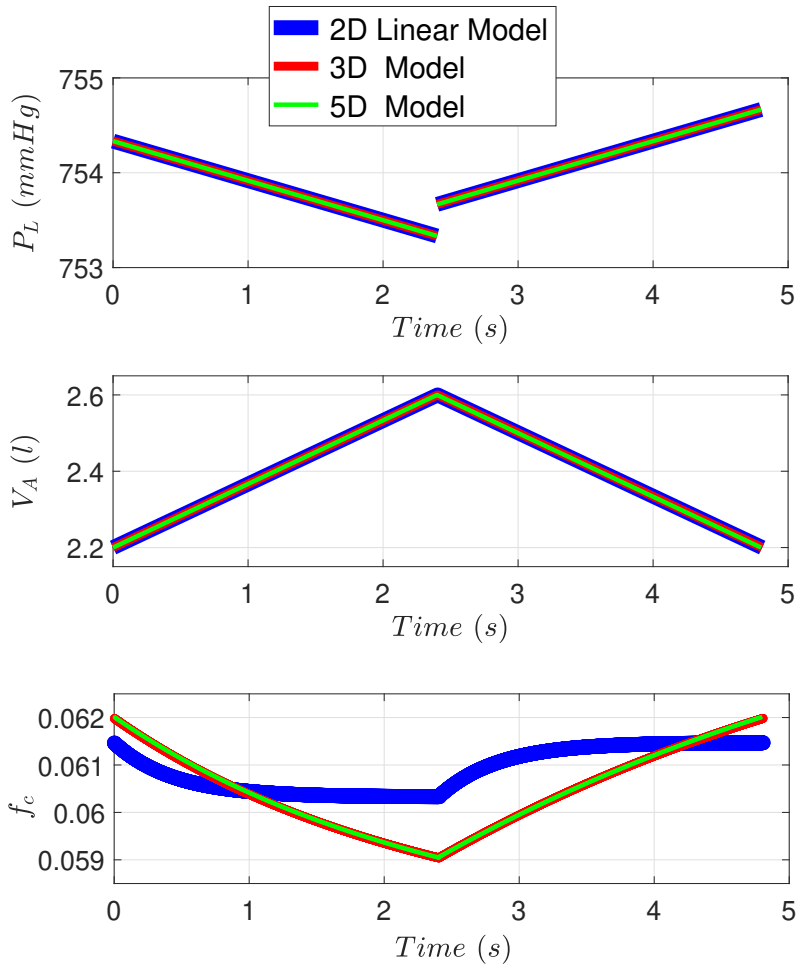

Fig. 4.4: Comparison of the optimal solution of P_L, V_A and f_c for the $2D$, $3D$ and $5D$ models when $V_T = 0.4\ l$ and $T = 4.82\ s$. Here we fixed T and T_i which leads to different average levels of f_c. For the $2D$ model, $P_L = P_m - RF$ (see Section 2.3). See Table 2, for all values of the parameters.

Next we solve the optimal control problem for the $3D$ and $5D$ models. We have obtained the optimal control problem for these models numerically, as the models are nonlinear. First, we observe how these different models effect the average value

of f_c for a given fixed V_T, T_i and T. Fig. 4.4 shows that the average value of f_c for the $3D$ and $5D$ models is approximately the same, but, for the $2D$ linear model the average value is slightly different. However, we have also observed an interesting fact that the optimal driving force (pleural pressure) is the same for all models with the given cost function (see Fig . 4.4). The simulations shown in Fig. 4.5 are for maintaining the concentration of CO_2 at 6.1%. This supports the hypothesis of a constant effective minute ventilation for all models, as the relationship between V_T and T is linear for the 2D model and almost linear for the other models.

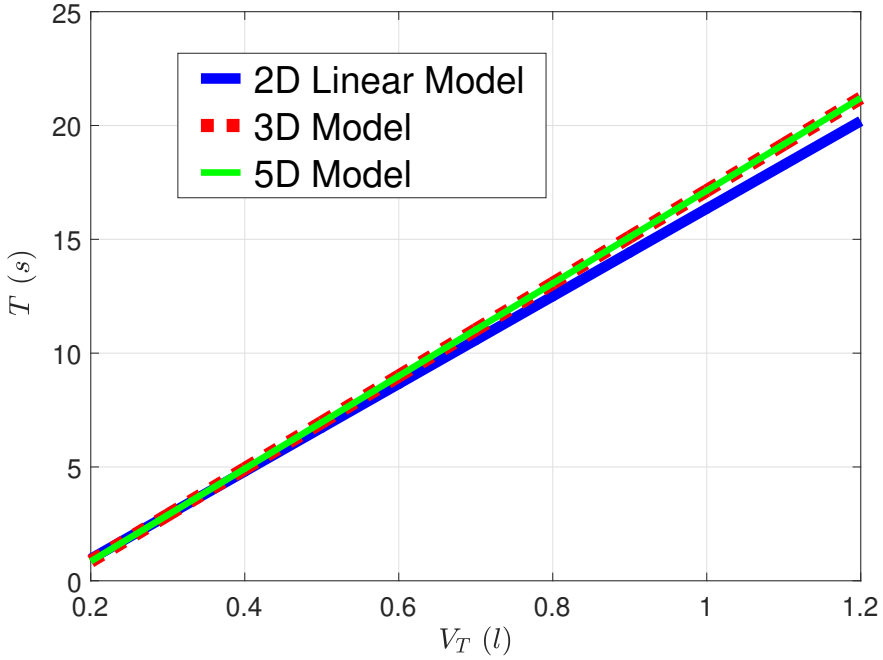

Fig. 4.5: Relationship between the tidal volume and breathing period for the $2D$, $3D$ and $5D$ models.

We found in this chapter that the optimal volume has a triangular shape with a constant flow rate (see Fig. 4.4). We showed in Fig. 3.18 that for any $V_T > V_D$, the sinusoidal pleural pressure (P_L) consumes about twenty-three percent more energy than the optimal P_L. However, the optimal P_L is discontinuous. This suggests that the work of breathing is not the optimization criterion for selecting a particular breathing pattern. Nevertheless, some observational data show that the human breathing pattern during exercise is triangular [69]. Thus, the criterion of minimum total work of breathing could predict the human breathing pattern under exercise conditions but not at rest.

Chapter 5

Solutions for other Cost Functions

In chapter 4, we found the optimal breathing pattern that minimizes the total work done by the respiratory muscles during each breath using optimal control theory. This gave an optimal pleural pressure that is discontinuous in time, and an optimal duration of inspiration equal to the duration of expiration. In this chapter we discuss some other mechanical cost functions that have been proposed previously in the literature for respiratory control optimization.

First, we define a weighted function that merges several of the previously suggested cost functions, specifically, the average square volumetric acceleration, work rate and average square force developed by the respiratory muscles. We then solve several special cases in which some of the functions are neglected. We show that the breathing pattern optimised by considering the work rate only is discontinuous and there is no optimal solution which minimizes the average square force. Finally, we find the breathing patterns associated with different weighting coefficients.

5.1 Weighted Cost Function

Hämäläinen and Viljanen [31] were the first to discuss two separate mechanical cost functions for the inhalation and exhalation phases of respiration. During inhalation, they merged weighted functions of the average square volumetric acceleration and work rate. During expiration they replaced the work rate term with the average square of the respiratory pressure. In this section, we consider various mechanical cost functions used previously to find the optimal breathing

pattern, as weighted functions in a single expression. The single cost function is represented as:

$$J_I = \frac{1}{T}\int_0^{T_i} \left[\eta_1 \ddot{V}_A{}^2 + \eta_2 (P_m - P_L)\, \dot{V}_A + \eta_3 (P_m - P_L)^2\right] dt, \tag{5.1}$$

$$J_E = \frac{1}{T}\int_{T_i}^{T} \left[\eta_1 \ddot{V}_A^2 + \eta_2 R \dot{V}_A^2 + \eta_3 (P_m - P_L)^2\right] dt, \tag{5.2}$$

J_I and J_E represent the cost function during inhalation and exhalation respectively. These cost functions interpreted as the weighted sum of the average square volumetric acceleration, work rate and the average square force developed by the respiratory muscles. During exhalation, the respiratory muscles relax and release the elastic energy that was stored during inhalation. So, there is no need to consider the elastic work during exhalation and we only consider the work caused by the airflow resistance during exhalation. The parameters η_1, η_2 and η_3 represent the weights for the average volumetric acceleration, work rate and the average square force respectively. The parameters η_1, η_2 and η_3 have the units $l^{-2}s^4$, $mmHg^{-1}l^{-1}s$ and $mmHg^{-2}$ respectively. This gives a non-dimensional cost function.

The cost function includes $\ddot{V}_A$, so we present $\ddot{V}_A$ in terms of other variables. By differentiating Eq. (2.6) with respect to time and substituting $\dot{V}_A$, we get:

$$\ddot{V}_A = \frac{E^2}{R^2} V_A - \frac{E}{R^2}(P_m - P_L) - \frac{1}{R}\dot{P}_L \tag{5.3}$$

Now, we can represent Eq. (5.3) as a system of two first order differential equations. Let:

$$\dot{P}_L = -G \tag{5.4}$$

$$\dot{V}_A = W \tag{5.5}$$

this implies that Eq. (5.3) can be written as:

$$\dot{W} = \frac{E^2}{R^2} V_A - \frac{E}{R^2}(P_m - P_L) + G \tag{5.6}$$

Here, W represents the airflow rate and G is the input control variable with conditions $W(0) = W(T_i) = W(T) = 0$ and $P_L(0) = P_L(T)$.

For the $2D$ model, the cost functions (5.1) and (5.2) are represented as:

$$J_I = \frac{1}{T}\int_0^{T_i} \left[\eta_1 \ddot{V}_A{}^2 + \eta_2 F\dot{V}_A + \eta_3 F^2\right] dt, \tag{5.7}$$

$$J_E = \frac{1}{T}\int_{T_i}^{T} \left[\eta_1 \ddot{V}_A^2 + \eta_2 R\dot{V}_A^2 + \eta_3 F^2\right] dt, \tag{5.8}$$

and Eq. (5.5) is the same as for the $5D$ model, however, Eq. (5.4) and (5.6) are replaced with:

$$\dot{F} = G \tag{5.9}$$

$$\dot{W} = \alpha^2 V_A - \alpha F + G \tag{5.10}$$

with conditions $W(0) = W(T_i) = W(T) = 0$ and $F(0) = F(T)$.

We solve the optimization problem for the $2D$ model that minimizes the cost function (5.7) and (5.8) when $G(t)$, T_i and T are unknown for a given V_T during one whole breath, subject to the following constraints:

i The differential equations (Eq. (2.19), (5.5), (5.9) and (5.10)) are satisfied.

ii The system of equations is in a periodic steady state with period T, that is $V_A(0) = V_A(T)$, $W(0) = W(T)$, $Y_c(0) = Y_c(T)$ and $F(0) = F(T)$.

iii The initial value and amplitude of $V_A(t)$ are given as B and V_T respectively. That is, $V_A(0) = B$ and $V_A(T_i) = B + V_T$, where T_i is the time to reach a maximum V_A.

iv The average value of Y_c is a given fixed value, $y_{av} = \frac{1}{T}\int_0^T Y_c(t)\, dt$, where y_{av} is a constant. (Recall that the variable Y_c provides a measure of CO_2 concentration in the lungs, $Y_c = D_c(E + K_1) f_c - D_c K_2$, see Section 2.2.2).

The constraint (iv) can be replaced by the differential equation

$$\frac{dM}{dt} = Y_c \tag{5.11}$$

with the boundary conditions $M(0) = 0$ and $M(T) = T\ y_{av}$.

5.2 Average Square Volumetric Acceleration

In this section, we first derive the optimal breathing pattern that minimizes the average square volumetric acceleration for the $2D$ model. By substituting $\eta_1 = 1$, $\eta_2 = 0$ and $\eta_3 = 0$ into Eqs. (5.1) and (5.2), we get the cost function:

$$J = \frac{1}{T}\int_0^T \ddot{V}_A^2 dt, \tag{5.12}$$

Let H_1 and H_2 be the Hamiltonians during inhalation ($0 < t \leq T_i$) and exhalation ($T_i < t \leq T$) respectively, that is:

$$H_1 = \frac{1}{T}\ddot{V}_{A1}^2 + \lambda_{11}(t)\dot{F}_1 + \lambda_{12}(t)\dot{V}_{A1} + \lambda_{13}(t)\dot{W}_1 + \lambda_{14}(t)\dot{Y}_{c1} + \lambda_{15}(t)\dot{M}_1 \tag{5.13}$$

$$H_2 = \frac{1}{T}\ddot{V}_{A2}^2 + \lambda_{21}(t)\dot{F}_2 + \lambda_{22}(t)\dot{V}_{A2} + \lambda_{23}(t)\dot{W}_2 + \lambda_{24}(t)\dot{Y}_{c2} + \lambda_{25}(t)\dot{M}_2 \tag{5.14}$$

where, λ_{ij} are unknown adjoint functions of time (known as Lagrange multipliers). During inhalation ($0 < t \leq T_i$), we can construct five additional differential equations for the Lagrange multipliers (see condition (ii) of section 4.1):

$$\dot{\lambda}_{11} = -\frac{\partial H_1}{\partial F_1} = -\frac{2\alpha^2}{T}F_1 + \frac{2\alpha^3}{T}V_{A1} + \frac{2\alpha}{T}G_1 + \alpha\lambda_{13} \tag{5.15}$$

$$\dot{\lambda}_{12} = -\frac{\partial H_1}{\partial V_{A1}} = \frac{2\alpha^3}{T}F_1 - \frac{2\alpha^4}{T}V_{A1} - \frac{2\alpha^2}{T}G_1 - \alpha^2\lambda_{13} \tag{5.16}$$

$$\dot{\lambda}_{13} = -\frac{\partial H_1}{\partial W_1} = -\lambda_{12} + \hat{\gamma}\lambda_{14} \tag{5.17}$$

$$\dot{\lambda}_{14} = -\frac{\partial H_1}{\partial Y_{c1}} = \beta\lambda_{14} - \lambda_{15} \tag{5.18}$$

$$\dot{\lambda}_{15} = -\frac{\partial H_1}{\partial M_1} = 0 \tag{5.19}$$

Similarly, during exhalation ($T_i < t \leq T$), we can construct differential equations for the Lagrange multipliers (see condition (iv) of section 4.1):

$$\dot{\lambda}_{12} = -\frac{\partial H_2}{\partial F_2} = -\frac{2\alpha^2}{T}F_2 + \frac{2\alpha^3}{T}V_{A2} + \frac{2\alpha}{T}G_2 + \alpha\lambda_{23} \tag{5.20}$$

$$\dot{\lambda}_{22} = -\frac{\partial H_2}{\partial V_{A2}} = \frac{2\alpha^3}{T}F_2 - \frac{2\alpha^4}{T}V_{A2} - \frac{2\alpha^2}{T}G_2 - \alpha^2\lambda_{23} \tag{5.21}$$

$$\dot{\lambda}_{23} = -\frac{\partial H_2}{\partial W_2} = -\lambda_{22} \tag{5.22}$$

$$\dot{\lambda}_{24} = -\frac{\partial H_2}{\partial Y_{c2}} = \beta\lambda_{24} - \lambda_{25} \tag{5.23}$$

$$\dot{\lambda}_{25} = -\frac{\partial H_2}{\partial M_2} = 0 \tag{5.24}$$

where G_1 and G_2 are the control variables during inhalation and exhalation respectively. By using the conditions $\partial H_1/\partial G_1 = 0$ and $\partial H_2/\partial G_2 = 0$ (see condition (i) and (iii) of section 4.1), we get:

$$G_1 = \alpha F_1 - \alpha^2 V_{A1} - \frac{T}{2}\lambda_{11} - \frac{T}{2}\lambda_{13} \tag{5.25}$$

$$G_2 = \alpha F_2 - \alpha^2 V_{A2} - \frac{T}{2}\lambda_{21} - \frac{T}{2}\lambda_{23} \tag{5.26}$$

By using (5.25) and (5.26), we get the following differential system:

$$\dot{\mathbf{B}}_1 = \begin{bmatrix} \alpha & -\alpha^2 & 0 & 0 & 0 & -\frac{T}{2} & 0 & -\frac{T}{2} & 0 & 0 \\ 0 & 0 & 1 & 0 & 0 & 0 & 0 & 0 & 0 & 0 \\ 0 & 0 & 0 & 0 & 0 & -\frac{T}{2} & 0 & -\frac{T}{2} & 0 & 0 \\ 0 & 0 & \hat{\gamma} & -\beta & 0 & 0 & 0 & 0 & 0 & 0 \\ 0 & 0 & 0 & 1 & 0 & 0 & 0 & 0 & 0 & 0 \\ 0 & 0 & 0 & 0 & 0 & -\alpha & 0 & 0 & 0 & 0 \\ 0 & 0 & 0 & 0 & 0 & \alpha^2 & 0 & 0 & 0 & 0 \\ 0 & 0 & 0 & 0 & 0 & 0 & -1 & 0 & -\hat{\gamma} & 0 \\ 0 & 0 & 0 & 0 & 0 & 0 & 0 & 0 & \beta & -1 \\ 0 & 0 & 0 & 0 & 0 & 0 & 0 & 0 & 0 & 0 \end{bmatrix} \mathbf{B}_1 \tag{5.27}$$

$$\dot{\mathbf{B}}_2 = \begin{bmatrix} \alpha & -\alpha^2 & 0 & 0 & 0 & -\frac{T}{2} & 0 & -\frac{T}{2} & 0 & 0 \\ 0 & 0 & 1 & 0 & 0 & 0 & 0 & 0 & 0 & 0 \\ 0 & 0 & 0 & 0 & 0 & -\frac{T}{2} & 0 & -\frac{T}{2} & 0 & 0 \\ 0 & 0 & 0 & -\beta & 0 & 0 & 0 & 0 & 0 & 0 \\ 0 & 0 & 0 & 1 & 0 & 0 & 0 & 0 & 0 & 0 \\ 0 & 0 & 0 & 0 & 0 & -\alpha & 0 & 0 & 0 & 0 \\ 0 & 0 & 0 & 0 & 0 & \alpha^2 & 0 & 0 & 0 & 0 \\ 0 & 0 & 0 & 0 & 0 & 0 & -1 & 0 & 0 & 0 \\ 0 & 0 & 0 & 0 & 0 & 0 & 0 & 0 & \beta & -1 \\ 0 & 0 & 0 & 0 & 0 & 0 & 0 & 0 & 0 & 0 \end{bmatrix} \mathbf{B}_2 \tag{5.28}$$

where $\hat{\gamma} = \gamma\left(\frac{V_T - V_D}{V_T}\right)$, $\mathbf{B_1} = \begin{bmatrix} F_1 & V_{A1} & W_1 & Y_{c1} & M_1 & \lambda_{11} & \lambda_{12} & \lambda_{13} & \lambda_{14} & \lambda_{15} \end{bmatrix}^\top$ and $\mathbf{B_2} = \begin{bmatrix} F_2 & V_{A2} & W_2 & Y_{c2} & M_2 & \lambda_{21} & \lambda_{22} & \lambda_{23} & \lambda_{24} & \lambda_{25} \end{bmatrix}^\top$. We also have the following 20 boundary conditions for the state variables and Lagrange multipliers, λ_{ij}:

$$
\begin{aligned}
&F_1(0) = F_2(T), && F_1(T_i) = F_2(T_i), && V_{A1}(0) = B,\\
&V_{A2}(T) = B, && V_{A1}(T_i) = B + V_T, && V_{A2}(T_i) = B + V_T,\\
&W_1(0) = 0, && W_1(T_i) = 0, && W_2(T_i) = 0,\\
&W_2(T) = 0, && Y_{c1}(0) = Y_{c2}(T), && Y_{c1}(T_i) = Y_{c2}(T_i),\\
&u_1(0) = 0, && u_1(T_i) = u_2(T_i), && \lambda_{11}(0) = \lambda_{21}(T),\\
&\lambda_{11}(T_i) = \lambda_{21}(T_i), && \lambda_{14}(0) = \lambda_{24}(T), && \lambda_{14}(T_i) = \lambda_{24}(T_i),\\
&\lambda_{15}(T_i) = \lambda_{25}(T_i), && \lambda_{25}(T) = 0.
\end{aligned}
$$

Recall that λ_1, λ_2, λ_3, λ_4 and λ_5 are the Lagrange multipliers associated with the variables F, V_A, W, Y_c and M respectively (see Eqs. (5.13) and (5.14)). As V_A and W are fixed at $t = 0$, T_i and T, it follows that λ_2 and λ_3 are free at these boundary points (see conditions (v) and (vi) of section 4.1). The variables F and Y_c are periodic and free, hence λ_1 and λ_4 are also periodic and free (see conditions (v) of section 4.1). F, Y_c and M are continuous and free at $t = T_i$, therefore λ_1, λ_2 and λ_3 are also continuous and free at $t = T_i$ (see conditions (vi) of section 4.1). The variable M is fixed at $t = 0$, and free at $t = T$, so λ_3 is free at $t = 0$ and zero at $t = T$.

Solving the differential equations (Eq. (5.27) and (5.28))and using the above conditions, we get the optimal driving force $F(t)$ for a given V_T:

$$
F(t) = \begin{cases} \alpha B - \frac{6V_T t(t-T_i)}{T_i^3} + \frac{\alpha V_T t^2(3T_i - 2t)}{T_i^3} & ; \quad 0 < t \le T_i \\ \\ \alpha B - \frac{6V_T(t-T)(t-T_i)}{(T_i-T)^3} + \frac{\alpha V_T(t-T)^2(3T_i - 2t - T)}{(T_i-T)^3} & ; \quad T_i < t \le T \end{cases} \tag{5.29}
$$

and the corresponding alveolar volume:

$$
V_A(t) = \begin{cases} B + V_T \frac{t^2(3T_i - 2t)}{T_i^3} & ; \quad 0 < t \le T_i \\ \\ B + V_T \frac{(t-T)^2(3T_i - 2t - T)}{(T_i-T)^3} & ; \quad T_i < t \le T \end{cases} \tag{5.30}
$$

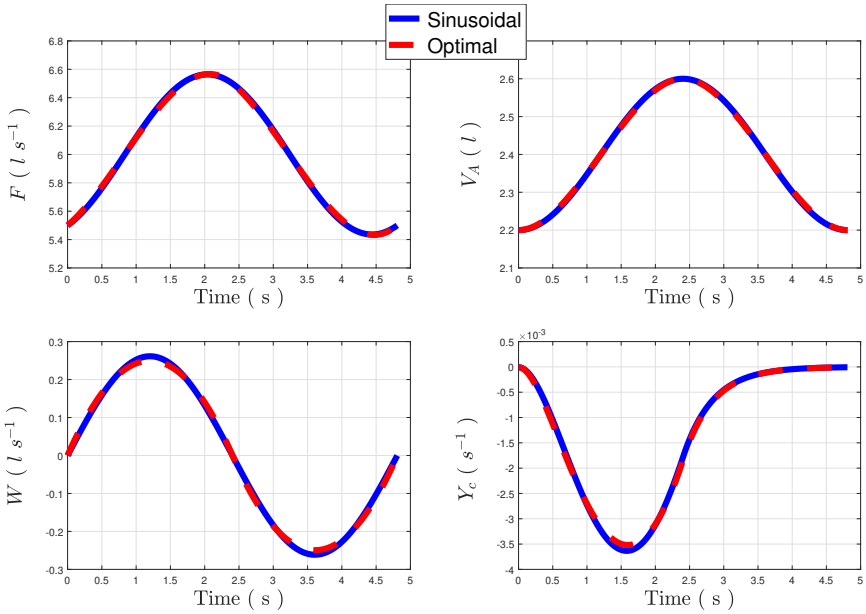

Fig. 5.1: Comparisons between trajectories of $F(t)$, $V_A(t)$, $W(t)$ and $Y_c(t)$ for sinusoidal and optimal airflows that minimizes Eq. (5.12). Calculations are done using the $2D$ linear model and both solutions maintain a specific value of $Y_{av} = -0.0013$, which is equivalent to $f_c = 6.1\%$. See Table 2, for all values of the arameters.

Using the conditions $M_2(T) = T\ y_{av}$ and $H_1(T_i) = H_2(T_i)$, the optimal durations T and T_i are:

$$T = \frac{\gamma\,(V_T - V_D)}{\beta\ y_{av}} \tag{5.31}$$

$$T_i = \frac{\gamma\,(V_T - V_D)}{2\ \beta\ y_{av}} = \frac{T}{2} \tag{5.32}$$

The optimal solution is a piecewise cubic function of time and the optimal T_i is half the period, which is the same result as when the total work was taken as the cost function. Figure (5.1) shows a comparison between trajectories derived for a sinusoidal airflow and the optimal piecewise cubic function constrained to maintaining the average concentration of CO_2 at 6.1%. The optimal airflow is symmetrical as is the sinusoidal signal, but it has a slightly lower peak.

Next we solve this optimal control problem for the $5D$ model. Figure 5.2 shows a comparison of the solutions of the $2D$ and $5D$ models for a given V_T and T. As can be seen, the shape of the breathing pattern is the same for both models, however,

the average level of concentration of CO_2 in the lungs is slightly lower for the $5D$ model. Figure 5.3 shows the optimal solution of the $2D$ and $5D$ model when the concentration of CO2 in the lungs is maintained at 6.1%. In order to achieve the same optimal duration, the breathing amplitude is lower for the $5D$ model (V_T = 0.375 l) than for the $2D$ model (V_T = 0.4 l).

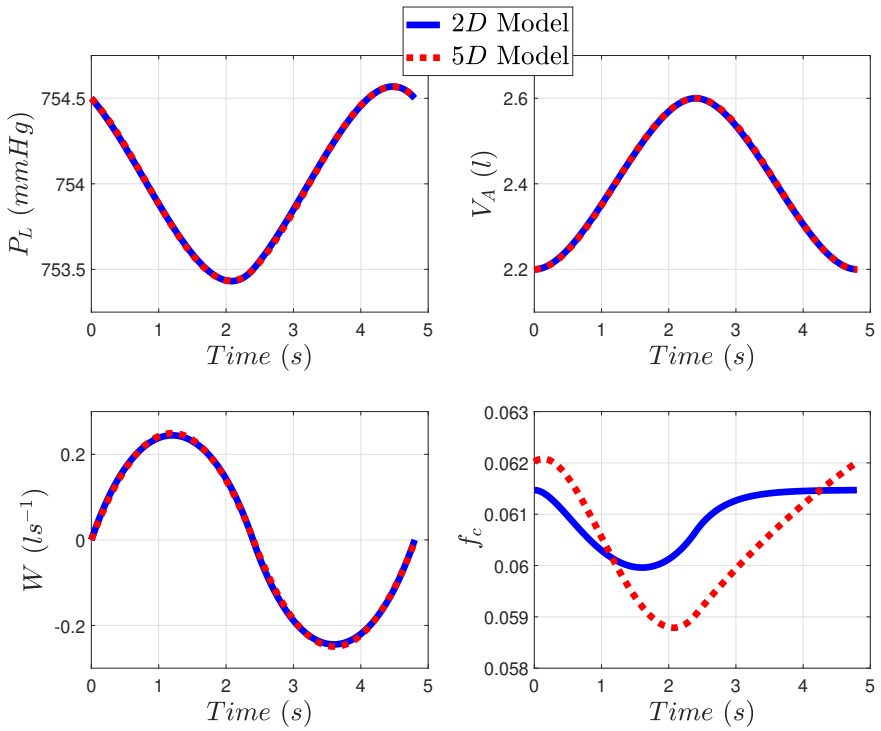

Fig. 5.2: Comparison of the optimal solution for the $2D$ linear model and $5D$ model for V_T = 0.4 l and T = 4.82 s that minimizes Eq. (5.12). Here we fixed T and T_i which leads to different average levels of f_c. For the $2D$ linear model, $P_L = P_m - RF$ (see Section 2.3). See Table 2, for all values of the parameters.

The optimal average square volume acceleration, when we solve the $2D$ model is:

$$J = \frac{1}{T}\int_0^T \ddot{V}_A^2 dt = \frac{192\beta Y_{cav} V_T^2}{\gamma^4 (V_T - V_D)^4} \tag{5.33}$$

For maintaining the same levels of CO_2, the average square volume acceleration for the sinusoidal airflow pattern is:

$$J = \frac{2\pi^4 \beta Y_{cav} V_T^2}{\gamma^4 (V_T - V_D)^4} \approx \frac{195\beta Y_{cav} V_T^2}{\gamma^4 (V_T - V_D)^4} \tag{5.34}$$

It is clear from Eqs. (5.33) and (5.34) that for every tidal volume, V_T, the optimal function gives a lower average square volumetric acceleration than the sinusoidal function. The average square volumetric acceleration is a strictly decreasing function of V_T (if $V_T > V_D$), therefore there is no optimal V_T that minimizes Eq. (5.33).

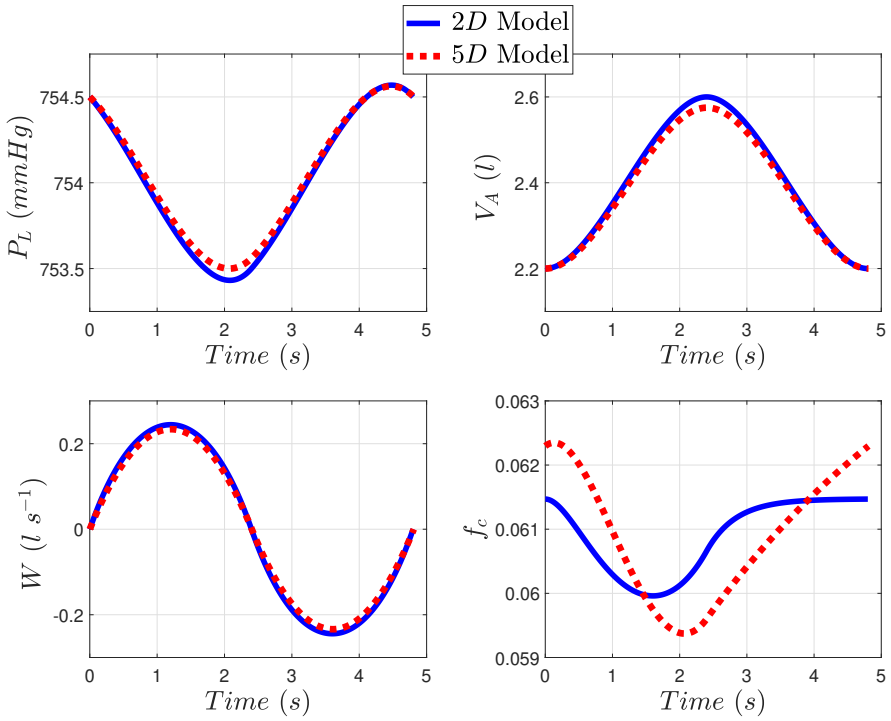

Fig. 5.3: Comparison of the optimal solution for the $2D$ linear model and $5D$ model for $V_T = 0.4$ l that minimizes Eq. (5.12). For the $2D$ linear model, $P_L = P_m - RF$ (see Section 2.3). Both solutions maintain a specific value of $f_c = 6.1\%$. See Table 2, for all values of parameters.

5.3 Work Rate

In this section, we derive the optimal breathing pattern that minimizes the work rate during a whole breathing period. By substituting $\eta_1 = 0$, $\eta_2 = 1$ and $\eta_3 = 0$ into

Eq. (5.1) and (5.2), the cost function becomes:

$$J_I = \frac{1}{T}\int_0^{T_i} F(t)\dot{V}_A dt, \tag{5.35}$$

$$J_E = \frac{1}{T}\int_{T_i}^{T} R\dot{V}_A^2 dt, \tag{5.36}$$

Let H_1 and H_2 be the Hamiltonians of the problem over the intervals $0 < t \leq T_i$ and $T_i < t \leq T$ respectively such that:

$$H_1 = \frac{1}{T}F_1(t)\dot{V}_{A_1}(t) + \lambda_{11}(t)\dot{V}_{A_1}(t) + \lambda_{12}(t)\dot{Y}_{c_1}(t) + \lambda_{13}(t)\dot{M}_1(t) \tag{5.37}$$

$$H_2 = \frac{1}{T}R\dot{V}_{A_2}^2 + \lambda_{21}(t)\dot{V}_{A_2}(t) + \lambda_{22}(t)\dot{Y}_{c_2}(t) + \lambda_{23}(t)\dot{M}_2(t) \tag{5.38}$$

By using the conditions $\partial H_1/\partial F_1 = 0$ and $\partial H_2/\partial F_2 = 0$, we get:

$$F_1 = \frac{1}{2}\left(\alpha V_{A1} - T\lambda_{11} + \hat{\gamma}T\lambda_{12}\right) \tag{5.39}$$

$$F_2 = \alpha V_{A2} - \frac{T}{2R}\lambda_{21} \tag{5.40}$$

We can construct additional differential equations for the Lagrange multipliers, λ_{ij} during inhalation, $T_i < t \leq T$, (see condition (ii) of section 4.1):

$$\dot{\lambda}_{11} = -\frac{\partial H_1}{\partial V_{A1}} = \frac{\alpha}{T}F_1 + \alpha\lambda_{11} - \alpha\hat{\gamma}\lambda_{12} \tag{5.41}$$

$$\dot{\lambda}_{12} = -\frac{\partial H_1}{\partial Y_{c1}} = \beta\lambda_{12} - \lambda_{13} \tag{5.42}$$

$$\dot{\lambda}_{13} = -\frac{\partial H_1}{\partial M_1} = 0 \tag{5.43}$$

Similarly, during exhalation, $T_i < t \leq T$, we can construct differential equations for the Lagrange multipliers (see condition (iv) of section 4.1):

$$\dot{\lambda}_{12} = -\frac{\partial H_2}{\partial V_{A2}} = \frac{2\alpha R}{T}F_2 - \frac{2\alpha^2 R}{T}V_{A_2} + \alpha\lambda_{12} \tag{5.44}$$

$$\dot{\lambda}_{22} = -\frac{\partial H_2}{\partial Y_{c2}} = \beta\lambda_{22} - \lambda_{23} \tag{5.45}$$

$$\dot{\lambda}_{23} = -\frac{\partial H_2}{\partial M_2} = 0 \tag{5.46}$$

Substituting Eq. (5.39) and Eq. (5.40) into the differential equations (2.17), (2.19), (4.17) and (5.41)-(5.46) yields the following systems of differential equations:

$$\dot{\mathbf{A}}_1 = \begin{bmatrix} -\frac{\alpha}{2} & 0 & 0 & -\frac{T}{2} & \frac{\hat{\gamma}T}{2} & 0 \\ \frac{\alpha\hat{\gamma}}{2} & -\beta & 0 & \frac{\hat{\gamma}T}{2} & -\frac{\hat{\gamma}^2T}{2} & 0 \\ 0 & 1 & 0 & 0 & 0 & 0 \\ \frac{\alpha^2}{2T} & 0 & 0 & \frac{\alpha}{2} & -\frac{\alpha\hat{\gamma}}{2} & 0 \\ 0 & 0 & 0 & 0 & \beta & -1 \\ 0 & 0 & 0 & 0 & 0 & 0 \end{bmatrix} \mathbf{A}_1 \tag{5.47}$$

and

$$\dot{\mathbf{A}}_2 = \begin{bmatrix} 0 & 0 & 0 & -\frac{T}{2R} & 0 & 0 \\ 0 & -\beta & 0 & 0 & 0 & 0 \\ 0 & 1 & 0 & 0 & 0 & 0 \\ 0 & 0 & 0 & 0 & 0 & 0 \\ 0 & 0 & 0 & 0 & \beta & -1 \\ 0 & 0 & 0 & 0 & 0 & 0 \end{bmatrix} \mathbf{A}_2 \tag{5.48}$$

We solve the differential equations (5.47) and (5.48) with boundary conditions (4.42) and obtain the optimal function $F(t)$ for a given V_T:

$$F(t) = \begin{cases} \alpha B + \frac{V_T}{T_i}(1+\alpha t) & ; \quad 0 < t \leq T_i \\ \\ \alpha B + \frac{V_T}{T_i}(\alpha T - \alpha t - 1) & ; \quad T_i < t \leq T \end{cases} \tag{5.49}$$

From the conditions $M_2(T) = T\ y_{av}$ and $H_1(T_i) = H_2(T_i)$, the optimal durations T and T_i are found:

$$T = \frac{\gamma(V_T - V_D)}{\beta\ y_{av}} \tag{5.50}$$

$$T_i = \frac{\gamma(V_T - V_D)}{2\,\beta\ y_{av}} = \frac{T}{2} \tag{5.51}$$

The optimal solution and duration that minimizes the total work rate are the same as that which minimizes the total work done by the respiratory muscles (see Eq. 4.43).

5.4 Average Square Force

Here we derive the optimal breathing pattern that minimizes the average square force developed by the respiratory muscles. By substituting $\eta_1 = 0$, $\eta_2 = 0$ and $\eta_3 = 1$ into Eq. (5.1) and (5.2), the cost function becomes:

$$J = \frac{1}{T}\int_0^T F(t)^2 dt, \tag{5.52}$$

Let H_1 and H_2 be the Hamiltonians of the problem over the intervals $0 < t \leq T_i$ and $T_i < t \leq T$ respectively such that:

$$H_1 = \frac{1}{T}F_1^2(t) + \lambda_{11}(t)\dot{V}_{A_1}(t) + \lambda_{12}(t)\dot{Y}_{c_1}(t) + \lambda_{13}(t)\dot{M}_1(t) \tag{5.53}$$

$$H_2 = \frac{1}{T}F_2^2(t) + \lambda_{21}(t)\dot{V}_{A_2}(t) + \lambda_{22}(t)\dot{Y}_{c_2}(t) + \lambda_{23}(t)\dot{M}_2(t) \tag{5.54}$$

By using the conditions $\partial H_1/\partial F_1 = 0$ and $\partial H_2/\partial F_2 = 0$, we get: (see conditions (i) and (iii) of section 4.1)

$$F_1 = \frac{T}{2}\left(\lambda_{11} + \hat{\gamma}\lambda_{12}\right) \tag{5.55}$$

$$F_2 = \frac{T}{2}\lambda_{21} \tag{5.56}$$

We can construct additional differential equations for the Lagrange multipliers, λ_{ij} during inhalation, $T_i < t \leq T$, (see condition (ii) of section 4.1):

$$\dot{\lambda}_{11} = -\frac{\partial H_1}{\partial V_{A_1}} = \alpha\lambda_{11} - \alpha\hat{\gamma}\lambda_{12} \tag{5.57}$$

$$\dot{\lambda}_{12} = -\frac{\partial H_1}{\partial Y_{c_1}} = \beta\lambda_{12} + \lambda_{13} \tag{5.58}$$

$$\dot{\lambda}_{13} = -\frac{\partial H_1}{\partial M_1} = 0 \tag{5.59}$$

Similarly, during exhalation, $T_i < t \leq T$, we can construct differential equations for the Lagrange multipliers (see condition (iv) of section 4.1):

$$\dot{\lambda}_{12} = -\frac{\partial H_2}{\partial V_{A_2}} = \alpha\lambda_{21} \tag{5.60}$$

$$\dot{\lambda}_{22} = -\frac{\partial H_2}{\partial Y_{c_2}} = \beta\lambda_{22} + \lambda_{23} \tag{5.61}$$

$$\dot{\lambda}_{23} = -\frac{\partial H_2}{\partial M_2} = 0 \tag{5.62}$$

Substituting Eq. (5.55) and Eq. (5.56) into the differential equations (2.17), (2.19), (4.17) and (5.57)-(5.62) yields the following systems of differential equations:

$$\dot{\mathbf{A}}_1 = \begin{bmatrix} -\alpha & 0 & 0 & -\frac{T}{2} & \frac{\hat{\gamma}T}{2} & 0 \\ \alpha\hat{\gamma} & -\beta & 0 & \frac{\hat{\gamma}T}{2} & -\frac{\hat{\gamma}^2T}{2} & 0 \\ 0 & 1 & 0 & 0 & 0 & 0 \\ 0 & 0 & 0 & \alpha & -\alpha\hat{\gamma} & 0 \\ 0 & 0 & 0 & 0 & \beta & -1 \\ 0 & 0 & 0 & 0 & 0 & 0 \end{bmatrix} \mathbf{A}_1 \tag{5.63}$$

and

$$\dot{\mathbf{A}}_2 = \begin{bmatrix} -\alpha & 0 & 0 & -\frac{T}{2} & 0 & 0 \\ 0 & -\beta & 0 & 0 & 0 & 0 \\ 0 & 1 & 0 & 0 & 0 & 0 \\ 0 & 0 & 0 & \alpha & 0 & 0 \\ 0 & 0 & 0 & 0 & \beta & -1 \\ 0 & 0 & 0 & 0 & 0 & 0 \end{bmatrix} \mathbf{A}_2 \tag{5.64}$$

where, $\mathbf{A_1} = \begin{bmatrix} V_{A1} & Y_{c1} & M_1 & \lambda_{11} & \lambda_{12} & \lambda_{13} \end{bmatrix}^\top$
and $\mathbf{A_2} = \begin{bmatrix} V_{A2} & Y_{c2} & M_2 & \lambda_{21} & \lambda_{22} & \lambda_{23} \end{bmatrix}^\top$
By solving the differential equations (5.63) and (5.64), we get:

$$V_{A1} = C_3 e^{-\alpha t} - C_4 \frac{T}{4\alpha} e^{\alpha t} - C_5 \frac{\beta\hat{\gamma}T}{2\left(\alpha^2 - \beta^2\right)} e^{\beta t} \tag{5.65}$$

$$Y_{c1} = C_1 - \frac{C_2}{\beta} e^{-\beta t} - C_3 \frac{\hat{\gamma}}{\alpha - \beta} e^{-\alpha t} + C_4 \frac{T\hat{\gamma}}{4\alpha\left(\alpha + \beta\right)} e^{\alpha t} + C_5 \frac{\hat{\gamma}^2 T}{4\left(\alpha^2 - \beta^2\right)} e^{\beta t} \tag{5.66}$$

$$M_1 = C_2 e^{-\beta t} - C_3 \frac{\alpha\hat{\gamma}}{\alpha - \beta} e^{-\alpha t} + C_4 \frac{T\hat{\gamma}}{4\left(\alpha + \beta\right)} e^{\alpha t} + C_5 \frac{\beta\hat{\gamma}^2 T}{4\left(\alpha^2 - \beta^2\right)} e^{\beta t} \tag{5.67}$$

$$\lambda_{11} = -C_3 \frac{\alpha\beta}{\hat{\gamma}} - C_4 \frac{\alpha\beta}{\hat{\gamma}} t + C_6 \frac{\alpha\hat{\gamma}}{2\beta} e^{\beta t} \tag{5.68}$$

$$\lambda_{12} = C_5 e^{\beta t} + \frac{C_6}{\beta} \tag{5.69}$$

$$\lambda_{13} = C_6 \tag{5.70}$$

$$V_{A2} = C_7 e^{-\alpha t} - C_{10} \frac{T}{4\alpha} e^{\alpha t} \tag{5.71}$$

$$Y_{c2} = C_9 e^{-\beta t} \tag{5.72}$$

$$M_2 = C_8 - \frac{C_9}{\beta} e^{-\beta t} \tag{5.73}$$

$$\lambda_{21} = C_{10} e^{\alpha t} \tag{5.74}$$

$$\lambda_{22} = \frac{C_{12}}{\beta} + C_{11} e^{\beta t} \tag{5.75}$$

$$\lambda_{23} = C_{12} \tag{5.76}$$

We have the same boundary conditions as Eq. (4.42). In terms of coefficients, the equations generated from those conditions are linear, so the augmented matrix is:

$$
\left(\begin{array}{cccccccccc|c}
0 & 0 & 1 & -\frac{T}{4\alpha} & \frac{\beta\hat{\gamma}T}{2(\beta^2-\alpha^2)} & 0 & 0 & 0 & 0 & 0 & B \\
0 & 0 & e^{-\alpha T_i} & -\frac{T\,e^{\alpha T_i}}{4\alpha} & \frac{\beta\hat{\gamma}Te^{\beta T_i}}{2(\beta^2-\alpha^2)} & 0 & 0 & 0 & 0 & 0 & A+B \\
0 & 0 & 0 & 0 & 0 & 0 & e^{-\alpha T_i} & 0 & -\frac{T\,e^{\alpha T_i}}{4\alpha} & 0 & A+B \\
0 & 0 & 0 & 0 & 0 & 0 & e^{-\alpha T} & 0 & -\frac{T\,e^{\alpha T}}{4\alpha} & 0 & B \\
0 & 1 & -\frac{\alpha\hat{\gamma}}{\alpha-\beta} & \frac{\hat{\gamma}T}{4(\alpha+\beta)} & \frac{\beta\hat{\gamma}^2T}{4(\alpha^2-\beta^2)} & 0 & 0 & -e^{-\beta T} & 0 & 0 & 0 \\
0 & e^{-\beta T_i} & -\frac{\alpha\hat{\gamma}e^{-\alpha T_i}}{\alpha-\beta} & \frac{\hat{\gamma}Te^{\alpha T_i}}{4(\alpha+\beta)} & \frac{\beta\hat{\gamma}^2Te^{\beta T_i}}{4(\alpha^2-\beta^2)} & 0 & 0 & -e^{-\beta T_i} & 0 & 0 & 0 \\
1 & -\frac{1}{\beta} & \frac{\hat{\gamma}}{\alpha-\beta} & \frac{T\hat{\gamma}}{4\alpha(\alpha+\beta)} & \frac{\hat{\gamma}^2T}{4(\alpha^2-\beta^2)} & 0 & 0 & 0 & 0 & 0 & 0 \\
1 & -\frac{e^{-\beta T_i}}{\beta} & \frac{\hat{\gamma}e^{-\alpha T_i}}{\alpha-\beta} & \frac{\hat{\gamma}Te^{\alpha T_i}}{4\alpha(\alpha+\beta)} & \frac{\hat{\gamma}^2Te^{\beta T_i}}{4(\alpha^2-\beta^2)} & 0 & 0 & -1 & \frac{e^{-\beta T_i}}{\beta} & 0 & 0 \\
0 & 0 & 0 & 0 & 1 & \frac{1}{\beta} & 0 & 0 & 0 & -e^{\beta T} & -\frac{1}{\beta} \\
0 & 0 & 0 & 0 & e^{\beta T_i} & \frac{1}{\beta} & 0 & 0 & 0 & -e^{\beta T_i} & -\frac{1}{\beta} \\
0 & 0 & 0 & 0 & 0 & 1 & 0 & 0 & 0 & 0 & -1 \\
0 & 0 & 0 & 0 & 0 & 0 & 0 & 0 & 0 & 0 & 1
\end{array}\right)
\tag{5.77}
$$

In order to solve for the coefficients we performed row operations on the augmented matrix that yields:

$$\left(\begin{array}{cccccccc|c|ccc|c}
1 & 0 & 0 & 0 & 0 & 0 & 0 & 0 & \kappa_1 & 0 & 0 & 0 & 0 \\
0 & 1 & 0 & 0 & 0 & 0 & 0 & 0 & \frac{\alpha+2e^{\,Ti(\alpha+\beta)-T\beta}\beta-\beta-e^{2\,Ti\alpha}(\alpha+\beta)}{\kappa_2} & 0 & 0 & 0 & 0 \\
0 & 0 & 1 & 0 & 0 & 0 & 0 & 0 & -\frac{e^{2\,Ti\alpha-T\beta}\left(-1+e^{T\beta}\right)\left(\alpha^2-\beta^2\right)}{\kappa_2\alpha\hat{\gamma}} & 0 & 0 & 0 & 0 \\
0 & 0 & 0 & 1 & 0 & 0 & 0 & 0 & \frac{4e^{-T\beta}\left(-1+e^{T\beta}\right)\left(\beta^2-\alpha^2\right)}{\kappa_2 T\hat{\gamma}} & 0 & 0 & 0 & 0 \\
0 & 0 & 0 & 0 & 1 & 0 & 0 & 0 & 0 & 0 & 0 & 0 & 0 \\
0 & 0 & 0 & 0 & 0 & 1 & 0 & 0 & 0 & 0 & 0 & 0 & 0 \\
0 & 0 & 0 & 0 & 0 & 0 & 1 & 0 & 0 & 0 & 0 & 0 & 0 \\
0 & 0 & 0 & 0 & 0 & 0 & 0 & 1 & \kappa_1 & 0 & 0 & 0 & 0 \\
0 & 0 & 0 & 0 & 0 & 0 & 0 & 0 & 0 & 1 & 0 & 0 & 0 \\
0 & 0 & 0 & 0 & 0 & 0 & 0 & 0 & 0 & 0 & 1 & 0 & 0 \\
0 & 0 & 0 & 0 & 0 & 0 & 0 & 0 & 0 & 0 & 0 & 1 & 0 \\
0 & 0 & 0 & 0 & 0 & 0 & 0 & 0 & 0 & 0 & 0 & 0 & 1
\end{array}\right) \tag{5.78}$$

where,
$\kappa_2 = -\alpha+\beta-2\beta e^{T_i(\alpha+\beta)}+(\alpha+\beta)e^{2\alpha T_i}$ and $\kappa_1 = -\frac{e^{-\beta T}}{\beta}\left(\frac{(\alpha^2-\beta^2)\left(e^{\beta T}-1\right)\left(e^{2\alpha T_i}-1\right)}{\alpha\kappa_2}+1\right)$.
The reduced augmented matrix shows that there is no combination of coefficients that satisfies all the boundary conditions. We therefore conclude that there exists no optimal solution that minimizes the average square force only.

5.5 Solution of the Weighted Cost Function

In section 5.2, we showed that there is no optimal V_T that minimizes the average volumetric acceleration. We also found that the optimal pleural pressure that minimizes the total work rate is discontinuous (see section 5.3) and no optimal solution exists that minimizes the average square force developed by the respiratory muscles (see section 5.4). None of these cost functions can account for the breathing pattern by themselves.

In this section, we discuss how the weighted sum of these cost functions affects the breathing pattern. We solve the optimization problem for the $5D$ model that minimizes Eq. (5.1) and (5.2), subject to the following constraints:

i The differential equations (Eqs. (1.8), (1.9), (1.19), (1.20), (5.4), (5.5) and (5.6)) are satisfied.

ii The system of equations is in a periodic steady state with period T, that is $V_A(0) = V_A(T)$, $P_L(0) = P_L(T)$, $W(0) = W(T)$, $f_c(0) = f_c(T)$, $f_o(0) = f_o(T)$, $p_c(0) = p_c(T)$ and $p_o(0) = p_o(T)$.

iii The initial value and amplitude of $V_A(t)$ are given as B and V_T respectively. That is, $V_A(0) = B$ and $V_A(T_i) = B + V_T$, where T_i is the time to reach a maximum V_A.

iv The average value of the concentration of CO_2 in the lung, f_c, is a given fixed value, $f_{c_{av}} = \frac{1}{T}\int_0^T f_c(t)\,dt$, where $f_{c_{av}}$ is a constant.

The constraint (iv) can be replaced by the differential equation

$$\frac{dM}{dt} = f_c \tag{5.79}$$

with the boundary conditions $M(0) = 0$ and $M(T) = T\ f_{c_{av}}$.

Let H_1 and H_2 be the Hamiltonians of the problem during inhalation and exhalation respectively such that:

$$\begin{aligned} H_1 =& \eta_1 \ddot{V}_{A1}^2 + \eta_2 (P_m - P_{L1})\dot{V}_{A1} + \eta_3 (P_m - P_{L1})^2 + \lambda_{11}(t)\dot{P}_{L1} + \lambda_{12}(t)\dot{V}_{A1} + \lambda_{13}(t)\dot{W}_1 \\ &+ \lambda_{14}(t)\dot{f}_{c1} + \lambda_{15}(t)\dot{\tilde{p}}_{c1} + \lambda_{16}(t)\dot{f}_{o1} + \lambda_{17}(t)\dot{\tilde{p}}_{o1} + \lambda_{18}(t)\dot{M}_1 \end{aligned} \tag{5.80}$$

$$\begin{aligned} H_2 =& \eta_1 \ddot{V}_{A2}^2 + \eta_2\ R\ \dot{V}_{A2}^2 + \eta_3 (P_m - P_{L2})^2 + \lambda_{21}(t)\dot{P}_{L2} + \lambda_{22}(t)\dot{V}_{A2} + \lambda_{23}(t)\dot{W}_2 + \lambda_{24}(t)\dot{f}_{c2} \\ &+ \lambda_{25}(t)\dot{\tilde{p}}_{c2} + \lambda_{26}(t)\dot{f}_{o2} + \lambda_{27}(t)\dot{\tilde{p}}_{o2} + \lambda_{28}(t)\dot{M}_2 \end{aligned} \tag{5.81}$$

Here subscripts 1 and 2 represent the variables in the interval $0 < t \le T_i$ (inhalation) and $T_i < t \le T$ (exhalation) respectively and λ_{ij} are the Lagrange multipliers. As G_1 and G_2 are the control variables during inhalation and exhalation respectively, by using the conditions $\partial H_1/\partial G_1 = 0$ and $\partial H_2/\partial G_2 = 0$ (see condition (i) and (iii) of section 4.1), we find G_1 and G_2 as:

$$G_1 = \frac{RT}{2\eta_1}(\lambda_{13} - R\lambda_{11}) + \frac{E}{R}(P_{L1} - P_m + EV_{A1}) \tag{5.82}$$

$$G_2 = \frac{RT}{2\eta_2}(\lambda_{23} - R\lambda_{21}) + \frac{E}{R}(P_{L2} - P_m + EV_{A2}) \tag{5.83}$$

We construct sixteen additional differential equations (eight for each phase) for the Lagrange multiplier, λ_{ij} (see conditions (ii) and (iv) of section 4.1).

$$\begin{aligned}\dot{\lambda_{11}} = -\frac{\partial H_1}{\partial P_{L1}} = {} & \frac{2\eta_1 E}{R^4 T}\left(RG_1 - E\left(P_{L1} - P_m + EV_{A1}\right)\right) + \frac{\eta_2}{T}W_1 + \frac{\eta_3}{T}\left(1 - 2P_{L1} + 2P_m\right) \\ & - \frac{D_o}{V_{A1}} f_{o1}\left(f_{c1}\lambda_{14} + \left(f_{o1} - 1\right)\lambda_{16}\right) - \frac{D_c}{V_{A1}} f_{c1}\left(f_{o1}\lambda_{16} + \left(f_{c1} - 1\right)\lambda_{14}\right) \\ & - \frac{1}{C_u V_c}\left(\frac{D_o f_{o1}\lambda_{17}}{\sigma} + \frac{D_c f_{c1}\lambda_{15}}{\sigma_c}\right) - \frac{E}{R^2}\lambda_{13} \end{aligned} \tag{5.84}$$

$$\begin{aligned}\dot{\lambda_{12}} = -\frac{\partial H_1}{\partial V_{A1}} = {} & \frac{2\eta_1 E^2}{R^4 T}\left(R\,G_1 - E\left(P_{L1} - P_m + EV_{A1}\right)\right) + \frac{E}{C_u V_c}\left(\frac{D_o f_{o1}\lambda_{17}}{\sigma} + \frac{D_c f_{c1}\lambda_{15}}{\sigma_c}\right) \\ & + \frac{D_o}{V_A^2}\left(f_{c1}\lambda_{14} + \left(f_{o1} - 1\right)\lambda_{16}\right)\left(f_{o1}\left(P_{L1} - p_w\right) - p_{o1}\right) \\ & + \frac{D_c}{V_{A1}^2}\left(f_{o1}\lambda_{16} + \left(f_{c1} - 1\right)\lambda_{14}\right)\left(f_{c1}\left(P_{L1} - p_w\right) - p_{c1}\right) - \frac{E^2}{R^2}\lambda_{13} \\ & - \frac{W_1}{V_{A1}^2}\left(f_{c1}\lambda_{14} + (f_{o1} - f_{om})\lambda_{16}\right)\left(1 - \frac{V_D}{V_T}\right) \end{aligned} \tag{5.85}$$

$$\dot{\lambda_{13}} = -\frac{\partial H_1}{\partial W_1} = \frac{\eta_2}{T}\left(P_{L1} - P_m\right) + \frac{1}{V_{A1}}\left(1 - \frac{V_D}{V_T}\right)\left(f_{c1}\lambda_{14} + \left(f_{o1} - f_{om}\right)\lambda_{16}\right) - \lambda_{12} \tag{5.86}$$

$$\begin{aligned}\dot{\lambda_{14}} = -\frac{\partial H_1}{\partial f_{c1}} = {} & \frac{\left(p_w - P_{L1} - EV_{A1}\right)}{V_{A1}}\left(D_o f_{o1}\lambda_{14} + D_c f_{o1}\lambda_{16} + D_c\left(2f_{c1} - 1\right)\lambda_{14}\right) \\ & + \frac{D_c}{C_u \sigma V_c}\lambda_{15}\left(p_w - P_{L1} - EV_{A1}\right) + \frac{\lambda_{14}}{V_{A1}}\left(D_c p_{c1} + D_o p_{o1}\right) - \lambda_{18} \\ & + \left(1 - \frac{V_D}{V_T}\right)\frac{W_1\lambda_{14}}{V_{A1}} \end{aligned} \tag{5.87}$$

$$\dot{\lambda_{15}} = -\frac{\partial H_1}{\partial p_{c1}} = \left(\frac{r_2}{h l_2 T_L} + \frac{D_c}{C_u \sigma_c V_c}\right)\lambda_{15} + \frac{D_c}{V_{A1}}\left(\left(f_{c1} - 1\right)\lambda_{14} + f_{o1}\lambda_{16}\right) \tag{5.88}$$

$$\begin{aligned}\dot{\lambda_{16}} = -\frac{\partial H_1}{\partial f_{o1}} = {} & \frac{\left(p_w - P_{L1} - EV_{A1}\right)}{V_{A1}}\left(D_o f_{c1}\lambda_{14} + D_c f_{c1}\lambda_{16} + D_o\left(2f_{o1} - 1\right)\lambda_{16}\right) \\ & + \frac{D_o}{C_u \sigma V_c}\lambda_{17}\left(p_w - P_{L1} - EV_{A1}\right) + \frac{\lambda_{16}}{V_{A1}}\left(D_c p_{c1} + D_o p_{o1}\right) \\ & + \left(1 - \frac{V_D}{V_T}\right)\frac{W_1\lambda_{16}}{V_{A1}} \end{aligned} \tag{5.89}$$

$$\dot{\lambda_{17}} = -\frac{\partial H_1}{\partial p_{o1}} = \frac{D_o}{V_{A1}}\left(f_{c1}\lambda_{14} + (f_{o1} - 1)\lambda_{16}\right) + \frac{D_o}{C_u \sigma V_c}\lambda_{17} + \frac{4T_h}{\sigma T_L}\lambda_{27} S'(p_{o1}) \tag{5.90}$$

$$\dot{\lambda_{18}} = -\frac{\partial H_1}{\partial M_1} = 0 \tag{5.91}$$

$$\dot{\lambda_{21}} = -\frac{\partial H_2}{\partial P_{L2}} = \frac{2\eta_1 E}{R^4 T}\left(RG_2 - E\left(P_{L2} - P_m + EV_{A2}\right)\right) + \frac{\eta_3}{T}\left(1 - 2P_{L2} + 2P_m\right)$$
$$- \frac{D_o}{V_{A2}} f_{o2}\left(f_{c2}\lambda_{24} + \left(f_{o2} - 1\right)\lambda_{26}\right) - \frac{D_c}{V_{A2}} f_{c2}\left(f_{o2}\lambda_{26} + \left(f_{c2} - 1\right)\lambda_{24}\right)$$
$$- \frac{1}{C_u V_c}\left(\frac{D_o f_{o2}\lambda_{27}}{\sigma} + \frac{D_c f_{c2}\lambda_{25}}{\sigma_c}\right) - \frac{E}{R^2}\lambda_{23} \tag{5.92}$$

$$\dot{\lambda_{22}} = -\frac{\partial H_2}{\partial V_{A2}} = \frac{2\eta_1 E^2}{R^4 T}\left(R\,G_2 - E\left(P_{L2} - P_m + EV_{A2}\right)\right) + \frac{E}{C_u V_c}\left(\frac{D_o f_{o2}\lambda_{27}}{\sigma} + \frac{D_c f_{c2}\lambda_{25}}{\sigma_c}\right)$$
$$+ \frac{D_o}{V_{A2}^2}\left(f_{c2}\lambda_{24} + \left(f_{o2} - 1\right)\lambda_{26}\right)\left(f_{o2}\left(P_{L2} - p_w\right) - p_{o2}\right)$$
$$+ \frac{D_c}{V_{A2}^2}\left(f_{o1}\lambda_{26} + \left(f_{c2} - 1\right)\lambda_{24}\right)\left(f_{c2}\left(P_{L2} - p_w\right) - p_{c2}\right) - \frac{E^2}{R^2}\lambda_{23} \tag{5.93}$$

$$\dot{\lambda_{23}} = -\frac{\partial H_2}{\partial W_2} = -\frac{2\eta_2}{T} RW_2 - \lambda_{22} \tag{5.94}$$

$$\dot{\lambda_{24}} = -\frac{\partial H_2}{\partial f_{c2}} = \frac{\left(p_w - P_{L2} - EV_{A2}\right)}{V_{A2}}\left(D_o f_{o2}\lambda_{24} + D_c f_{o2}\lambda_{26} + D_c\left(2f_{c2} - 1\right)\lambda_{24}\right)$$
$$+ \frac{D_c}{C_u \sigma V_c}\lambda_{25}\left(p_w - P_{L2} - EV_{A2}\right) + \frac{\lambda_{24}}{V_{A2}}\left(D_c p_{c2} + D_o p_{o2}\right) - \lambda_{28} \tag{5.95}$$

$$\dot{\lambda_{25}} = -\frac{\partial H_2}{\partial p_{c2}} = \left(\frac{r_2}{h l_2 T_L} + \frac{D_c}{C_u \sigma_c V_c}\right)\lambda_{25} + \frac{D_c}{V_{A2}}\left(\left(f_{c2} - 1\right)\lambda_{24} + f_{o2}\lambda_{26}\right) \tag{5.96}$$

$$\dot{\lambda_{26}} = -\frac{\partial H_2}{\partial f_{o2}} = \frac{\left(p_w - P_{L2} - EV_{A2}\right)}{V_{A2}}\left(D_o f_{c2}\lambda_{24} + D_c f_{c2}\lambda_{26} + D_o\left(2f_{o2} - 1\right)\lambda_{26}\right)$$
$$+ \frac{D_o}{C_u \sigma V_c}\lambda_{27}\left(p_w - P_{L2} - EV_{A2}\right) + \frac{\lambda_{26}}{V_{A2}}\left(D_c p_{c2} + D_o p_{o2}\right) \tag{5.97}$$

$$\dot{\lambda_{27}} = -\frac{\partial H_2}{\partial p_{o2}} = \frac{D_o}{V_{A2}}\left(f_{c2}\lambda_{24} + (f_{o2} - 1)\lambda_{26}\right) + \frac{D_o}{C_u \sigma V_c}\lambda_{27} + \frac{4T_h}{\sigma T_L}\lambda_{27} S'(p_{o2}) \tag{5.98}$$

$$\dot{\lambda_{28}} = -\frac{\partial H_2}{\partial M_2} = 0 \tag{5.99}$$

We also have the following 32 boundary conditions (see section 4.1 for more details):

$$P_{L1}(0) = P_{L2}(T), \quad P_{L1}(T_i) = P_{L2}(T_i), \quad V_{A1}(0) = B, \quad V_{A2}(T) = B,$$
$$V_{A1}(T_i) = B + V_T, \quad V_{A2}(T_i) = B + V_T, \quad W_1(0) = 0, \quad W_1(T_i) = 0,$$
$$W_2(T_i) = 0, \quad W_2(T) = 0, \quad f_{c1}(0) = f_{c2}(T), \quad f_{c1}(T_i) = f_{c2}(T_i),$$
$$p_{c1}(0) = p_{c2}(T), \quad p_{c1}(T_i) = p_{c2}(T_i), \quad f_{o1}(0) = f_{o2}(T), \quad f_{o1}(T_i) = f_{o2}(T_i),$$
$$p_{o1}(0) = p_{o2}(T), \quad p_{o1}(T_i) = p_{o2}(T_i), \quad M_1(0) = 0, \quad M_1(T_i) = M_2(T_i),$$

$$\lambda_{11}(0) = \lambda_{21}(T), \quad \lambda_{11}(T_i) = \lambda_{21}(T_i), \quad \lambda_{14}(0) = \lambda_{24}(T), \quad \lambda_{14}(T_i) = \lambda_{24}(T_i),$$
$$\lambda_{15}(0) = \lambda_{25}(T), \quad \lambda_{15}(T_i) = \lambda_{25}(T_i), \quad \lambda_{16}(0) = \lambda_{26}(T), \quad \lambda_{16}(T_i) = \lambda_{26}(T_i),$$
$$\lambda_{17}(0) = \lambda_{27}(T), \quad \lambda_{17}(T_i) = \lambda_{27}(T_i), \quad \lambda_{18}(T_i) = \lambda_{28}(T_i), \quad \lambda_{28}(T) = 0.$$

From Eqs. (5.80) and (5.81), we know that λ_1, λ_2, λ_3, λ_4, λ_5, λ_6, λ_7 and λ_5 are the Lagrange multipliers associated with variables P_L, V_A, W, f_c, $\bar{p}_c$, f_o, $\bar{p}_o$ and M respectively. As V_A and W are fixed at $t = 0$, T_i and T, it follows that λ_2 and λ_3 are free at these boundary points (see conditions (v) and (vi) of section 4.1). The variables P_L, f_c, $\bar{p}_c$, f_o and $\bar{p}_o$ are periodic and free, hence λ_1, λ_4, λ_5, λ_6 and λ_7 are also periodic and free (see conditions (v) of section 4.1). P_L, f_c, $\bar{p}_c$, f_o, $\bar{p}_o$ and M are continuous and free at $t = T_i$, therefore λ_1, λ_4, λ_5, λ_6, λ_7 and λ_8 are also continuous and free at $t = T_i$ (see conditions (vi) of section 4.1). The variable M is fixed at $t = 0$, and free at $t = T$, so λ_3 is free at $t = 0$ and zero at $t = T$.

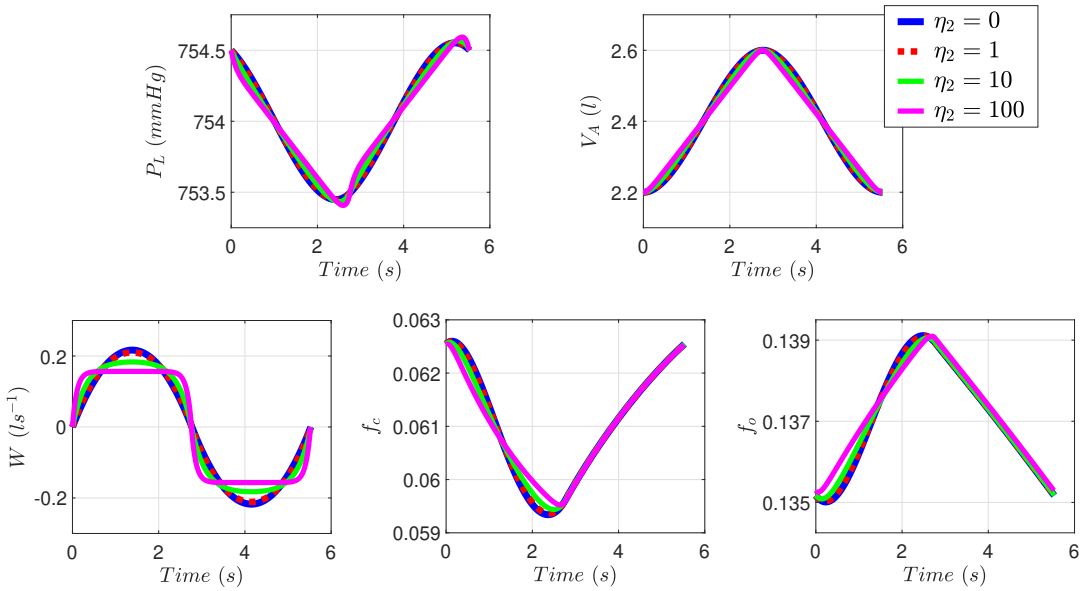

Fig. 5.4: The optimal solution for different values of η_2 with $\eta_1 = 1$ and $\eta_3 = 0$ that minimizes Eq. (5.1) and (5.2) for $V_T = 0.4\ l$. All solutions maintain a specific value of $f_c = 6.1\%$. All calculations are done using the $6D$ model. See Table 2, for all values of the parameters.

Figure (5.4) shows that for all values of the weighting parameter associated with the work rate (η_2), the optimal airflow, W is symmetric. As η_2 increases, the optimal airflow peak reduces and the optimal volume approaches a triangular shape. For

all values of the weighting parameter associated with average square force ($\eta_3 > 0$), the optimal airflow is not symmetric during inhalation (the peak of the optimal airflow shifts from the middle) as shown in Fig. (5.5). As η_3 increases, the airflow peak increases; there is no solution when η_3 is high enough. We have also found that the optimal value of T associated with V_T such that f_{cav} is maintained at a given value, does not vary due to changes in η_2 and η_3 and the optimal duration of inhalation (T_i) is half of T for all cases.

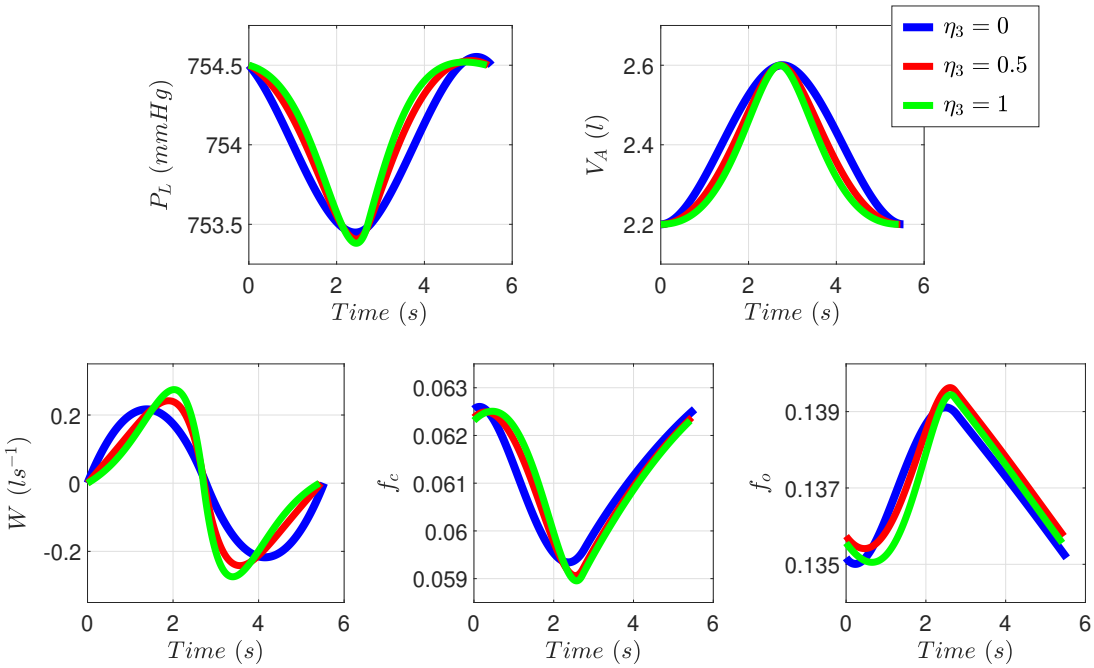

Fig. 5.5: The optimal solution for different values of the η_3 when $\eta_1 = 1$ and $\eta_2 = 0$ that minimizes Eq. (5.1) and (5.2) for $V_T = 0.4\ l$. All solutions maintain a specific value of $f_c = 6.1\%$. All calculations are done using the $6D$ model. See Table 2, for all values of the parameters.

Fig. (5.6) shows the optimal solution of the special case that minimizes the sum of Eq. (5.1) and (5.2), when the weights associated with each component has equal magnitude, $\eta_1 = 1$, $\eta_2 = 1$ and $\eta_3 = 1$. Once again the optimal solution has equal durations of inhalation and exhalation. This breathing pattern is similar to the one we got when $\eta_2 = 0$. This shows that in equal weights the cost is dominated by the volumetric acceleration and the average square force.

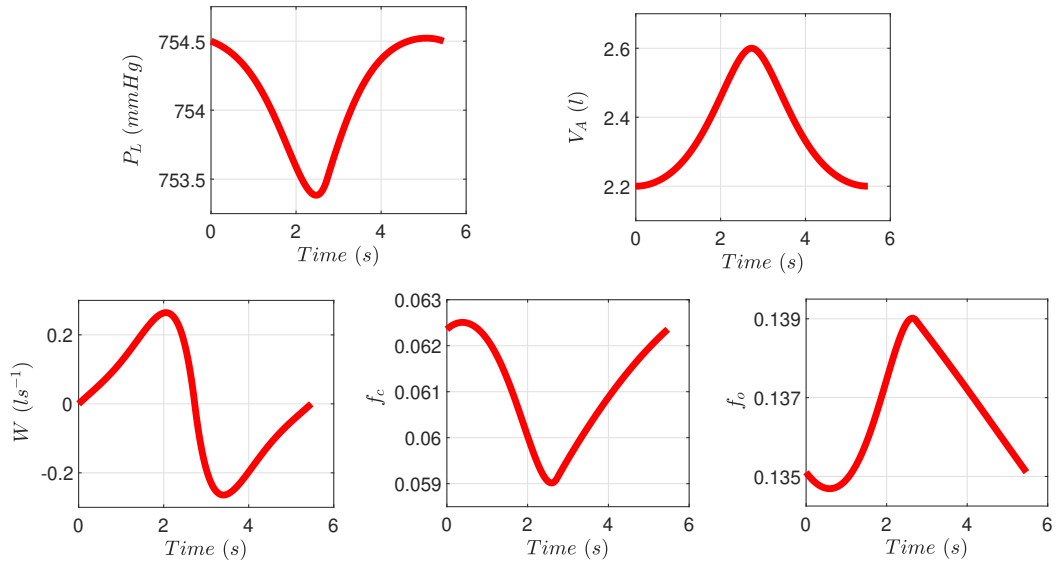

Fig. 5.6: The optimal solution that minimizes Eq. (5.1) and (5.2) while maintaining f_c at 6.1% for $V_T = 0.4\ l$ when $\eta_1 = 1$, $\eta_2 = 1$ and $\eta_3 = 1$. All calculations are done using the $6D$ model. See Table 2, for all values of parameters.

Chapter 6

Conclusion

The main aim of this thesis was to check the hypothesis that an observed combination of breathing frequency and amplitude is optimal with respect to some objective function. Many previous studies of the respiratory system considered neural control of breathing as a black box and used the total minute ventilation (product of rate and amplitude of breathing) as a variable, hence did not distinguish between the amplitude and frequency of breathing. Studies concerning the question at the centre of this thesis, were able to find optimal amplitude and frequency within physiologically acceptable range. However, this was achieved with different objective functions and by using $1D$ models that do not take into account gas exchange directly.

The models we used in this thesis ranged from $2D$ to $6D$. We used the previously published $6D$ and $5D$ models that explain more accurately the coupling between lung mechanics and gas exchange (see Sections 1.3 and 1.4). We modified the pleural pressure (driving force) to portray better the neural signal (see Section 2.1). We then reduced the 5D model to $3D$ and $2D$ models, which we presented in this thesis for the first time (see Section 2.3). The simplest $2D$ model consists of two piecewise linear differential equations. We showed that this simple model is a good approximation of the more complex $5D$ model of gas exchange and gas transport (see Section 2.3).

The use of higher dimension models required the formulation of a new optimization problem as minimizing a given objective function subject to several constraints, such as satisfying the differential equations and maintaining one of

the variables at a given average value. The last constraint stems from the physiological observation that the average arterial partial pressure of CO_2 is maintained at a constant value. We solved the optimization problem in two cases: (1) when the shape of the pleural pressure was given (see Chapter 3) and (2) when the shape of the pleural pressure was unknown (see Chapters 4 and 5).

For the given pleural pressure, we tested three different cost functions: (i) the work rate during inhalation; (ii) the total work done during a whole breath and (iii) the weighted sum of volumetric acceleration and work rate during inhalation. All three cost functions were studied on healthy and diseased affected lungs using the $6D$ model with two different predefined pleural pressures: sinusoidal and exponential (see Chapter 3). In both cases the optimal frequency obtained for the work rate and weighted cost functions was within the physiological range for healthy humans (12–18 breaths per minute); it was slightly higher for the total work. For diseased lungs, the optimal frequencies for the work rate and the weighted cost functions were significantly lower than those under normal conditions for both sinusoidal and exponential pleural pressures (see Figs. 3.5, 3.8, 3.11 and 3.13), which shows a movement of the optimal breathing frequency in the wrong direction. However, the optimal frequency was almost the same for healthy and diseased lungs when the cost function was taken as the total work over one breath and the pleural pressure was sinusoidal (see Fig. 3.6), and slightly lower when the pleural pressure was exponential (see Fig. 3.12).

The optimization problem for the $2D$ linear model was solved analytically with sinusoidal and linear predefined driving forces (see Chapter 3). The calculation was done when the cost function was taken as the total work during a whole breath. We found that the relationship between the tidal volume and the breathing period is linear. The same result was obtained for the sinusoidal and the linear breathing patterns (see Eq. (3.27) and (3.36)). By considering a generalized breathing pattern described by a Fourier series, we showed that in the $2D$ linear model, the average levels of CO_2 in the lungs are only affected by the tidal volume and the period of breathing and are not affected by the shape of the driving force (see Section 3.4).

The solution of the optimization problem when the driving force was not given required the development of a new methodology. We developed the necessary

conditions for the solution of the optimal control problem when the constraints consisted of a piecewise system of differential equations. Other constraints included unknown durations of phases with an interior point constraint (see Section 4.1). We solved the optimal problem analytically for the $2D$ linear model when the total work was minimized (see Section 4.2). The optimal forcing function, $F(t)$ was found to be piecewise linear and discontinuous with optimal durations of time that are the same as for the sinusoidal case (see Fig. 4.3). We also developed a numerical algorithm and verified it by comparing the numerical calculation with the analytical solution (see Section 4.3). The numerical algorithm we developed was then used to solve the more complex models (the nonlinear $2D$ model and the $3D$ and $5D$ models). We still found that the optimal forcing function, $P_L(t)$ was discontinuous and that the optimal duration of inhalation was half of the duration of a whole breath.

Our new methodology allowed us to solve the optimization problem for different cost functions that have previously been suggested in the literature. When taking the volumetric acceleration as a cost function, the optimal pattern was very close to being sinusoidal, although the airflow had a lower peak compared to the sinusoidal breathing pattern (see Fig. 5.1). For work rate, the optimal alveolar volume was triangular, the same as for total work (see Section 5.3) and there was no optimal solution that minimized the average force developed by the respiratory muscles (see Section 5.4). We also considered a weighted cost function of average volumetric acceleration, work rate and square force, and found an optimal breathing pattern in which the driving force (P_L) was continuous. However, the optimal duration of inhalation and exhalation was the same (see Section 5.5). In the physiological context, the time duration of the first phase is expected to be shorter than that of the second phase.

Our study does not support the hypothesis that an observed combination of breathing frequency and amplitude is optimal with respect to some objective function. In all the cases we checked, when the pleural pressure was a given function the optimal frequency of the diseased lungs moved in the wrong direction. When the optimal shape of the pleural pressure was calculated, inspiration time was found to be equal to expiration time, which is different from physiological observations

under normal conditions. However, this outcome might change by altering the model as we discuss below.

6.1 Limitation of the Study and Future Directions

As is the case for most studies, our study also has some limitations. In all the models we used in this study, the relationship between the respiratory pressure and the volume was considered as a linear differential equation due to the assumption that the resistance to airflow was static (constant). However, adding nonlinear resistance to the model could potentially change the model outcome. For example, three types of resistances were discussed in [63]: linear (resistance due to laminar airflow), quadratic (resistance due to turbulence) and dynamic (where the resistance to airflow varied with a change in lung volume). The study tested two objective functions: work rate and average force using a $1D$ model. When work rate was taken as a cost function, the optimal airflow was found to be constant for a linear and quadratic resistances, however, it was no longer constant for a dynamic resistance. When taking the average force as a cost function, there were no optimal solutions for linear and dynamic resistances, however, an optimal solution existed for a quadratic resistance. It was shown in [38] that imposing different resistances to airflow during inhalation and exhalation could affect the optimal ratio between the durations of both phases, making them unequal (see Eq. 1.28). An unequal optimal inhalation-to-exhalation ratio could also result from adding resistance due to turbulence (see Eq. 1.28). We note however, that Otis. et al. [53] did include resistance due to turbulence, but the optimal frequency they obtained when minimizing the work rate during inhalation with a sinusoidal breathing pattern was similar to our results.

Future directions following this thesis could include adding a dynamic resistance to the different models, and computing the effect of it on the optimal solution when the weighted cost function is minimized. The heart function and the interaction between the heart and the lungs could also be taken into account.

References

[1] Adrian, E. (1933). Afferent impulses in the vagus and their effect on respiration. *The Journal of Physiology*, 79(3):332–358.

[2] Alheid, G. F., Milsom, W. K., and McCrimmon, D. R. (2004). Pontine influences on breathing: an overview. *Respiratory Physiology & Neurobiology*, 143(2-3):105–114.

[3] Barrett, K. E. and Ganong, W. F. (1963). *Review of medical physiology*. Lange Medical Publications.

[4] Bates, J. (1986). The minimization of muscular energy expenditure during inspiration in linear models of the respiratory system. *Biological Cybernetics*, 54(3):195–200.

[5] Ben-Tal, A. (2006). Simplified models for gas exchange in the human lungs. *Journal of Theoretical Biology*, 238(2):474 – 495.

[6] Ben-Tal, A., Shamailov, S., and Paton, J. (2012). Evaluating the physiological significance of respiratory sinus arrhythmia: looking beyond ventilation–perfusion efficiency. *The Journal of Physiology*, 590(8):1989–2008.

[7] Ben-Tal, A. and Smith, J. C. (2008). A model for control of breathing in mammals: Coupling neural dynamics to peripheral gas exchange and transport. *Journal of Theoretical Biology*, 251(3):480 – 497.

[8] Ben-Tal, A. and Smith, J. C. (2010). Control of breathing: two types of delays studied in an integrated model of the respiratory system. *Respiratory Physiology & Neurobiology*, 170(1):103–112.

[9] Berkovitz, L. D. and Medhin, N. G. (2012). *Nonlinear optimal control theory*. CRC press.

[10] Bianchi, A. L., Denavit-Saubie, M., and Champagnat, J. (1995). Central control of breathing in mammals: neuronal circuitry, membrane properties, and neurotransmitters. *Physiological Reviews*, 75(1):1–45.

[11] Butera Jr, R. J., Rinzel, J., and Smith, J. C. (1999). Models of respiratory rhythm generation in the pre-botzinger complex. i. bursting pacemaker neurons. *Journal of Neurophysiology*, 82(1):382–397.

[12] Cabrera, M. E., Saidel, G. M., and Kalhan, S. C. (1999). Lactate metabolism during exercise: analysis by an integrative systems model. *American Journal of Physiology-Regulatory, Integrative and Comparative Physiology*, 277(5):R1522–R1536.

[13] Campbell, E. J. M., Agostoni, E., and Davis, J. N. (1970). *The Respiratory Muscles: Mechanics and Neural Control*. WB Saunders.

[14] Cherniack, N. S., Longobardo, G., Staw, I., and Heymann, M. (1966). Dynamics of carbon dioxide stores changes following an alteration in ventilation. *Journal of Applied Physiology*, 21(3):785–793.

[15] Clark, C. W. (1976). *Mathematical Bioeconomics: The optimal management of renewable resources*. Wiley.

[16] Cohen, M. I. (1979). Neurogenesis of respiratory rhythm in the mammal. *Physiological Reviews*, 59(4):1105–1173.

[17] de Pinho, M. R. and Vinter, R. B. (1997). Necessary conditions for optimal control problems involving nonlinear differential algebraic equations. *Journal of Mathematical Analysis and Applications*, 5:493–516.

[18] Dobbins, E. G. and Feldman, J. L. (1994). Brainstem network controlling descending drive to phrenic motoneurons in rat. *Journal of Comparative Neurology*, 347(1):64–86.

[19] Duffin, J. (2004). Functional organization of respiratory neurones: a brief review of current questions and speculations. *Experimental Physiology*, 89(5):517–529.

[20] Duron, B. (1981). Intercostal and diaphragmatic muscle endings and afferents. *Regulation of Breathing*, 17(part I):473–540.

[21] Engwall, M., Smith, C., Dempsey, J., and Bisgard, G. (1994). Ventilatory afterdischarge and central respiratory drive interactions in the awake goat. *Journal of Applied Physiology*, 76(1):416–423.

[22] Ezure, K., Tanaka, I., and Miyazaki, M. (1998). Pontine projections of pulmonary slowly adapting receptor relay neurons in the cat. *Neuroreport*, 9(3):411–414.

[23] Farhi, L. E. and Rahn, H. (1960). Dynamics of changes in carbon dioxide stores. *Anesthesiology: The Journal of the American Society of Anesthesiologists*, 21(6):604–614.

[24] Feldman, J. L. and Del Negro, C. A. (2006). Looking for inspiration: new perspectives on respiratory rhythm. *Nature Reviews Neuroscience*, 7(3):232.

[25] Fowle, A., Matthews, C., and Campbell, E. (1964). The rapid distribution of 3h2o and 11co2 in the body in relation to the immediate carbon dioxide storage capacity. *Clinical Science*, 27:51–65.

[26] Gelfand, R. and Lambertsen, C. (1973). Dynamic respiratory response to abrupt change of inspired co2 at normal and high po2. *Journal of Applied Physiology*, 35(6):903–913.

[27] Gray, J. S. (1946). The multiple factor theory of the control of respiratory ventilation. *Science*, 103(2687):739–744.

[28] Grodins, F. S., Buell, J., and Bart, A. J. (1967). Mathematical analysis and digital simulation of the respiratory control system. *Journal of Applied Physiology*, 22(2):260–276.

[29] Grodins, F. S., Gray, J. S., Schroeder, K. R., Norins, A. L., and Jones, R. W. (1954). Respiratory responses to co2 inhalation. a theoretical study of a nonlinear biological regulator. *Journal of Applied Physiology*, 7(3):283–308.

[30] Hall, J. E. (2011). Guyton and hall textbook of medical physiology. 12. philadelphia, pa: Saunders.

[31] Hämäläinen, R. and Viljanen, A. (1978). A hierarchical goal-seeking model of the control of breathing. *Biological Cybernetics*, 29(3):151–158.

[32] Hämäläinen, R. P. and Sipilä, A. (1984). Optimal control of inspiratory airflow in breathing. *Optimal Control Applications and Methods*, 5(2):177–191.

[33] Harada, Y., Kuno, M., and Wang, Y. Z. (1985). Differential effects of carbon dioxide and ph on central chemoreceptors in the rat in vitro. *The Journal of Physiology*, 368(1):679–693.

[34] Hestenes, M. R. (1966). *Calculus of variations and optimal control theory*. John Wiley and Sons.

[35] Hjelt, E. and Tigerstedt, R. (1910). Johan gadolin 1760–1852 in memoriam. *Acta Soc. Sci. Fenn*, 39(96):287.

[36] Hodgkin, A. L. and Huxley, A. F. (1952). Propagation of electrical signals along giant nerve fibres. *Proceedings of the Royal Society of London. Series B-Biological Sciences*, 140(899):177–183.

[37] Hull, D. G. (2013). *Optimal control theory for applications*. Springer Science and Business Media.

[38] Johnson, A. T. and Masaitis, C. (1976). Prediction of inhalation time/exhalation time ratio during exercise. *IEEE Transactions on Biomedical Engineering*, (5):376–380.

[39] Khoo, M., Gottschalk, A., and Pack, A. I. (1991). Sleep-induced periodic breathing and apnea: a theoretical study. *Journal of Applied Physiology*, 70(5):2014–2024.

[40] Khoo, M., Kronauer, R. E., Strohl, K. P., and Slutsky, A. S. (1982). Factors inducing periodic breathing in humans: a general model. *Journal of Applied Physiology*, 53(3):644–659.

[41] Lahiri, S., Rozanov, C., Roy, A., Storey, B., and Buerk, D. G. (2001). Regulation of oxygen sensing in peripheral arterial chemoreceptors. *The international Journal of Biochemistry & Cell Biology*, 33(8):755–774.

[42] Lenhart, S. and Workman, J. T. (2007). *Optimal control applied to biological models*. CRC Press.

[43] Liberzon, D. (2011). *Calculus of variations and optimal control theory: A concise introduction*. Princeton University Press.

[44] Lindsey, B. G., Rybak, I. A., and Smith, J. C. (2012). Computational models and emergent properties of respiratory neural networks. *Comprehensive Physiology*, 2(3):1619–1670.

[45] Luck, J. (1970). Afferent vagal fibres with an expiratory discharge in the rabbit. *The Journal of Physiology*, 211(1):63–71.

[46] McIlroy, M., Marshall, R., and Christie, R. (1954). The work of breathing in normal subjects. *Clinical Science*, 13(1):127.

[47] Mead, J. (1960). Control of respiratory frequency. *Journal of Applied Physiology*, 15(3):325–336.

[48] Mines, A. H. (1981). *Respiratory physiology*. Raven Press New York.

[49] Molkov, Y. I., Shevtsova, N. A., Park, C., Ben-Tal, A., Smith, J. C., Rubin, J. E., and Rybak, I. A. (2014). A closed-loop model of the respiratory system: focus on hypercapnia and active expiration. *PloS one*, 9(10):e109894.

[50] Monod, J., Wyman, J., and Changeux, J.-P. (1965). On the nature of allosteric transitions: a plausible model. *J Mol Biol*, 12(1):88–118.

[51] Nakagawa, M., Hattori, N., Haruta, Y., Sugiyama, A., Iwamoto, H., Ishikawa, N., Fujitaka, K., Murai, H., Tanaka, J., and Kohno, N. (2015). Effect of increasing respiratory rate on airway resistance and reactance in COPD patients. *Respirology*, 20(1):87–94.

[52] O'Regan, R. and Majcherczyk, S. (1982). Role of peripheral chemoreceptors and central chemosensitivity in the regulation of respiration and circulation. *Journal of Experimental Biology*, 100(1):23–40.

[53] Otis, A. B., Fenn, W. O., and Rahn, H. (1950). Mechanics of breathing in man. *Journal of Applied Physiology*, 2(11):592–607.

[54] Paintal, A. (1953). The conduction velocities of respiratory and cardiovascular afferent fibres in the vagus nerve. *The Journal of Physiology*, 121(2):341–359.

[55] Peever, J. H., Tian, G.-F., and Duffin, J. (1998). Bilaterally independent respiratory rhythms in the decerebrate rat. *Neuroscience Letters*, 247(1):41–44.

[56] Pontryagin, L. S., Boltyanskii, V. G., Gamkrelidze, R. V., and Mishechenko, E. F. (1962). *The Mathematical Theory of Optimal Processes*. John Wiley and Sons.

[57] Poon, C.-S. (1987). Ventilatory control in hypercapnia and exercise: optimization hypothesis. *Journal of Applied Physiology*, 62(6):2447–2459.

[58] Potturu, S. R., Pal, T., and Maka, S. (2019). Modelling and analysis of respiratory system with congestive heart failure. In *2019 Fifth Indian Control Conference (ICC)*, pages 266–270. IEEE.

[59] Prabhakar, N. R. (2000). Oxygen sensing by the carotid body chemoreceptors. *Journal of Applied Physiology*, 88(6):2287–2295.

[60] Rigatto, H., Fitzgerald, S., Willis, M., and Yu, C. (1992). In search of the central respiratory neurons: Ii. electrophysiologic studies of medullary fetal cells inherently sensitive to co2 and low ph. *Journal of Neuroscience Research*, 33(4):590–597.

[61] Rigatto, H., Wilson, C., Koshiya, N., House, S., and Smith, J. (2001). Stationary organotypic culture of the pre-bötzinger complex from the newborn rat. In *Frontiers in Modeling and Control of Breathing*, pages 139–145. Springer.

[62] Rohrer, F. (1925). Physiologie der Atembewegung. In *Handbuch der Normalen und Pathologischen Physiologie*, pages 70–127. Springer Berlin Heidelberg, Berlin, Heidelberg.

[63] Ruttimann, U. E. and Yamamoto, W. S. (1972). Respiratory airflow patterns that satisfy power and force criteria of optimality. *Annals of Biomedical Engineering*, 1(2):146–159.

[64] Rybak, I., Shevtsova, N., Paton, J., Dick, T., John, W. S., Mörschel, M., and Dutschmann, M. (2004). Modeling the ponto-medullary respiratory network. *Respiratory Physiology & Neurobiology*, 143(2-3):307–319.

[65] Rybak, I. A., Shevtsova, N. A., St-John, W. M., Paton, J. F., and Pierrefiche, O. (2003). Endogenous rhythm generation in the pre-bötzinger complex and ionic currents: modelling and in vitro studies. *European Journal of Neuroscience*, 18(2):239–257.

[66] Saidel, G. M. and Chester, E. H. (1976). Breathing pattern effects on pulmonary oxygen uptake. *Medical and Biological Engineering*, 14(4):402–407.

[67] Saunders, K. B., Bali, H. N., and Carson, E. R. (1980). A breathing model of the respiratory system: the controlled system. *Journal of Theoretical Biology*, 84(1):135–161.

[68] Shevtsova, N. A., Marchenko, V., and Bezdudnaya, T. (2019). Modulation of respiratory system by limb muscle afferents in intact and injured spinal cord. *Frontiers in Neuroscience*, 13.

[69] Silverman, L., Lee, G., Plotkin, T., Sawyers, L. A., Yancey, A. R., et al. (1951). Air flow measurements on human subjects with and without respiratory resistance at several work rates. *Arch. Indust. Hyg. & Occupational Med.*, 3(5):461–78.

[70] Smith, J. C., Ellenberger, H. H., Ballanyi, K., Richter, D. W., and Feldman, J. L. (1991). Pre-botzinger complex: a brainstem region that may generate respiratory rhythm in mammals. *Science*, 254(5032):726–729.

[71] Stornetta, R. L., Rosin, D. L., Wang, H., Sevigny, C. P., Weston, M. C., and Guyenet, P. G. (2003). A group of glutamatergic interneurons expressing high levels of both neurokinin-1 receptors and somatostatin identifies the region of the pre-bötzinger complex. *Journal of Comparative Neurology*, 455(4):499–512.

[72] Teppema, L. J. and Dahan, A. (2010). The ventilatory response to hypoxia in mammals: mechanisms, measurement, and analysis. *Physiological Reviews*, 90(2):675–754.

[73] Upreti, S. R. (2013). *Optimal Control for Chemical Engineers*. CRC Press,.

[74] Vinter, R. and Zheng, H. (1998). Necessary conditions for optimal control problems with state constraints. *Transactions of the American Mathematical Society*, 350:1181–1204.

[75] West, J. B. (2012). *Respiratory physiology: the essentials*. Lippincott Williams & Wilkins.

[76] Widdicombe, J. (1981). Nervous receptors in the respiratory tract and lungs. *Regulation of Breathing*.

[77] Yamashiro, S. and Grodins, F. (1971). Optimal regulation of respiratory airflow. *Journal of Applied Physiology*, 30(5):597–602.